AFCRL-65-490

SEISMIC NOISE IN DEEP BOREHOLES

A. J. Seriff, J. H. Rosenbaum, C. J. Velzeboer, R. J. Haase

Shell Development Company
A Division of Shell Oil Company
Exploration and Production Research Division
Houston, Texas

Contract No. AF19(628)-2785

Project No. 8652

Task No. 865204

FINAL REPORT

June 21, 1965

Work Sponsored by Advanced Research Projects Agency
Project VELA-UNIFORM
ARPA Order No. 292
Project Code No. 8100, Task 2

Prepared
for

AIR FORCE CAMBRIDGE RESEARCH LABORATORIES
OFFICE OF AEROSPACE RESEARCH
UNITED STATES AIR FORCE
BEDFORD, MASSACHUSETTS

Request for additional copies by agencies of the Department of Defense, their contractors, and other government agencies should be directed to:

DEFENSE DOCUMENTATION CENTER (DDC)
CAMERON STATION
ALEXANDRIA, VIRGINIA 22314

Department of Defense Contractors must be established for DDC services or have their "need-to-know" certified by the cognizant military agency of their project or contract.

All other persons and organizations should apply to the:

Clearinghouse for Federal Scientific and Technical Information (CFSTI)
Sills Building
5285 Port Royal Road
Springfield, Virginia 22151

AFCRL-65-490

SEISMIC NOISE IN DEEP BOREHOLES

A. J. Seriff, J. H. Rosenbaum, C. J. Velzeboer, R. J. Haase

Shell Development Company
A Division of Shell Oil Company
Exploration and Production Research Division
Houston, Texas

Contract No. AF19(628)-2785

Project No. 8652

Task No. 865204

FINAL REPORT

June 21, 1965

Work Sponsored by Advanced Research Projects Agency
Project VELA-UNIFORM
ARPA Order No. 292
Project Code No. 8100, Task 2

Prepared
for

AIR FORCE CAMBRIDGE RESEARCH LABORATORIES
OFFICE OF AEROSPACE RESEARCH
UNITED STATES AIR FORCE
BEDFORD, MASSACHUSETTS

TABLE OF CONTENTS

SEISMIC NOISE IN DEEP BOREHOLES

BY

A. J. SERIFF, J. H. ROSENBAUM, C. J. VELZEBOER, R. J. HAASE

ABSTRACT

Seismic noise in the frequency range 0.2 to 5.0 cps was observed in three wells approximately 10,000 feet deep. The wells are in the Texas Gulf Coast, the Val Verde Basin of West Texas and the Williston Basin of North Dakota. Observations were made at 1000 foot intervals in each well and simultaneous observations were made in a 500 foot reference hole and at four surface stations approximately 1500 feet apart. These seismometers were vertical component Benioffs. Two surface horizontal components were also recorded. Power spectral ratio, coherence and cross correlation phase were computed for most seismometer pairs, particularly the deep well seismometer and the 500 foot reference.

The theoretical response of appropriate plane layered elastic models to trapped Rayleigh and Love waves as well as to plane P, SV, and SH waves incident from below was investigated in detail over the applicable frequency range for each of the three sites. Two essentially independent models for the noise have been investigated. One is based on the assumption that at a given frequency the average energy density is the same for each trapped surface mode (Rayleigh and Love) and that the modes are independent; the other assumes that at a given frequency independent plane P, SV, and SH waves with equal energy flux in all directions are incident from the lower half space.

The theoretical response parameters for the two noise models applied to a given layered model have many similar features. The observed noises at all three sites vary systematically with depth and exhibit a behavior roughly predicted by an average of the two noise models. Both trapped waves and plane waves are probably present. Similar conclusions apply to the noise observed on the surface array and the surface horizontal components.

SEISMIC NOISE IN DEEP BOREHOLES

FINAL REPORT

INTRODUCTION

This Final Report begins with the results of previously unreported work carried out during the five month period October 1964 through February 1965. The work consists primarily of experimental observations and theoretical computations for the deepwell site at Trotters, North Dakota. The data and some comparisons with theory are presented in the section on Noise Observations. The section on Theoretical Studies contains extensions of the calculations for previous deepwell sites in addition to complete calculations for Trotters. The remainder of the report contains a comparison of data and calculations for all three of the sites studied and a summary of the salient conclusions of this research. Although we have appended to this report for ease of reference, some of the data previously reported for our Hempstead and Juno deepwell sites we have not attempted to repeat here the bulk of the material given in our Semi-Annual Reports.[1,2,3] Those reports contain an introduction to the purposes of this research; descriptions of the experimental equipment and procedures, the data analysis techniques and the bases for the theoretical calculations; and detailed analyses of the measurements at our first two sites. Together with this Final Report they form the complete documentation of our efforts.

NOISE OBSERVATIONS AT THE TROTTERS WELL

Site Information

General. The Trotters well is the Shell-N.P.Brown et al. 41-24-1 deep test drilled in 1961 to a total depth of 9830 feet (3000 meters). It is located in the southwest corner of North Dakota near the center of the Williston Basin (see Figure 1). Its position is N 47°07.3' and E 103°40.6'; the elevation is 2675 feet (815 meters). The hole was plugged and abandoned in June 1961, after the appropriate well surveys had been made, including a continuous velocity log with check shots. The 10 3/4-inch casing, which was set to a depth of 714 feet, was left in the hole.

In July 1964 it was decided to use the hole for our deep well noise studies, and preparations for reopening it and setting and cementing casing were initiated. Drilling operations started in mid August. Some delays were

experienced on account of rain, but by mid September the job was completed, including the drilling and casing of a 500-foot deep reference hole. The deep hole was completely cased with 7-inch casing, totally cemented from bottom to surface in three stages (see Figure 3). The reference hole also had 7-inch casing which was completely cemented. The bottom hole temperature of the deep hole was 194°F. The total cost of the site preparation was approximately $136,000.

The noise observation instrument crew started their preparation of the site in mid September and by the end of that month the first noise data were taken. Observations were continued until mid January, 1965, when Shell's operations at this location had been completed.

During this period of observation a wide variety of weather conditions was met. The first part of October was characterized by mild temperatures, and intermittent moderate winds, with speeds up to 10-25 mph, a delightful Indian summer. During the second part of October and the first half of November cool temperatures and frequent generally stronger winds were experienced. Winter started about mid November and lasted until the termination of the observations. Very low temperatures ($< -20°F$) and very strong winds (> 50 mph) were measured during this period, but normally the temperature was just below freezing, and wind moderate and intermittent. Snow was rather abundant.

The prevailing wind was generally from a northerly direction predominantly from the Northwest. There was a strong tendency for the wind to slacken drastically at dusk and pick up speed again during the later part of the night or in the morning.

Physiographically, the well is situated near the western edge of a broad zone of "bad lands" straddling the Little Missouri River. The zone is approximately 20 miles wide and extends in a roughly north-south direction. These "bad lands" are characterized by a deep and erratic erosion of the soft and rather sparsely vegetated soil, which gives rise to a very rough topography. Elevation differences of over 200 feet in distances of 1000 feet are common.

Geological setting. The well is situated near the center of the Williston Basin which is a generally flat, undisturbed rather shallow basin.[4] Figure 2 shows in cross section the basin configuration. The basin is about 600 miles long in a generally east-west direction and about 300 miles

wide in the north-south direction. At basement depth the steepest dips, at the sides of the basin, are on the north, south, and east but do not exceed 50 feet per mile. The local geology is very simple as can be surmised from Figure 2. There is only one significant tectonic feature in the basin; namely, the Cedar Creek Anticline which is about 50 miles from the well near the North Dakota-South Dakota-Montana junction. Its effect would be barely visible on cross-sections of the scale shown.

Velocity and density. The P-wave velocities measured in the Trotters well are shown in Figure 3. The lateral changes of the compressional wave velocity are very small as can be seen from Figure 4, which shows velocities measured in several nearby wells. In order to avoid difficulties arising from the different surface elevations of the wells shown and from the use of various datum planes for the velocity surveys, the time-depth data were plotted with respect to a fixed geological marker, viz, the top of the Mississippian Limestone. From Figure 4 and Figure 2 it is evident that the stratigraphic column of the Trotters well and its velocity distribution are representative of a wide area surrounding the well.

A composite log of the well combined with the P-wave velocity model is shown on Figure 3. No measured shear wave velocity data were available, nor were the densities known. The formation densities were assumed to increase gradually from 2.0 g/cm^3 at the surface to 2.8 for basement. A density reversal was taken to be present at the layer of Mississippian Salt, which was given a density of 2.2 g/cm^3. It was both under- and overlain by sediments of 2.5 g/cm^3. A complete tabulation of the densities used for the model can be found in Table 2, in the section on Theoretical Studies.

The shear wave velocities were derived from the compressional velocities, using assumed velocity ratios. The values chosen for these ratios are consistent with those found in the literature for the various types of sediments present. The sediments near the surface showed a physical similarity to those found at the surface at the Hempstead well site. Consequently, the variation of the V_p/V_s ratio with depth indicated by some measurements at the latter site was thought to be applicable to the Trotters site, viz, a rapid decrease from high V_p/V_s ratios at the surface to normal values at a depth of 150 meters. The values used are visible in Table 2 of the section on Theoretical Studies.

An unknown factor in the model is the depth and velocity of the basement. From regional geological studies a basement depth could be deduced which is some 1300 meters (± 10%) below the total depth of the well. No local P-wave velocity data were available for basement, it was assumed to be 6.9 km/sec with a V_p/V_s ratio of 1.9. Some very widely scattered determinations of the basement velocities in the northern U.S.A. and in Canada showed the velocity to be in excess of 6 km/sec, suggesting the absence in the upper part of the crust of a velocity reversal of the type found in Hempstead.[1]

Seismometer configuration. The setup of the field instruments is shown in Figure 5. The general arrangement was identical to that used in the two previous well surveys described in our semi-annual reports. The seismometer clamped at various depths in the deep well is referred to as DW-1. The seismometer in the 500-foot deep reference hole is referred to as DW-2.

Near the deep hole and reference hole, three seismometers were placed in buried vaults. One measured the vertical component of the ground motion (SPZo); the others (SPRo and SPTo) measured the horizontal components in E-W and N-S directions respectively. The array seismometers (SPZn, SPZse and SPZsw) were first placed in equilateral triangular configuration with the deep well at the center. The sides of the triangle were 1300 meters long. Very early during the noise observations at the Trotters site it became evident that the SPZsw location was unduly noisy during windy periods and it was moved to the second location shown on Figure 5. The array used at Trotters differed from previous arrays in size and symmetry, being somewhat larger and more symmetrical than any previously employed.

Local noise sources. The area around the Trotters well is thinly populated; outside the bad lands farms are found scattered at distances of 3 to 5 miles between small towns with a spacing of some 30 to 50 miles.

The bad lands were uninhabited except for some isolated farms along the river. The sole use of the soil in the bad lands is cattle grazing; outside the bad lands the main use is wheat farming with some cattle grazing. The nearest farm was about 3/4 mile from the well site. Except for daytime plowing activity during October, it made no noticeable contribution to the general noise level. Infrequent vehicular traffic on the dirt road passing the farm was noticeable.

Though dirt roads are abundant in the area, paved roads are few. The nearest highway is about 15 miles due south. Although traffic on this highway was quite heavy, it did not contribute any recognizable pattern to the ambient noise at the site of observation. In contrast to the road traffic, rail traffic on a line paralleling the highway could be clearly detected in the noise observations.

The deep well site is apparently situated in a busy airway traffic lane, and it is suspected that some strong high-frequency almost sinusoidal noise bursts are due to airplanes above. It must be noted however that these bursts were also found at times when no airplane could be heard or seen.

Wild life was abundant in the area and some sudden and local noise bursts may be explained by their presence near a seismometer vault.

A frequent source of noise near the Trotters well was the local winds. The wind conditions are described above. Fortunately, these winds were intermittent so that relatively quiet data could be obtained during most 24-hour periods. The effectiveness of these winds in producing noise varied considerably over distances of the order of a few tenths of a kilometer and seemed to be closely associated with the local topography. Results from the five surface stations occupied suggested that sites in valleys protected from the local winds were quieter than the high exposed sites. The SPZsw seismometer which was originally in a position on the edge of a rather high plateau and near a fence post, was much noisier than the other seismometer locations which were situated in or near valleys. The noise of the former site was of a high frequency character and strongly wind dependent and only during periods of little or no wind did the seismometer output resemble in level and appearance the noise of the other stations. As mentioned above, the SPZsw location was shifted into a valley some

335 meters towards the north (note the difference in elevations). There the seismometer had an output comparable to that of the other seismometers of the array. The manner in which local wind produced the noise observed at the seismometers was not clear. In some cases wind induced motion of vault covers, fence posts, etc. was partly responsible. In most cases, however, no such obvious agents were found.

In spite of the precautions mentioned in previous reports some tube wave noise was noticed in the deep well. The noises were infrequent, and the levels small and apparently not bothersome. The distinctive repeated bursts could occasionally be identified, however, particularly during periods immediately following a change of the depth of the DW-1 seismometer.

In general, all of these recognizable local noises were avoided in selecting portions of the recorded noise for detailed analysis. As in the previous reports noise samples were from "typical quiet" periods unless otherwise noted.

Experimental Procedures

Instrumentation. Both the field and office instrumentation used at Trotters were identical to those used for the Juno site. These are described in detail in our previous reports.[1,2,3] The field system employed standard Benioff short-period seismometers with photo-tube amplification. Signals were recorded both on film and magnetic tape. The deep well instruments were the Geotech seismometers described previously; they were locked to the well casing during observation. These seismometers have the same frequency response as the standard short-period Benioff. An anemometer signal was also recorded on film.

Calibration procedures and results were the same as those described in previous reports. Amplitudes are reliable to about 15%; phase errors affecting time estimates by as much as 0.020 seconds were not observed. Overall system noise at Trotters was well below the recorded data levels as shown by the power spectra of Figure 6.

Data acquisition. The procedures for data acquisition established at our other well sites were followed at Trotters also. All seismometers (DW-1, at variable depths; DW-2, at 500 feet; SPZo, SPZn, SPZsw, SPZse, SPRo, and SPTo at the surface) were recorded continuously. The depth of the DW-1 seismometer was changed approximately once a week, adequate time

being allowed for stabilization of the instrument and for sampling of a variety of noise conditions. Observations were made at 500 feet, 1000 feet, and at approximately 1000-foot intervals down to 9750 feet. Deep and shallow depths were alternated so as to eliminate the possibility that gradual changes of noise or system parameters would be interpreted as variations with depths.

In addition to the set of observations taken also at other sites, we have recorded data at depths of 100, 200, 300, and 400 feet.

Calculations. With the exception of the horizontal velocity calculations shown in Figure 19, all calculations performed on the Trotters data were of types described in detail in our previous reports. All quantitative data analyses were performed on signals played back from the magnetic tape and digitized every 0.050 seconds at record time. The tape was played back at 7-1/2 cps.

Except where specifically noted, analyses were performed on data selected as representative of "typical quiet" noise. This selection involved visual inspection of the photographically recorded noise and wind velocity information; the criteria for such a selection have been discussed in detail previously. Some additional comments appear in the section on Local Noise Sources.

All spectra were computed from auto- or cross-correlations of 150-second long noise samples. These correlations were truncated with a triangular weighting function 20-seconds long before Fourier analysis.

Experimental Results

Signal amplitudes - seismometer coupling. Except for the very near surface, the Trotters well was protected over its entire length by a single string of completely cemented casing so that good coupling of the seismometer to the formation was expected. The first 714 feet contained two strings of casing, but both were cemented. Direct comparisons of noise recorded at 470 feet in the deep well and in the 500-foot reference hole gave identical results for all frequencies below 3.0 cps.

Seismometer coupling at deeper depths was investigated by comparing the levels of clearly defined earthquake P-waves recorded at depth and at the surface and near surface stations. The observed signal levels agreed with the levels predicted for plane P-waves arriving vertically from below the well within the expected error of measurement. The results obtained at

Trotters were the same as those reported for both Hempstead and Juno; seismometer coupling appeared to be good at all depths, and signal amplitudes decreased with depth approximately as predicted by simple theory.

General noise levels. Figure 7 shows several power spectra for "typical quiet" noise from various depths at the Trotters site. These spectra and all the spectra shown in reports of this project are corrected to true ground motion only at 1.0 cps; they have not been corrected at other frequencies for the response characteristics of the seismometer and recording system used. In general the levels recorded here were comparable to those observed at our Hempstead site and somewhat greater than the levels observed at Juno. The Trotters site could be classed as fairly noisy in a comparison of general levels observed in the United States.

The shape of these spectra are very similar to those observed during quiet periods at Hempstead, except for the 2.0 cps peak which is much weaker at Trotters. The large decrease in level between the surface and 500-foot observations at Hempstead is also present at Trotters (cf. Figure 10). This decrease is approximately 20 db in power (a factor of about 3 in amplitude) at 2.5 cps and only about 2 db at 1.0 cps. Surface and 500-foot levels are almost equal below 1.0 cps. The additional gradual decrease with depth observed at our other sites is also found at Trotters. The power levels at the maximum depth of observation are between 10 and 20 db below those observed at 500 feet. This decrease, corresponding to a decrease in amplitude by a factor ranging from about 1.7 to 3.0, is of the same order as the observed decrease in earthquake signal levels. Thus, only a slight improvement in general signal-to-noise ratio is to be expected at depths below 500 feet at the Trotters site. At frequencies above 1.0 cps, however, a definite gain can be obtained by shallow burial of the seismometer.

Noise stationarity. The noise observed at Trotters during preselected "typical quiet" periods was quite stable in its general characteristics. Surface power spectra for a number of different quiet periods are shown in Figures 7, 10, 11 and 12. These were periods of low wind which showed no unusual noise conditions on the develocorder records. In general, these spectra fall within a few db of each other for frequencies of the order of 2.0 cps and lower. At Trotters occasional variations were visible, however, in the amplitudes of fairly well defined

peaks observed at approximately 0.65, 0.95, and 1.2 cps. For example, the quiet noise of Figure 11 shows an increase at 0.65 and 0.95 cps of about 6 to 10 db over the usual level at these frequencies. These variations in spectrum shape were not usually observed at other sites; their origin at Trotters is not understood. Some of this variability is eliminated from the deep data by normalization to the 500-foot reference level.

The stationarity of the power spectra for the deep observations and particularly for the relative power spectra between the deep observations and the 500-foot reference signals was fairly satisfactory at Trotters; typical examples are shown on Figures 7-11. Figures 8 and 9 also give some indication of the stationarity of phase and coherence spectra for comparisons of deep well and 500-foot data.

Figures 7, 8, 10 and 11 also show some data recorded during rather extreme noise conditions. Such data was generally not used in making detailed noise studies, but the results are interesting in themselves and for the extent to which they indicate the effectiveness of normalization with the 500-foot observations in removing some of the variability of the data.

Figures 7 and 8 contain data taken during a blizzard involving very high winds. The surface noise power during the blizzard increased by as much as 40 db between 1.0 and 2.0 cps. In the same frequency range the noise at 500 feet increased by only 10 to 15 db. The increase at 5000 feet was such that the power ratio of the 5000-foot and 500-foot data is almost the same as the ratio observed during quiet periods. Clearly the increased noise seen at the surface contains a component which decreases with depth in approximately the same fashion as typical quiet noise and a much larger component which is confined to depths shallower than 500 feet.

Figure 11 contains a comparison of surface, 500-foot, and 6000-foot observations for a quiet period and a period during which extreme noise from an eastbound train is visible at all three depths. The train is at a distance of approximately 15 miles. The increase in surface noise is almost as great as that observed during the blizzard, however, it begins at a higher frequency (about 1.0 cps) and is obviously of a different nature. The large increase from this distant source is present at all depths at levels such that the ratio of surface to 500-foot power as well

as the ratio of 6000-foot to 500-foot power are unchanged. The entire increase observed here acts like the small portion of the blizzard noise which attenuates with depth in the same fashion as the typical quiet noise. These observations are consistent with the hypothesis that the extreme wind noise contains a strong component generated near the seismometers as well as a weaker component generated at reasonably large distances.

Near surface noise. At Trotters we have investigated the near surface noise behavior in some detail. Figure 10 shows (lower curves) the relative power spectra for deep well observations at 100 and 200 feet normalized to the 500-foot reference. The corresponding simultaneous observations at the surface (upper curves) and the surface power spectra normalized to 500 feet (middle curves) are also shown. For each deep well depth data are shown for a quiet period and period of moderate to strong wind.

Several interesting phenomena should be noted:

1) From the lower curves we can see that the normal quiet noise decreases gradually from the surface to 500 feet. At 100 and 200 feet approximately one third to one fourth of the decrease observed at 500 feet has occurred. The straight line drawn with these curves is taken from the middle group of curves and is the approximate value of the ratio surface/500-foot for typical quiet noise.

2) During windy periods much of the large increase in surface noise above 0.5 cps is not present at 500 feet. Comparing the upper and middle curves we can see that almost none of the increase on 64-12-18 and only about one half of the increase on 65-01-13 are present at 500 feet.

3) During windy periods the ratios of noise power at 100 feet and 500 feet or 200 feet and 500 feet do not change. Since the largest part of the surface noise increase is not present at 500 feet, we can conclude that it does not extend even to a depth of 100 feet.

These observations are consistent with the conclusion that a large fraction of the surface noise increase observed during windy periods does not behave like typical quiet noise and is confined to depths shallower than 100 feet. It is our present belief that much of this noise is generated at or very near the seismometer vaults.

The horizontal components. In Figure 12 we have plotted the ratio of radial-to-vertical power as a function of frequency for several

periods of quiet noise. The ratios of transverse-to-vertical and radial-to-transverse power are also shown along with the actual vertical component power spectra. The Trotters data shown on Figure 12 demonstrate several features of the noise which were not observed at our other sites. First, the ratios SPRo/SPZo and SPTo/SPZo are much more variable with time than the ratios observed at other sites. This probably results, at least in part, from the fact that the SPZo station seemed to be somewhat noisy; it frequently showed an increase in noise above 0.5 cps which was not seen on all the other vertical component detectors and was probably of very local origin. Second, the ratio SPRo/SPTo is consistently greater than 1.0 for frequencies below 2.0 cps. There thus appears to be a considerable asymmetry in the azimuthal noise distribution.

The points plotted on the SPRo/SPZo data are taken from the theoretical calculations described in the section on Theoretical Studies. The circles are for an energy equipartition mixture of all Rayleigh and Love modes. The crosses are for the isotropic plane wave noise model referred to under Theoretical Studies. The points computed for the ratio of total horizontal-to-total vertical power have been reduced by 4 db to allow approximately for the observed proportion of the total horizontal power present in the radial component. It is quite interesting to note that the two quiet different noise models give very similar results for the predicted ratio of horizontal-to-vertical power.

The agreement between the observed and predicted points is not spectacular, however the general level of the predicted ratio is approximately correct. Both the predicted and observed level at Trotters are larger than those for either of the other sites. The local minimum predicted at about 0.25 cps may correspond to a minimum occasionally observed at about this frequency; the strong observed minimum at 0.95 cps does not appear in the predictions of either model, however.

It is perhaps worth noting that at Trotters the theoretical calculations for energy equipartition among all trapped modes predict that for most frequencies below 2.0 cps about 50 percent of the horizontal component energy is in the form of Love waves. Such a strong Love wave component would be consistent with the generally low coherence observed at Trotters (and at our other sites) between the vertical and horizontal noise components at the surface.

Synthetic deep well traces. At the Juno site one of the most striking features of the deep well data was the appearance in the typical noise of numerous pulses which appeared to travel with P-wave velocity vertically upward to the surface where they were totally reflected. This phenomenon was investigated by preparing synthetic deep well traces on the hypothesis that the noise visible at depth consists of incident and reflected copies of the surface noise. Figure 13 contains a number of comparisons of deep well noise recordings and synthetic deep well traces for the Trotters site. Simultaneous recordings of the 500-foot reference trace are also shown. The synthetic deep well trace consists of the sum of two time shifted copies of the 500-foot reference trace; the shifts are $+\tau$ and $-\tau$, where τ is the one-way vertical travel time for P-waves. The level of the synthetic traces has been arbitrarily adjusted to give a good visual comparison with the deep well signal. The computations were performed on a digital computer. Data for two depths of observation are shown; with the one exception indicated on the figure the recording periods were fairly quiet.

The similarity between the synthetic and actual deep well traces of Figure 13 is very slight. A few relatively short intervals (< 10 seconds) of rough agreement are found, but the striking coincidences seen at Juno are not visible here. An obvious difference between the synthetic and real traces at Trotters is the great relative strength of the high frequencies in the synthetic signal. The ratio of power at frequencies $\gtrsim 1.0$ cps to power at about 0.25 cps is clearly too high on the synthetic traces. It is possible that band-pass filtering would produce more comparable records in some limited frequency ranges. From the records shown, however, we can only conclude that simple surface reflected P-waves do not frequently appear to dominate the noise over the whole frequency band recorded.

Amplitude-depth observations. The basic data for the study of the noise variation with depth are shown in Figures 14-16 which contain plots of the power ratios, coherences and cross-correlation phases for the deep well noise and the 500-foot reference noise as a function of frequency for a number of depths of obeservation. These spectra were calculated as in previous reports from auto and cross-correlations of preselected quiet noise samples. In the figures only one spectrum is shown for each depth, but some data on the stationarity of the noise have been shown in previous figures and discussed above. Although the details of

the spectra are not as stationary at Trotters as at the previous sites, a number of general trends are obviously reproducible. In Figure 17 we have summarized part of these data in the form of plots of power ratio and signed coherence as a function of depth for a number of discrete frequencies. In Figure 17 data from a number of different spectra are shown at each depth. It is clear that the scatter in the data from different noise samples at the same depth is less on the average than the variations due to consistent trends in the noise. The points plotted on Figure 17 for a depth of 500 feet are interesting in this regard as they show the calibration uncertainties and other systematic differences between noise measured with the deep well seismometer and with the reference instrument when both are at the same depth.

The power ratio, coherence and phase spectra from Trotters show in general all of the previously described features of the Juno and Hempstead wells.[1,2,3] Having seen the previous spectra one can by rather judicious averaging find the rough outline of the same features in the Trotters results. The first minima in the power ratio and coherence are fairly clearly defined and both the first and second phase transitions are well marked. The frequencies of these features vary with depth as they did at the previous sites and even the slight displacement in frequency between the first power ratio and coherence minima at a given depth is visible. The spectra are in general somewhat more ragged, however, and the broad secondary maxima and minima in the power ratio and coherence seen at Juno and Hempstead are difficult to identify at Trotters due to the presence of numerous narrow local maxima and minima in the spectra. Most of these narrow features are not always observed but there seems to be a tendency for them to occur at the same frequencies if they are visible. Thus, one can find in the power ratio spectra at several depths minima at about 0.70, 0.95 and 1.25 cps. Such minima, which seem to occur at a fixed frequency independent of depth, were not prominent in the spectra of the other sites. These features could result from signals which are strong only at the 500-foot reference level either being unique to that hole or dying out rapidly with depth. Minima which appear at a frequency independent of depth could also be due to the presence of tube waves in the deep well. An interval of about 0.25 cps between minima would be expected for tube waves reflected at the top and bottom of the well. As mentioned

previously, tube waves were observed at Trotters, however, the recordings selected fo analysis appeared on the develocorder records to be relatively free from this type of disturbance. Thus far we have not been able to draw any useful conclusions about these finer features of the spectra at Trotters and in most of what follows we will be discussing the larger features which are discernible if the curves shown are somewhat smoothed.

Comparisons with theory. In addition to the experimental data, Figures 14-17 contain two sets of curves adapted from those given in the section on Theoretical Studies. [It should be noted that whereas the theoretical curves shown in Figure 17 were available at closely spaced points, the curves of Figures 14 and 15 are simply an estimated smooth curve running through the calculated points shown. At the greater depths these points were not available at close enough intervals to define the maxima and minima of the curves with much certainty.] The curves show the theoretical variation of the noise for two different mixtures of the modes computed for a plane layered model of the Trotters site. The first model is an energy equipartition mixture of the trapped modes only; the second model has in addition an admixture of the isotropic plane wave noise described in the Theoretical Studies section. We have arbitrarily taken an amount of isotropic plane wave noise which has at all frequencies the same vertical component power at the surface as the mixture of trapped modes. The purpose of choosing such a mixture was to demonstrate the effect of the presence of a plane wave component large enough to be visible on a surface array without completely obscuring the Rayleigh wave component. It can be seen on Figure 27 that this mixture will begin to be dominated by the plane waves at depths below about 5000 feet.

In our previous report[3] we have compared our experimental data with trapped waves and with plane waves incident at specific angles, in particular nearly vertical P-waves. In Figure 14 we have indicated the locations of the first minima in the power ratio curves predicted for vertical P-waves alone. In this regard Figure 25 reveals a most interesting feature of the theoretical calculations: the power ratio variation with depth for the isotropic plane wave model is almost identical to that predicted for vertical P-waves alone. Moreover, from Figure 26 we can see that the coherence for the isotropic plane waves is approximately ±1 with

sign changes near the depths of the expected sign changes in the coherence of the vertical P-waves.

This striking similarity of the isotropic plane wave noise and the nearly vertical P-waves suggests that it may be quite difficult to distinguish with a vertical array between noise from sources sufficiently distant to produce almost vertical arrivals and noise from many local sources or scatterers. Such a distinction could be quite important, since those two types of plane wave noise might be expected to behave quite differently in another regard. Whereas the level of plane wave noise from distant sources might be expected to be fairly constant over the continent and relatively independent of the trapped wave level, the plane wave level from local sources or scatterers might bear a close relation to the level of the trapped wave noise.

The theoretical calculations for Trotters demonstrate also the great similarity between the depth variation of an equipartition mixture of trapped modes and the depth variation of an isotropic mixture of plane waves. At any given depth the agreement between the two theories is fairly good for frequencies up to about two times the frequency of the first minimum in power ratio or coherence. At higher frequencies the oscillations in the theoretical power level curves are more extreme for plane waves than for the Rayleigh modes, and the coherence levels for the plane wave mixtures are much higher than those for Rayleigh modes alone. At the lower frequencies, however, the general shape of the amplitude-depth curves and such features as the location of the first minima are hardly diagnostic of the two noise models. The coherence predictions (with sign) are somewhat more sensitive to the model than the power ratio and should definitely be included in any comparison of theory and experiment.

An additional feature of the theoretical curves should be noted. The general level of the power ratio with respect to 500 feet becomes very sensitive to the plane layered model parameters at frequencies for which the power at 500 feet approaches a minimum. For example the theoretical power ratio curves at 2.00 cps can be shifted considerably in level (though not in general shape) by a slight change in the depth of the predicted power minimum near 500 feet.

The power ratio data of Figures 14 and 17 show many points of agreement with the theoretical curves. The general levels as a function of depth and the first minimum at each depth are in reasonable agreement with the theories. (Note that the theoretical curves at the greater depths of Figure 14 are not very well defined by the points.) From Figure 14 it appears that the levels at frequencies above the first minimum are somewhat better predicted by the mixture containing plane waves.

It is interesting to note that the rapid decay in the first 500 feet of the noise above 1.0 cps is fairly well predicted by the theories.

The coherence and phase data should be considered together as they are very closely related. We can see from Figures 15, 16 and 17 that the first coherence minimum is predicted by both noise models and is visible both on the coherence and phase plots. The second phase change predicted by the mixture including plane waves is in fairly good agreement with the observed phase data; however, the coherence data are much more complicated than the plane wave predictions at frequencies above the first minimum and the observed coherence levels are generally somewhat lower than the predictions. On the other hand, the predicted coherence for the model containing only trapped waves seems far two low to fit the data. One must recall, however, that the computations presented here can give erratic coherences well below 0.25 (i.e., -12 db).

At 1.0 cps we have computed two least square error fits to the data by the techniques described in our previous reports. In one case both Rayleigh and plane waves were used; in the other case only the Rayleigh modes were included. The results are shown in Table 1, along with the relative surface amplitudes for the case of energy equipartition of the trapped modes alone. As expected, the addition of plane waves improves the fit. The reduction in average error, σ, is not great however. These results are similar to the results obtained at Juno, where the significance of the reduction in σ was enhanced by the consistency of the results for numerous frequencies. The results for the fit including plane waves are plotted on Figure 17. The fit with Rayleigh waves only gave a very similar curve for power-ratio, however, the sign change in the observed coherence at 8000 feet could not be duplicated without the addition of plane waves.

These comparisons at Trotters demonstrate again the fact that both trapped and plane wave models give a reasonable fit to the deep well

TABLE 1

RELATIVE SURFACE VERTICAL AMPLITUDE FOR LEAST SQUARE ERROR

f = 1.0 cps

R_1	R_2	R_3	R_4	R_5	R_6	$P_{vert.}$	σ
1.0	2.8	0.4	0.4	1.2	1.0	–	*
1.0	1.9	0.3	0.3	1.0	1.7	–	0.24
1.0	1.5	0.2	0.2	0.8	1.7	1.1	0.15

*Energy equipartition distribution.

noise data; though the use of plane waves enhances the fit somewhat, the improvement is not such as to demonstrate unequivocally the presence of this type of noise at the Trotters site.

Horizontal propagation velocities - the surface array. A representative sample of the basic data from the surface array at Trotters is given in Figures 18, 19 and 20. These are the data from which inferences may be drawn concerning the propagation directions and velocities of the near surface noise.

Cross-correlation phases between all pairs of surface seismometers are shown in Figure 18 for two different noise samples. The data for the short distances ($\approx$ .8 km) and the long distances ($\approx$ 1.3 km) are separated. At numerous frequencies below about 1.5 cps a number of the noise observations at Trotters have phases which can be interpreted in terms of approximately unidirectional noises propagating from a generally NE direction with velocities ranging from about 3.0 km/sec to 6.0 km/sec and greater; velocities of the order of 4.0 to 6.0 km/sec are most common. Such observations were quite rare at our other sites. Both of the samples shown in Figure 18 are of this type. The very low phases consistent with a more isotropic noise distribution which are usually observed at low frequencies at Juno are occasionally observed at Trotters, but they are not predominant.

In Figure 19 we have plotted the very low frequency phase observations for two other noise samples in a different manner. For a number of frequencies the "apparent velocity" for each seismometer pair is plotted as a vector along the direction joining the seismometers. Apparent velocity is defined here as $2\pi f\Delta x/\phi$; where f is the frequency, Δx the seismometer separation and ϕ the cross-correlation phase. For a simple unidirectional noise the apparent velocity points should lie on a straight line perpendicular to the direction of propagation. The vector from the origin to the line is proportional to the horizontal propagation velocity. As can be seen the data of Figure 19 give results quite consistent with unidirectional noise from the SW. In the figure the vertical direction is north. For frequencies below 0.5 cps such observations are common at Trotters; for higher frequencies similar results are also often observed though the computed velocities are somewhat higher than those of Figure 19. For example, the data of Figure 18 show some intermediate frequencies around

0.7 cps where all phases are low suggesting interference of noises from various directions. Near 1.0 cps the phases give a picture very roughly consistent with unidirectional propagation from the NE with velocities of the order of 7.0 km/sec. Above about 1.5 cps the phase curves become very erratic suggesting the presence of numerous phases $\gtrsim \pi$; no well defined zones of phase reversal, such as might be expected for very uniform isotropic noise, are observed, however.

The surface array phase data at Trotters have not provided a clear picture of the nature of the horizontal propagation velocities of the near surface noise. There seems to be fair evidence at frequencies below 0.5 cps for measurable unidirectional velocities above the theoretical velocities computed for Rayleigh waves. At higher frequencies much less reliable measurements occasionally suggest even higher velocities. Phases consistent with a picture of a very uniform isotropic noise are not often observed.

In Figure 18 we have also shown the coherence for all the seismometer pairs in the surface array. In addition, Figure 20 shows similar results for four additional noise samples. The coherence plots of Figure 20 are separated according to seismometer pair and are shown in order of increasing Δx. Figure 20 also shows theoretical computations for three noise models.

Although the surface array coherence data at Trotters have not been interpreted to any significant degree certain features of the experimental curves can be noted. In general the curves show a gradual decrease with frequency similar to those previously observed; the results for any given seismometer pair are fairly stationary in time; the curves do not show any marked variation with direction but do seem to depend somewhat on Δx; the coherences for the larger distances decrease with frequency somewhat more rapidly than those for the shorter distances; the larger distances show a fairly well defined minimum in the coherence at about 0.5 cps. Most of these features are consistent with an isotropic distribution of propagation directions, however the phase curves do not seem to support this conclusion. Moreover, an isotropic distribution of Rayleigh waves with an equipartition distribution of energy among the modes gives a predicted coherences well below those observed at all distances. It is interesting to note, however, that the observed coherence minimum near 0.5 cps is near

the frequency of a predicted minimum for the equipartition mixture. Isotropic noises with velocities somewhat higher than those expected for the Rayleigh waves would give coherence values more nearly in agreement with the observations. Curves for constant velocities of 3.6 km/sec and 8.0 km/sec are shown for reference. Of course, high coherence values can also be obtained with a strong unidirectional noise and it may be possible to explain both the phase and coherence data with a mixture of fairly isotropic Rayleigh waves and a more unidirectional component of somewhat higher velocity.

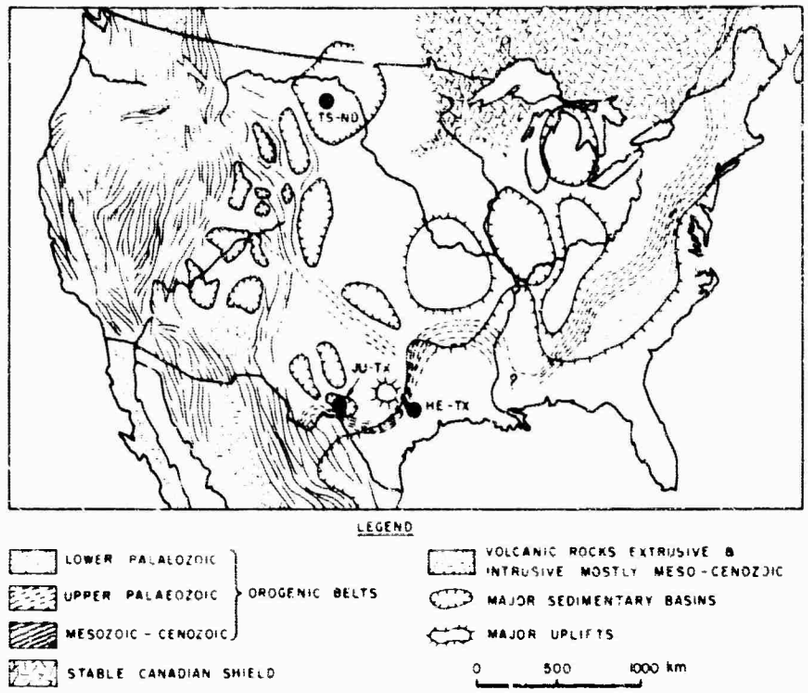

Fig. 1 - Location and geological environment of the three deep wells surveyed.

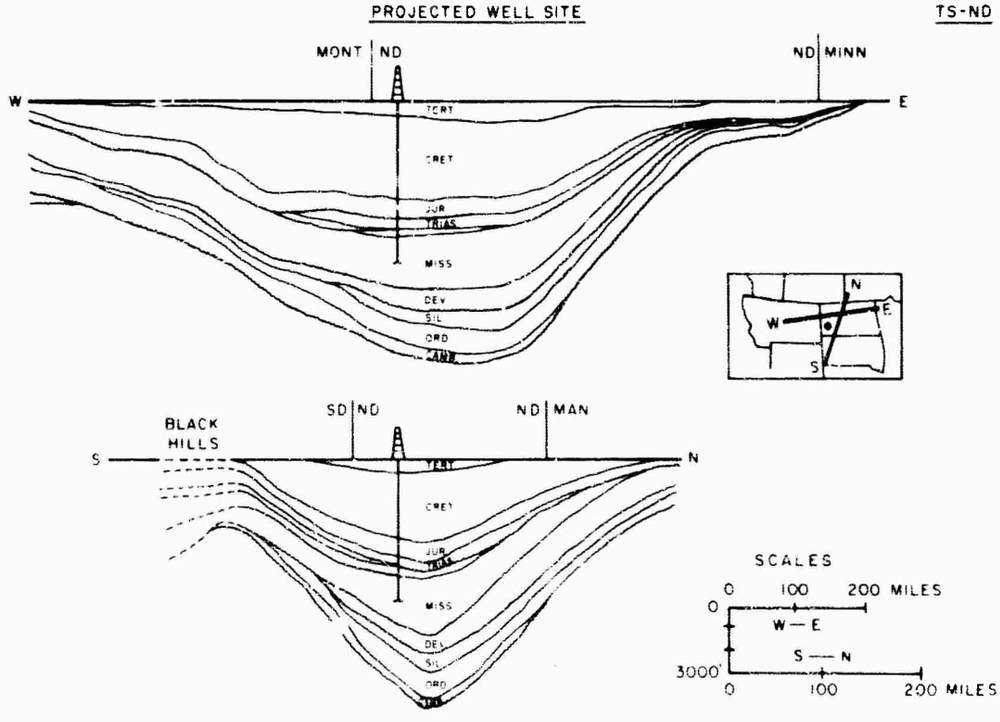

Fig. 2 - Geological cross-sections of the Williston Basin showing the Trotters well.

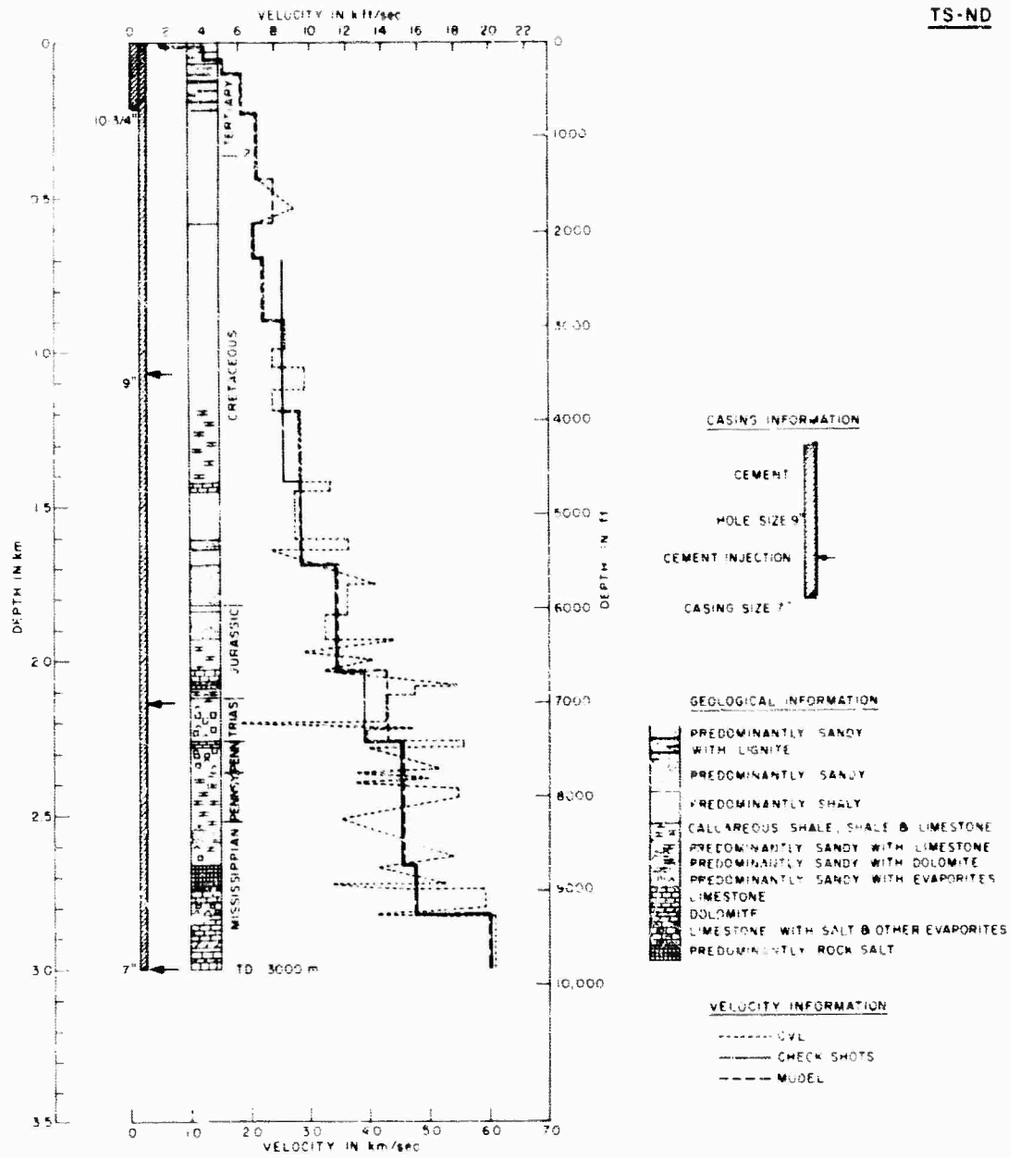

Fig. 3 - Casing, geological and velocity logs for the Trotters well. The P-wave velocity model used for theoretical computations is also shown.

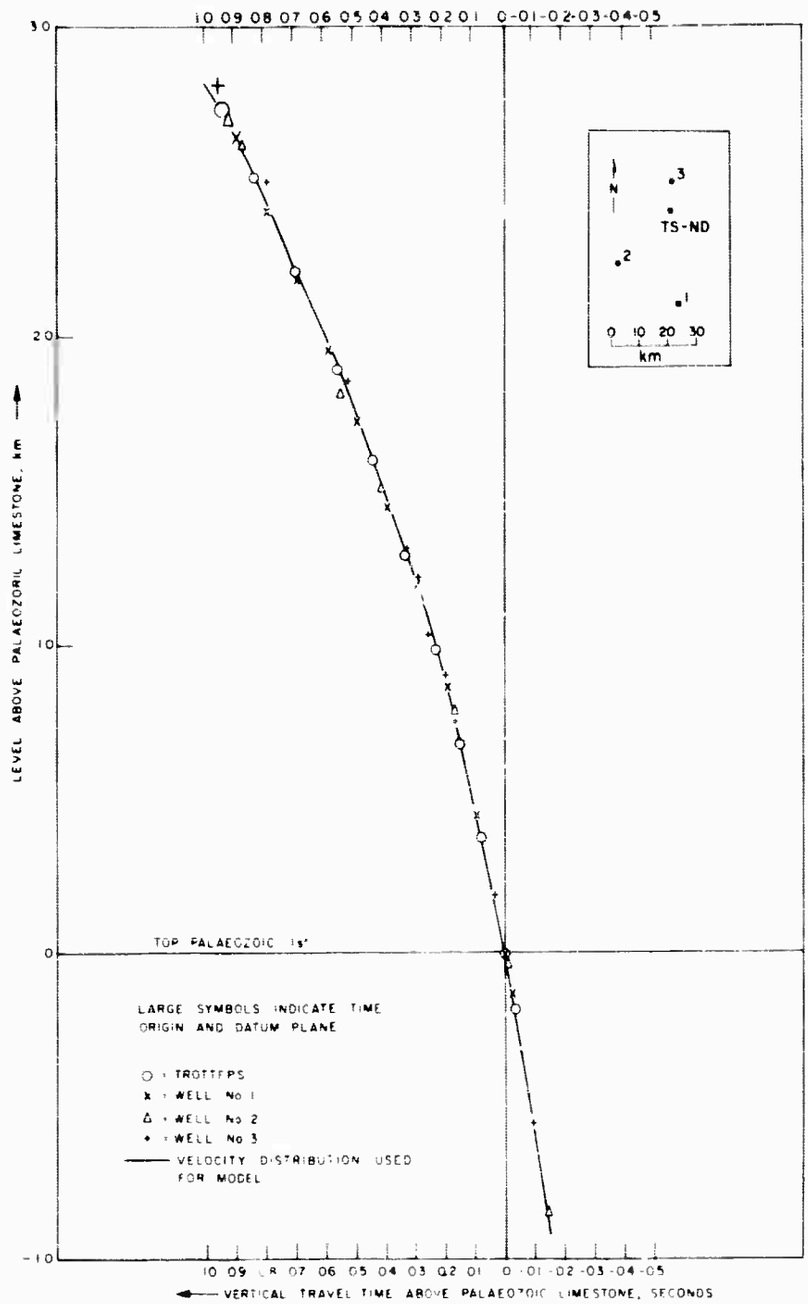

Fig. 4 - Vertical travel times for P-waves in the vicinity of the Trotters well. Data for three additional wells are shown.

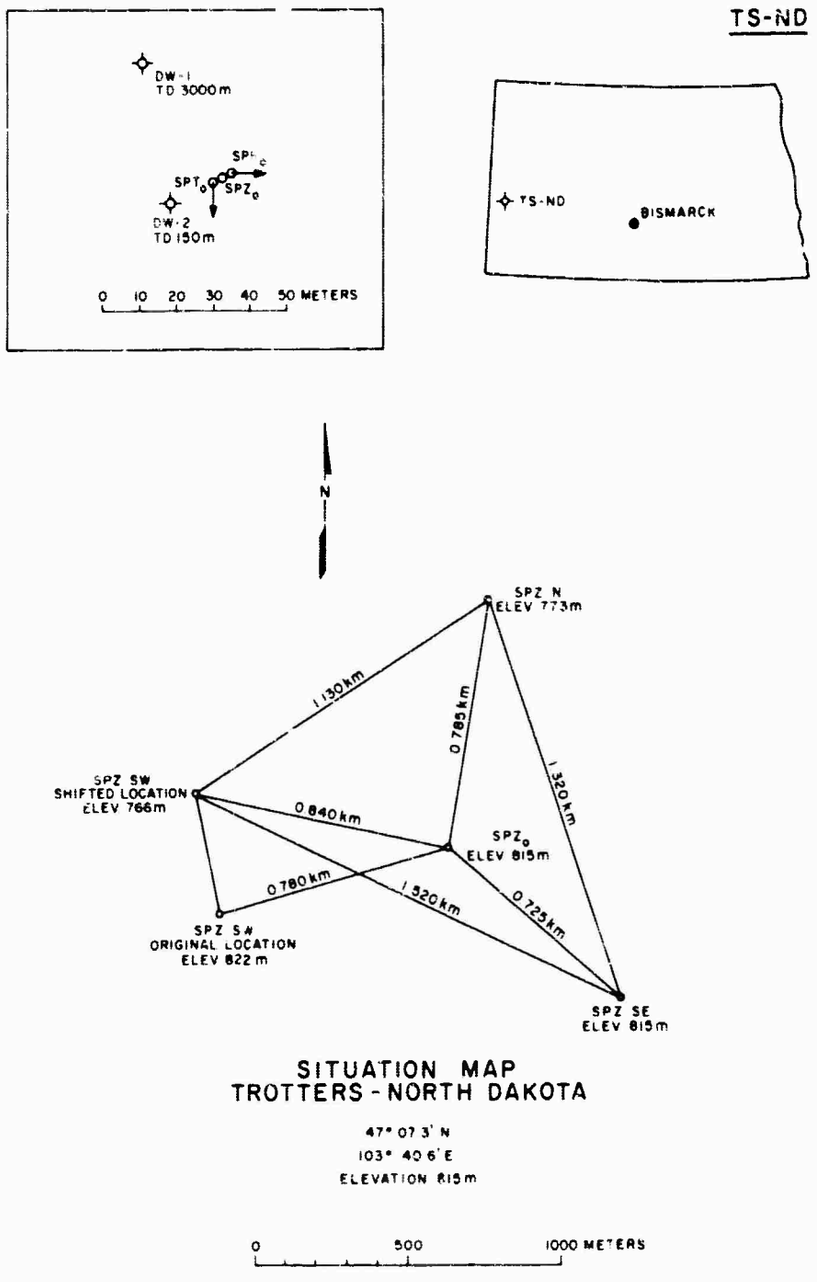

Fig. 5 - Site plan, showing seismometer locations, for TS-ND.

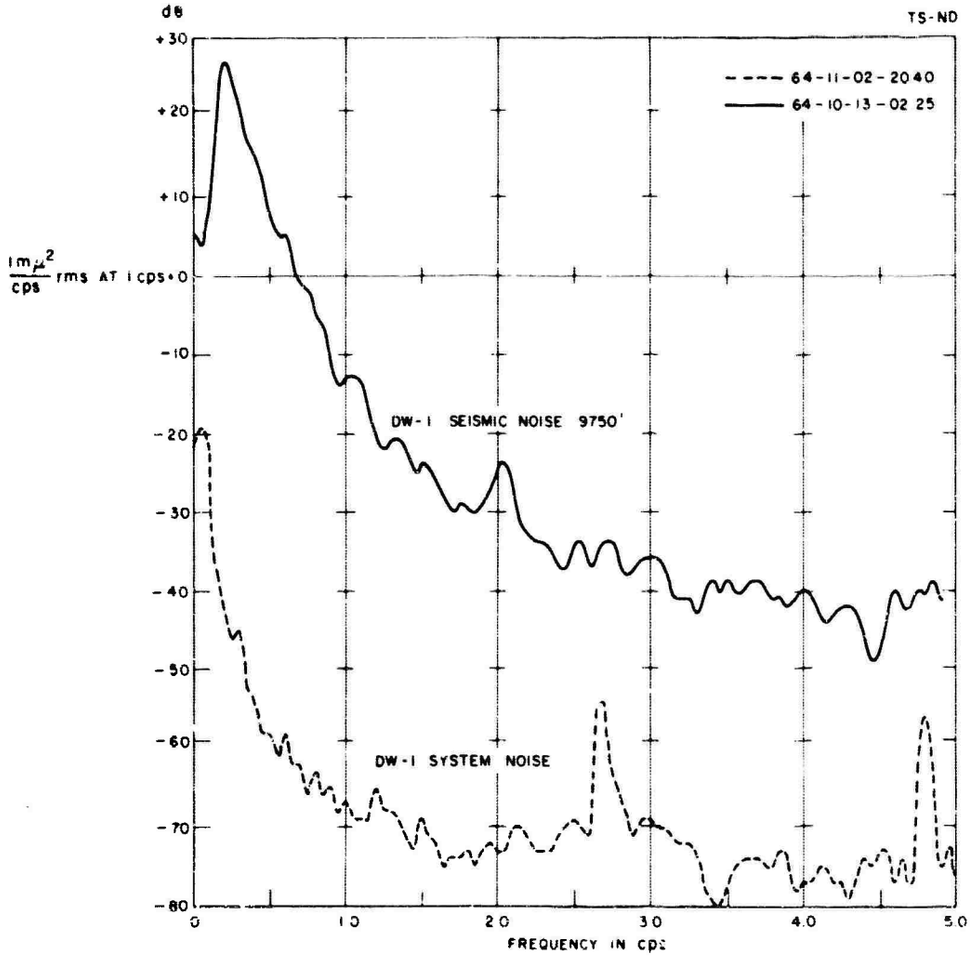

Fig. 6 - System noise for the deep well seismometer channel including office playback equipment. The upper curve shows the power spectrum of the seismic noise recorded at 9750 feet. The lower curve shows the power spectrum of the signal recorded on the same channel with a dummy load in place of the seismometer.

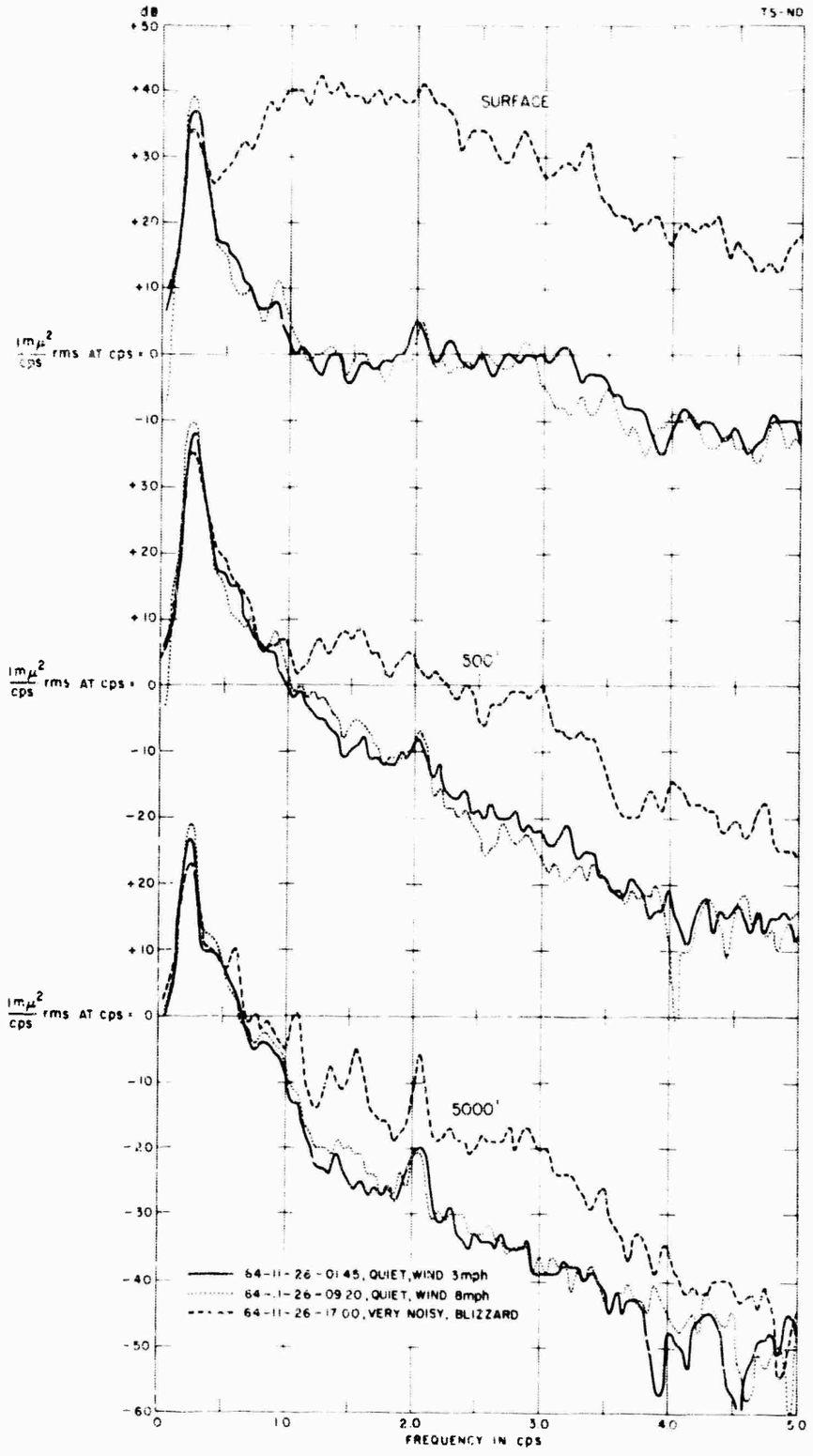

Fig. 7 - Power spectra for simultaneous observations at the surface, 500 feet and 5000 feet. Two examples of "typical quiet" noise are shown. A sample taken during the extremely windy conditions of a blizzard is also shown.

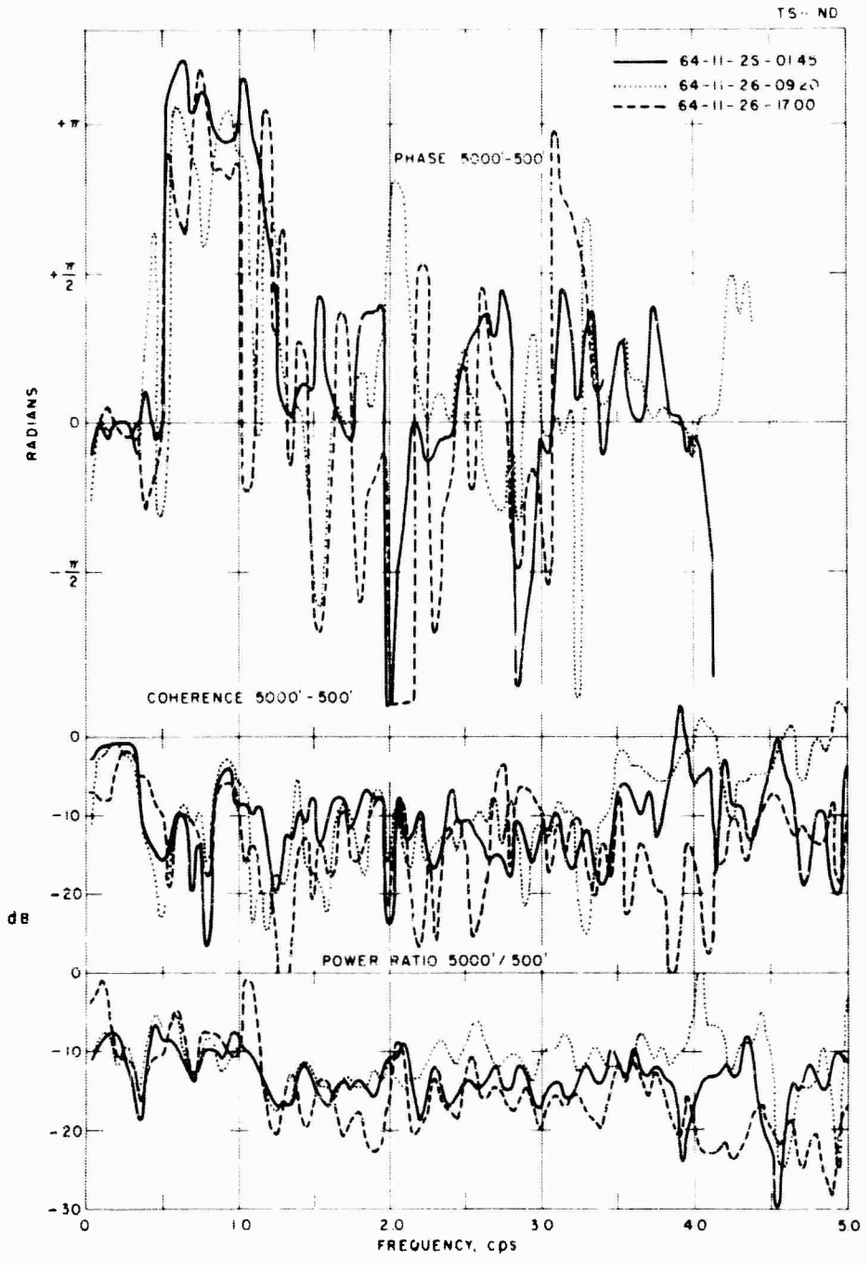

Fig. 8 - Cross-correlation phase, coherence and power ratio for the 5000-foot and 500-foot signals shown in Figure 7. Note stationarity of the data.

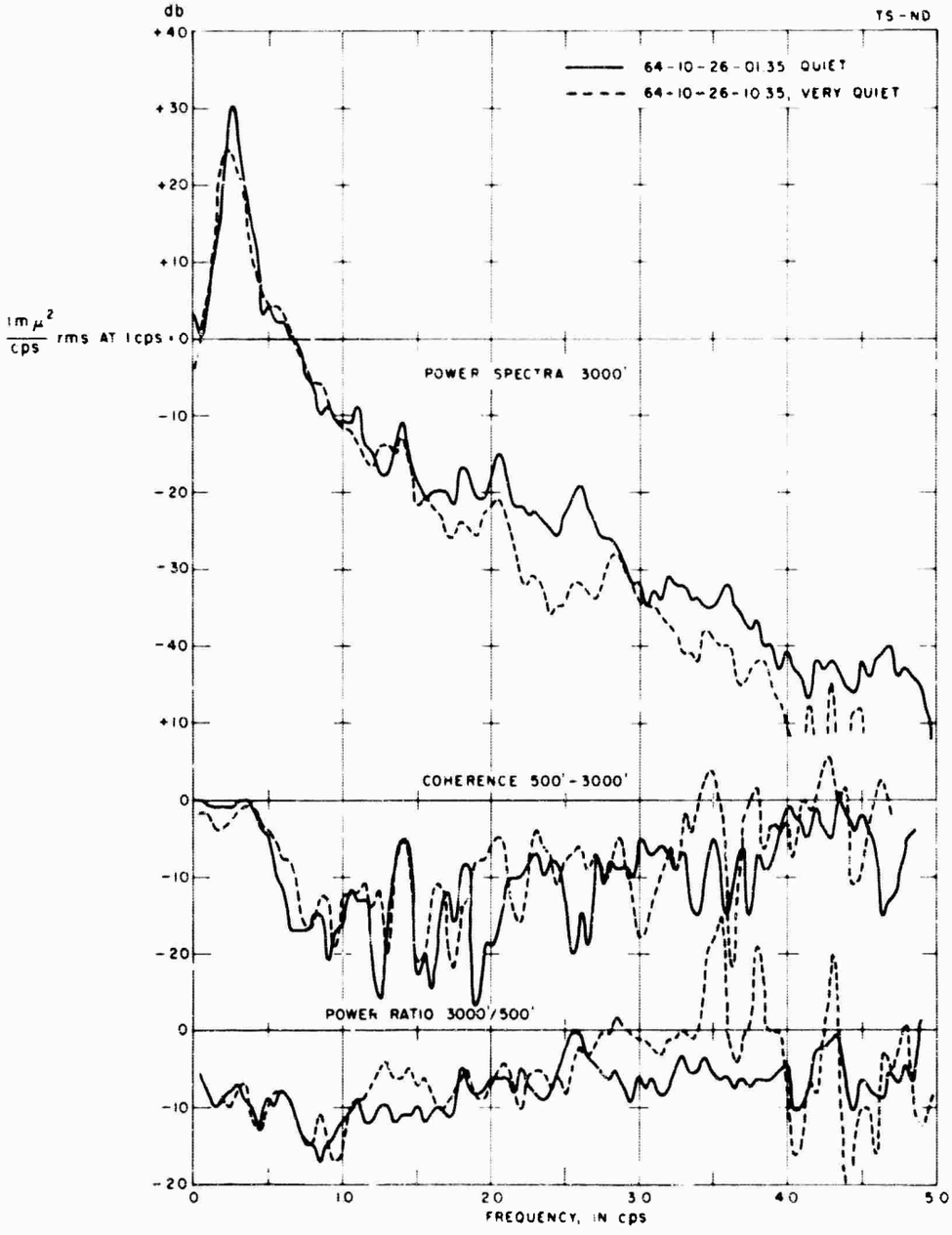

Fig. 9 - Power spectra for 3000-foot observations. Note stationarity of the data.

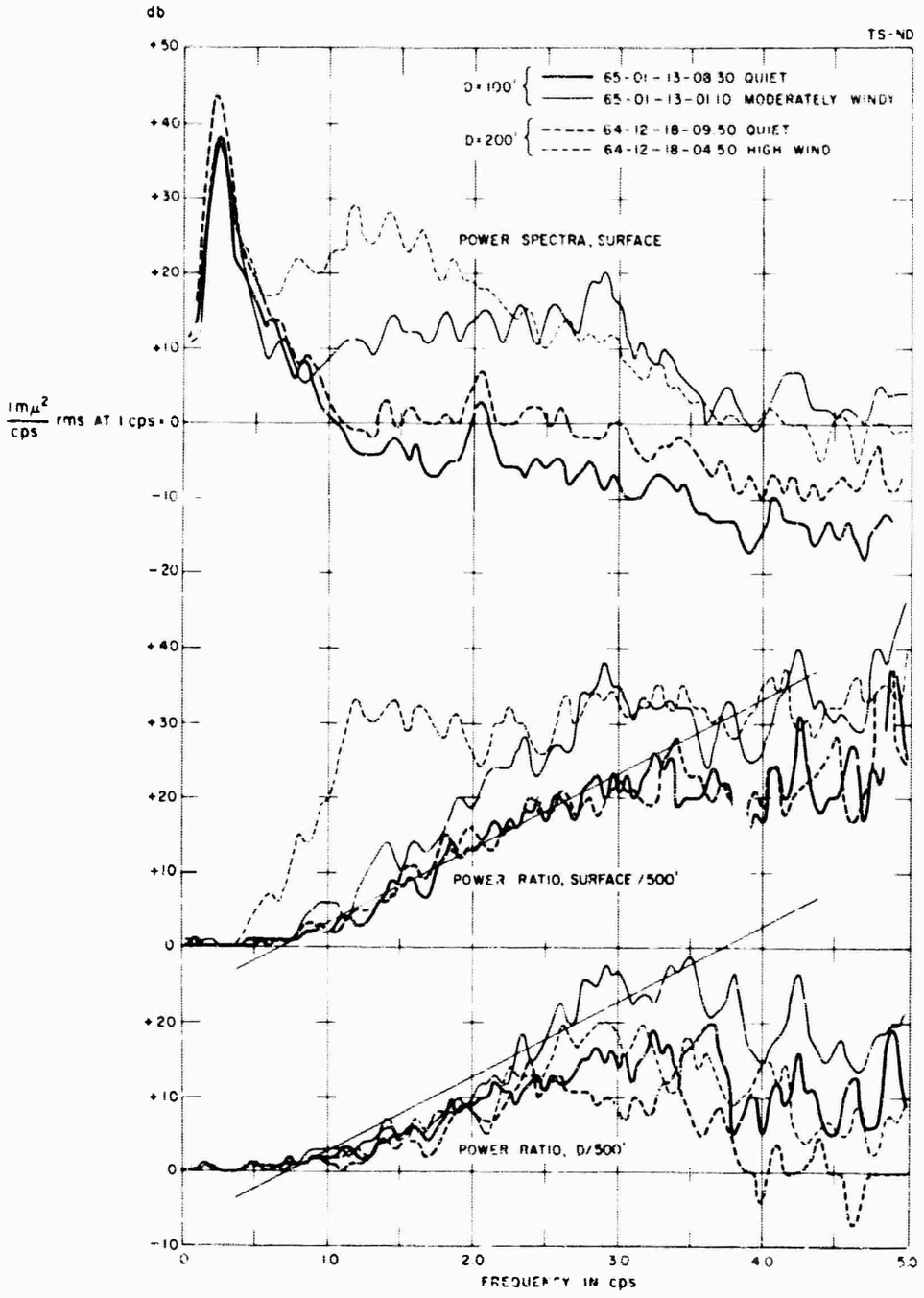

Fig. 10 - Near surface noise during quiet and windy conditions. The upper curves are surface power spectra; the middle curves are power ratios of the surface noise with respect to 500 feet; the lower curves are the power ratios deep well/500 feet. The straight lines with the middle and lower curves give an approximation to the ratio surface/500 feet for typical quiet noise.

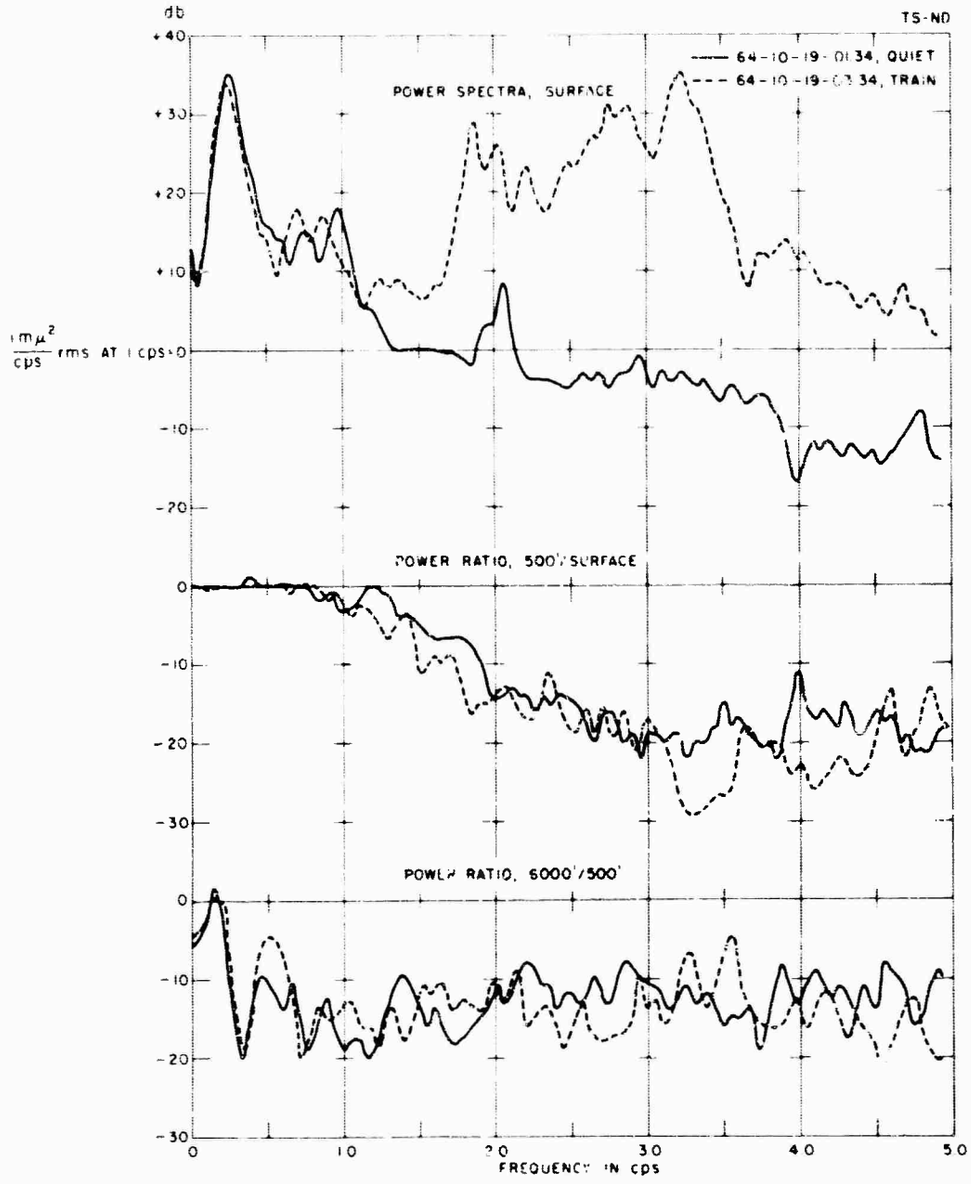

Fig. 11 - Train noise. Power spectra and ratios for simultaneous surface, 500-foot and 6000-foot observations are shown for a typical quiet period and for a period during which a train is passing.

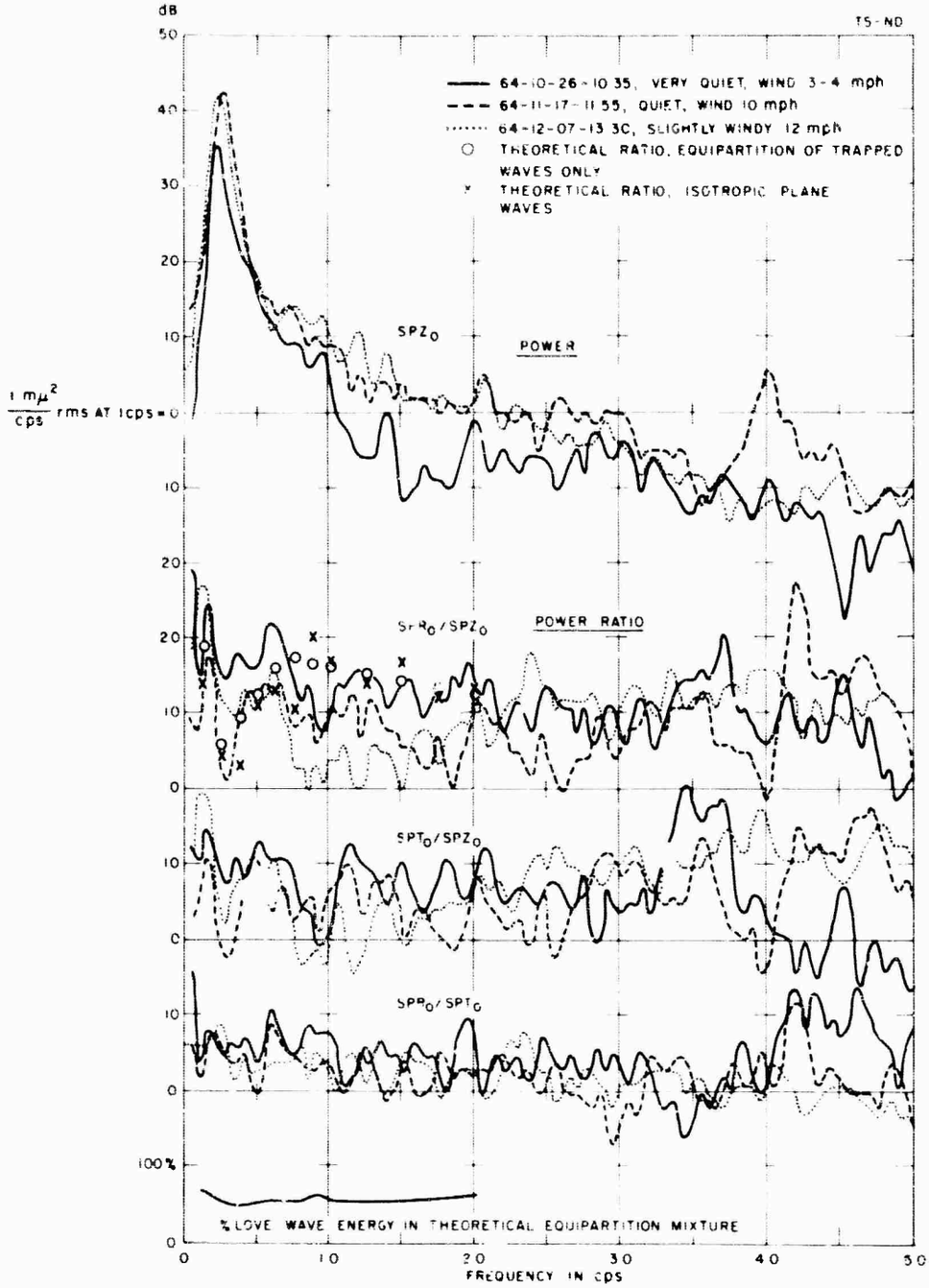

Fig. 12 - Horizontal components of surface noise. The points shown on the SPRo/SPZo curves are from theoretical computations of mixtures of trapped modes or of body waves. The theoretical points, computed for an isotropic azimuthal distribution, have been adjusted for the case in which approximately two thirds of the horizontal energy appears in the radial component.

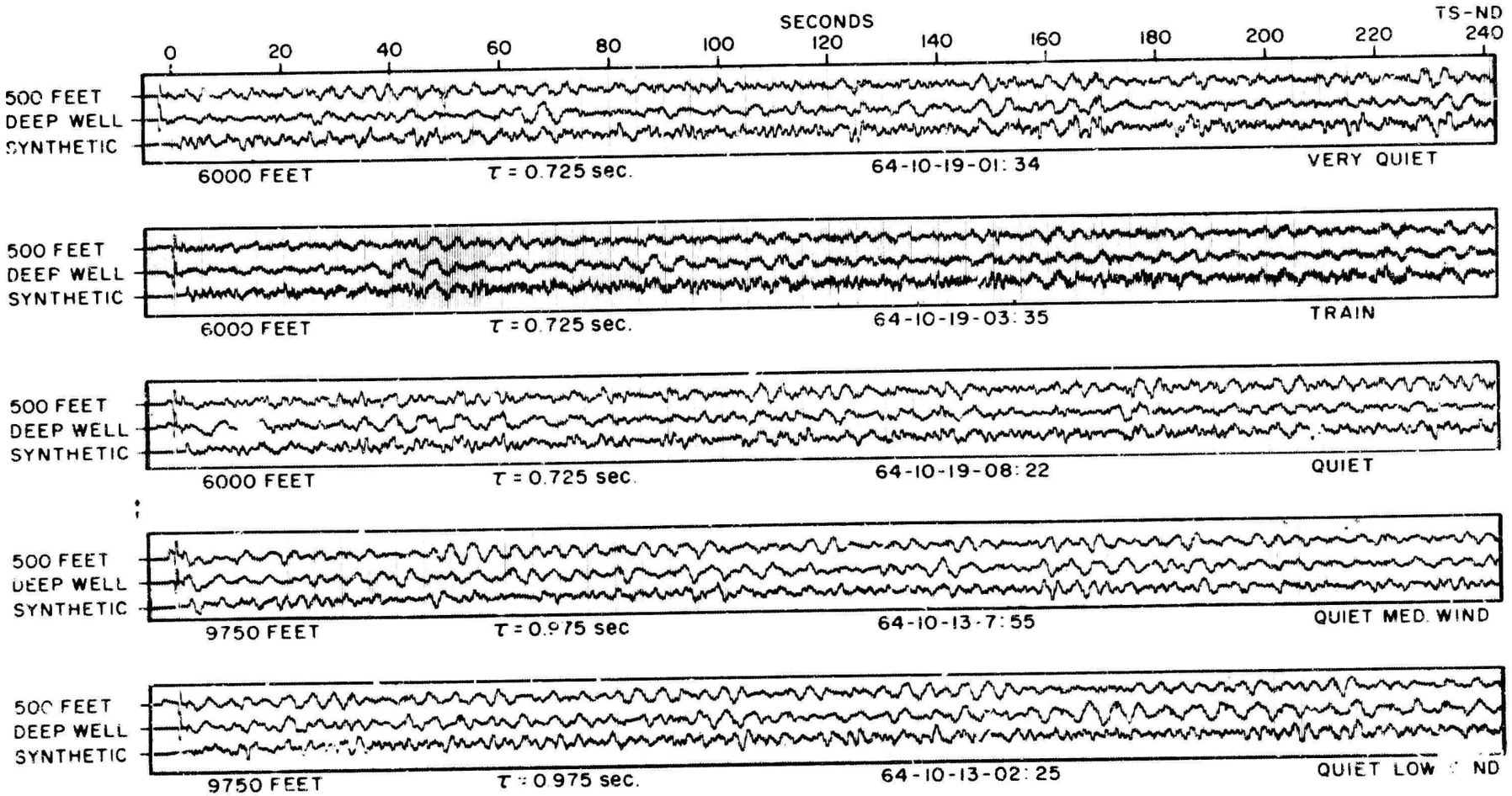

Fig. 13 - Synthetic deep well traces. Five samples from two depths of observations are shown. At each depth simultaneous 500-foot and deep well recordings are shown along with the synthetic trace constructed from the 500-foot recording. τ is the one-way travel time for P-waves.

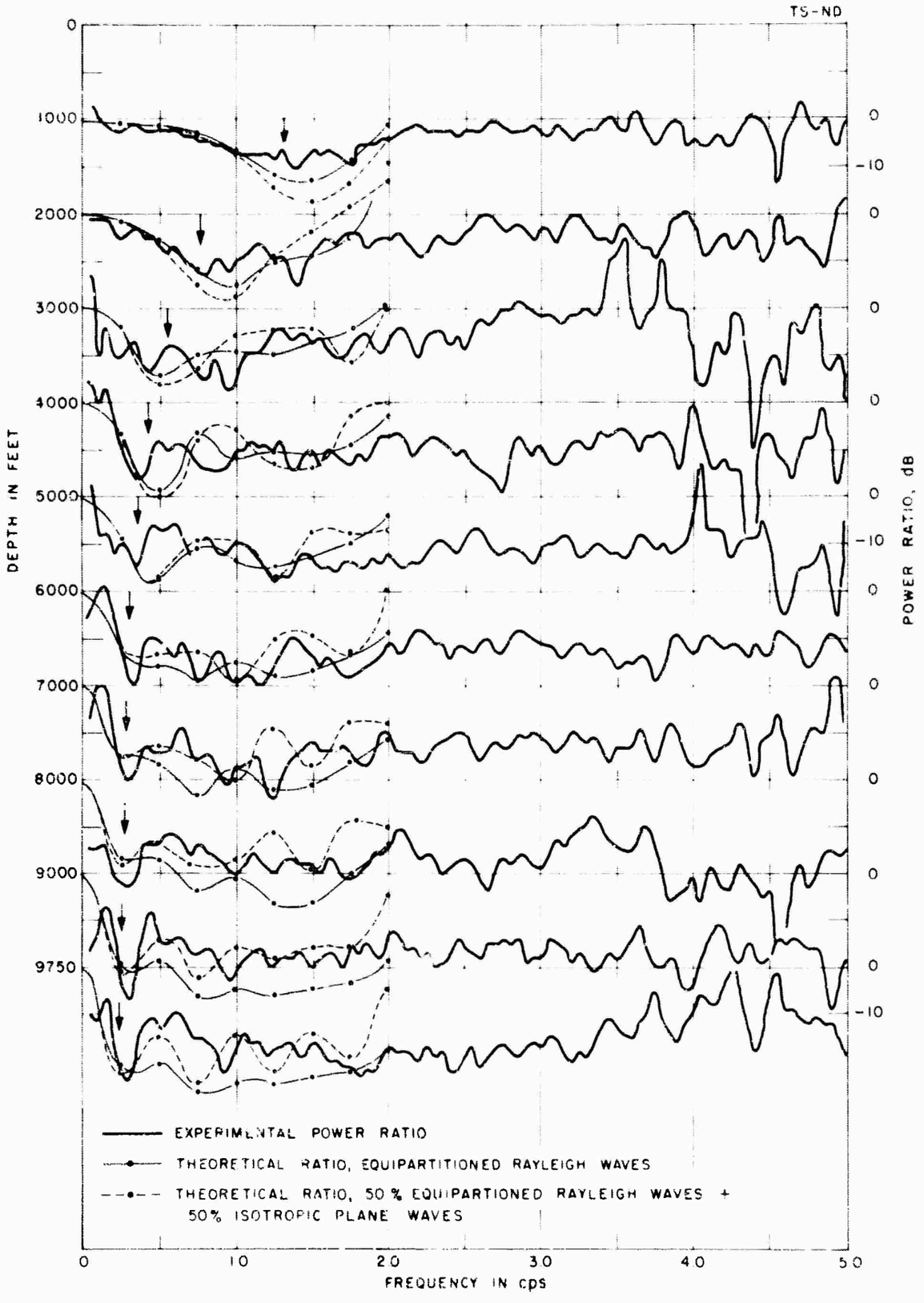

Fig. 14 - Power ratio, deep well/500-fcot, versus frequency for various depths at Trotters. The experimental observations are for typical quiet noise. Points for two theoretical noise models are shown connected by estimated smooth lines. The arrows are at the frequencies of expected first minima for vertical P-waves.

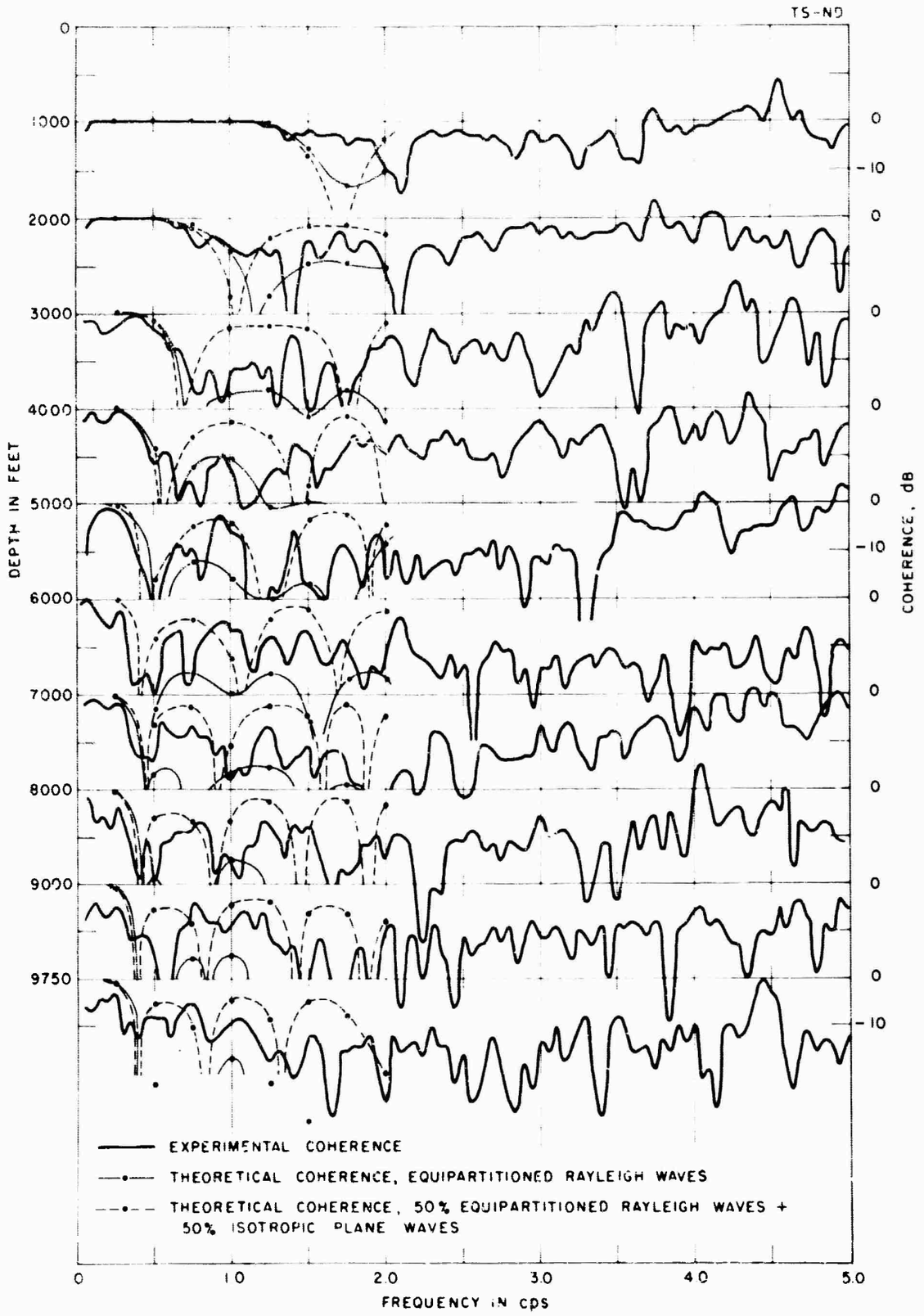

Fig. 15 - Coherence of deep well and 500-foot noise versus frequency for various depths at Trotters. Noise samples and theoretical curves same as Figure 14.

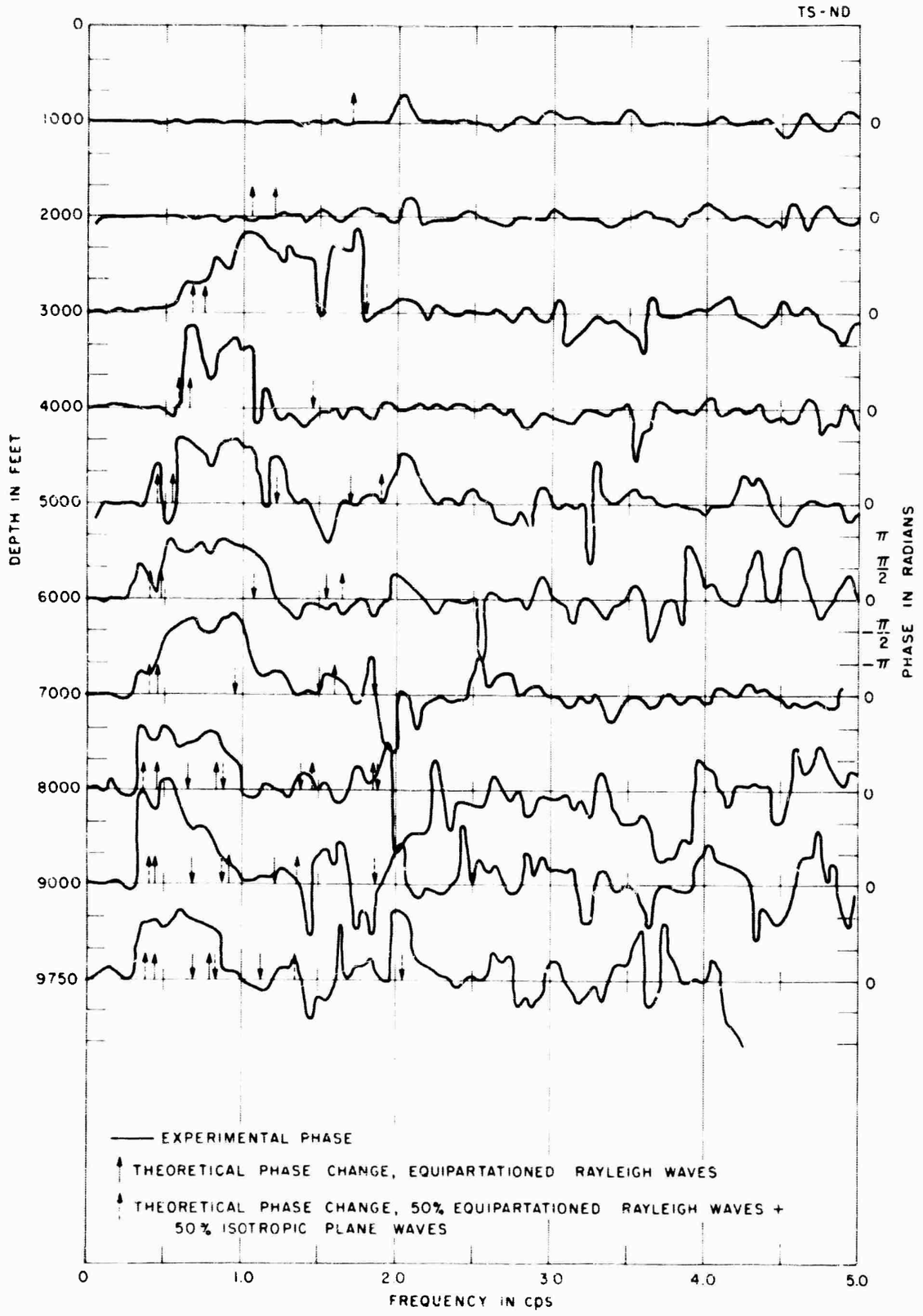

Fig. 16 - Cross-correlation phase for deep well and 500-foot noise versus frequency for various depths at Trotters. Noise samples are same as Figure 14. Theoretical phases are 0 and π; the transition frequencies are shown by arrows.

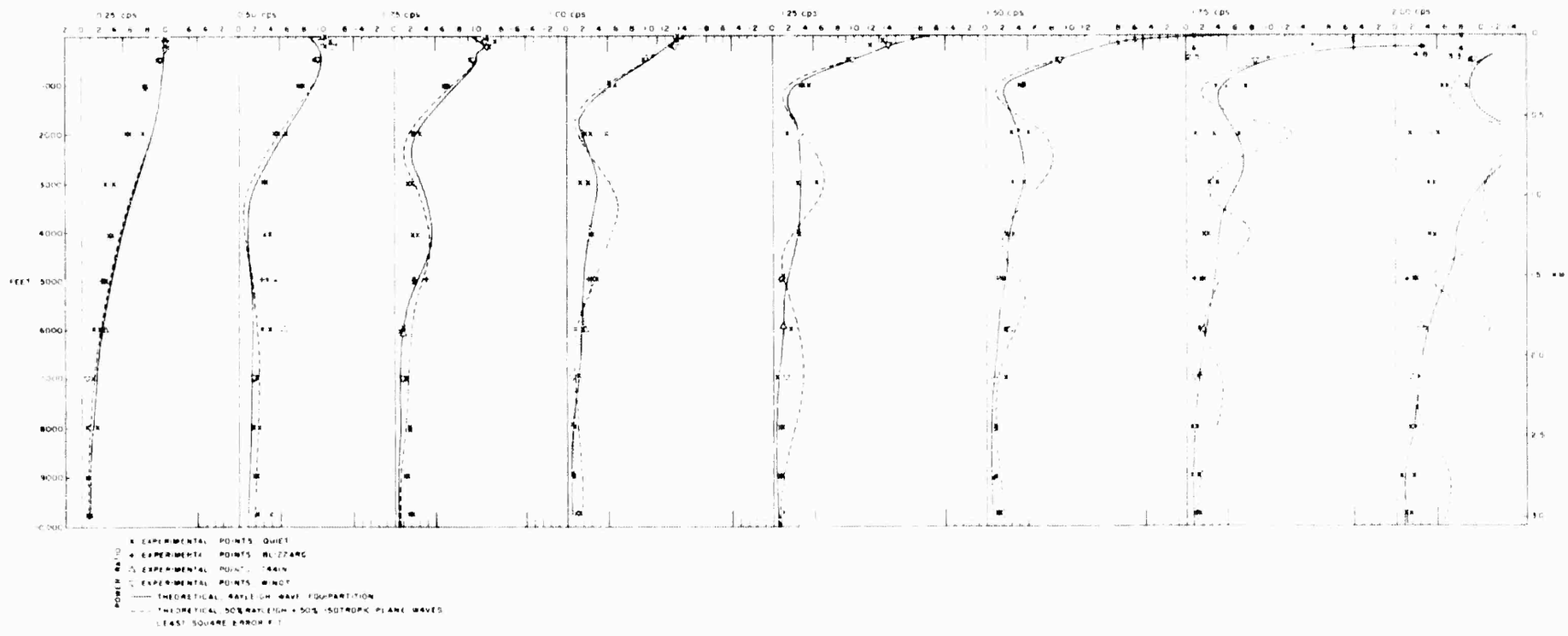

Fig. 17a - Power rati deep well/500-foot versus depth at various frequencies at Trotters. Points for various noise conditi ns and theoretical curves for two noise models are shown. At 1.0 cps a least square error fit of Rayleigh waves and vertical P-waves is shown.

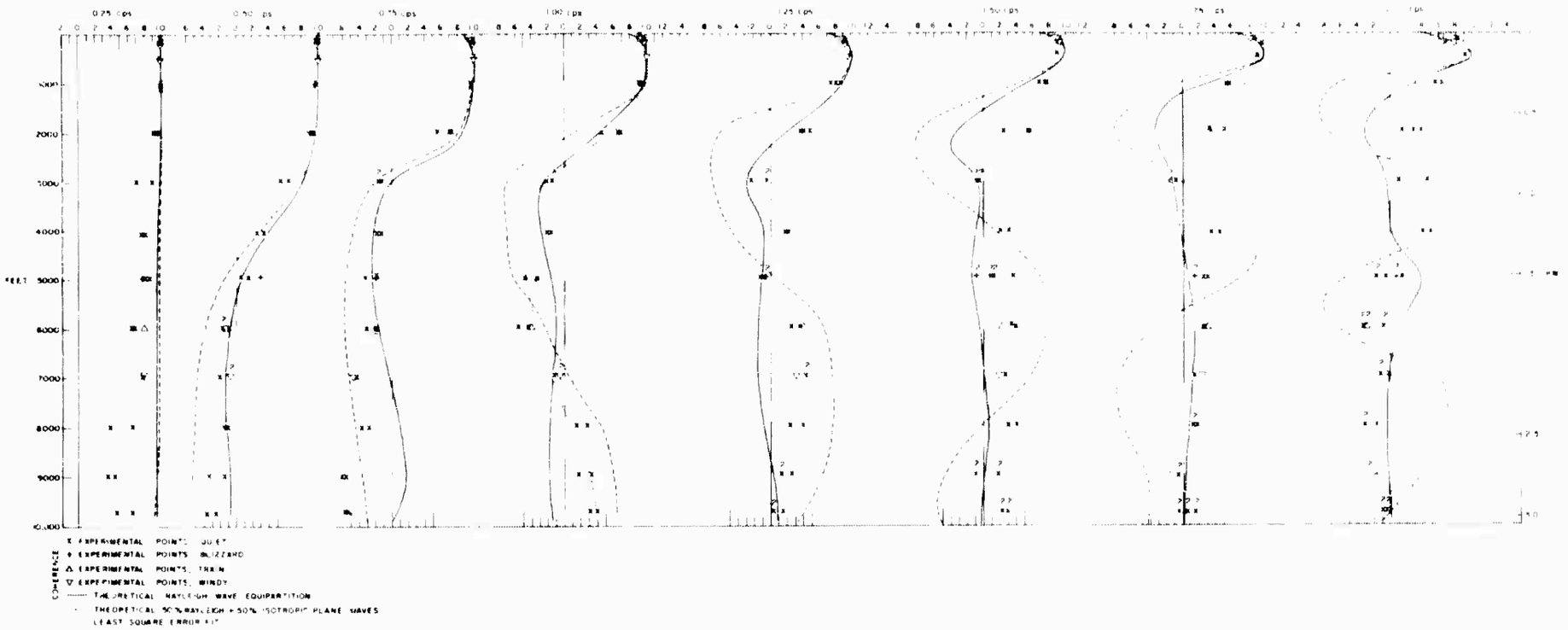

Fig. 17b - Coherence between deep well and 500-foot noise versus depth for several frequencies at Trotters. Data and theories same as Figure 17a. At 1.0 cps a least square error fit of Rayleigh waves and vertical P-waves is shown.

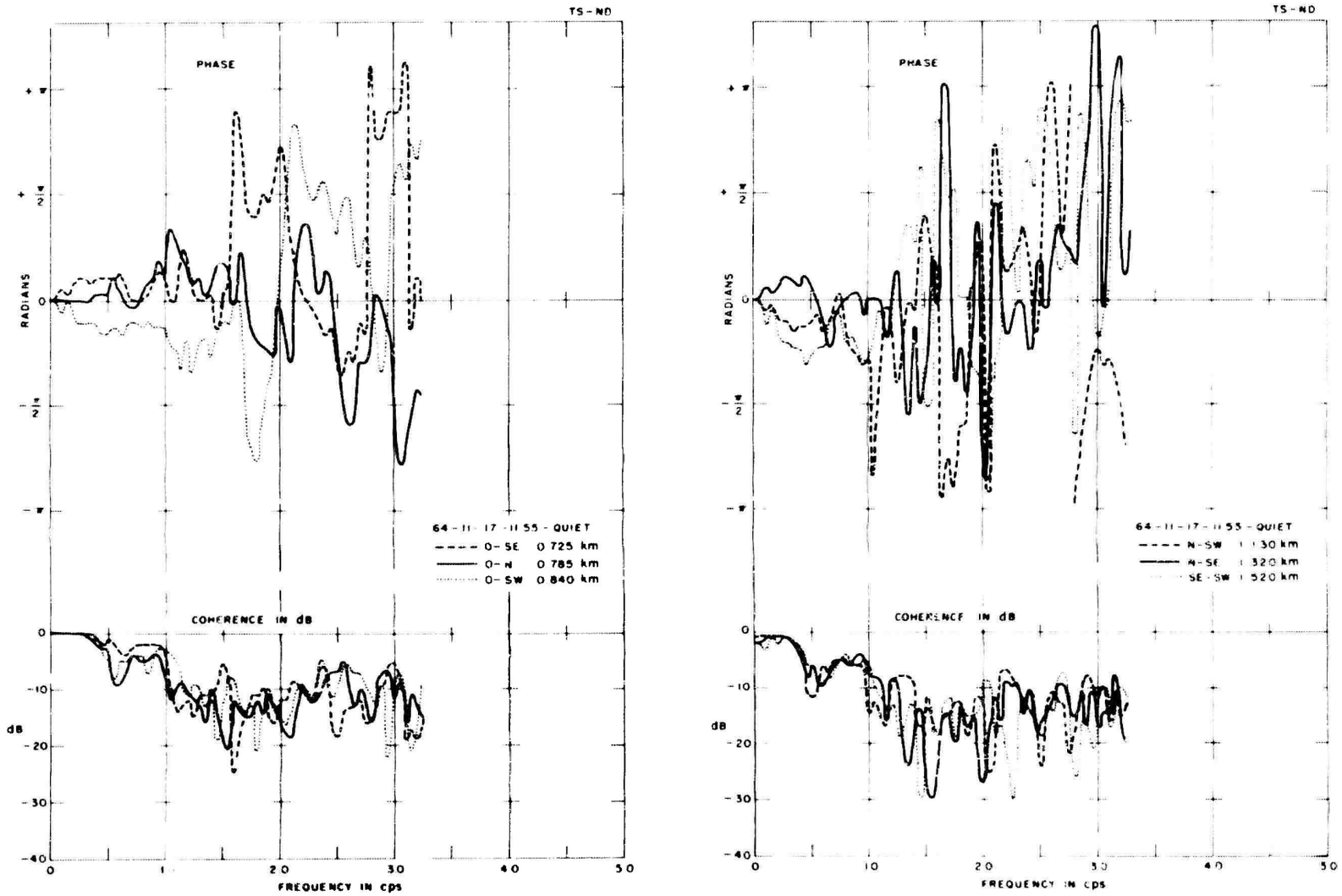

Fig. 18 - Coherence and cross-correlation phase versus frequency for noise from pairs of seismometers in the surface array. Results for two different noise samples are shown. The results for the short and long distances are shown separately. Continued on next figure.

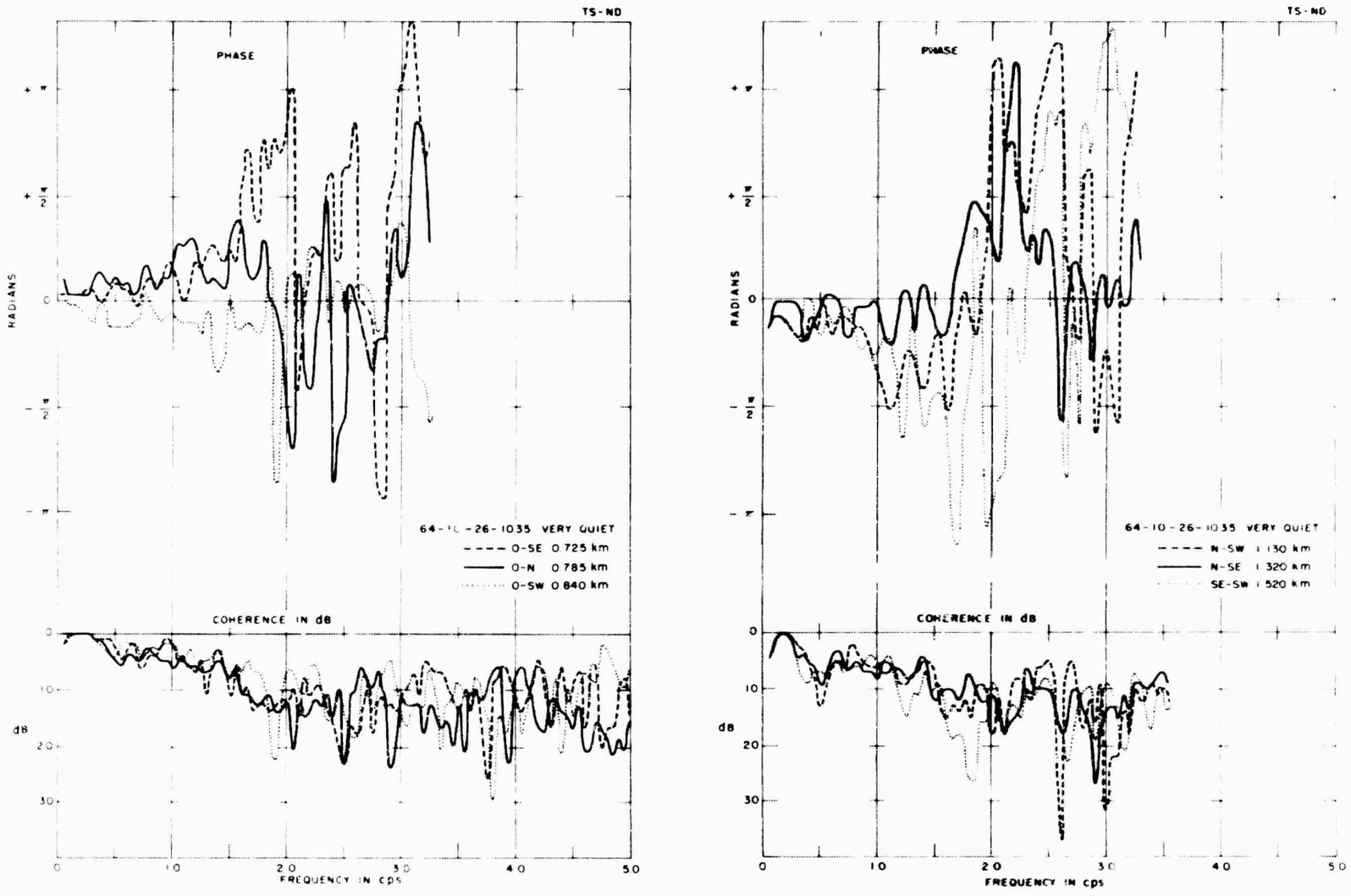

Fig. 18 - Continued.

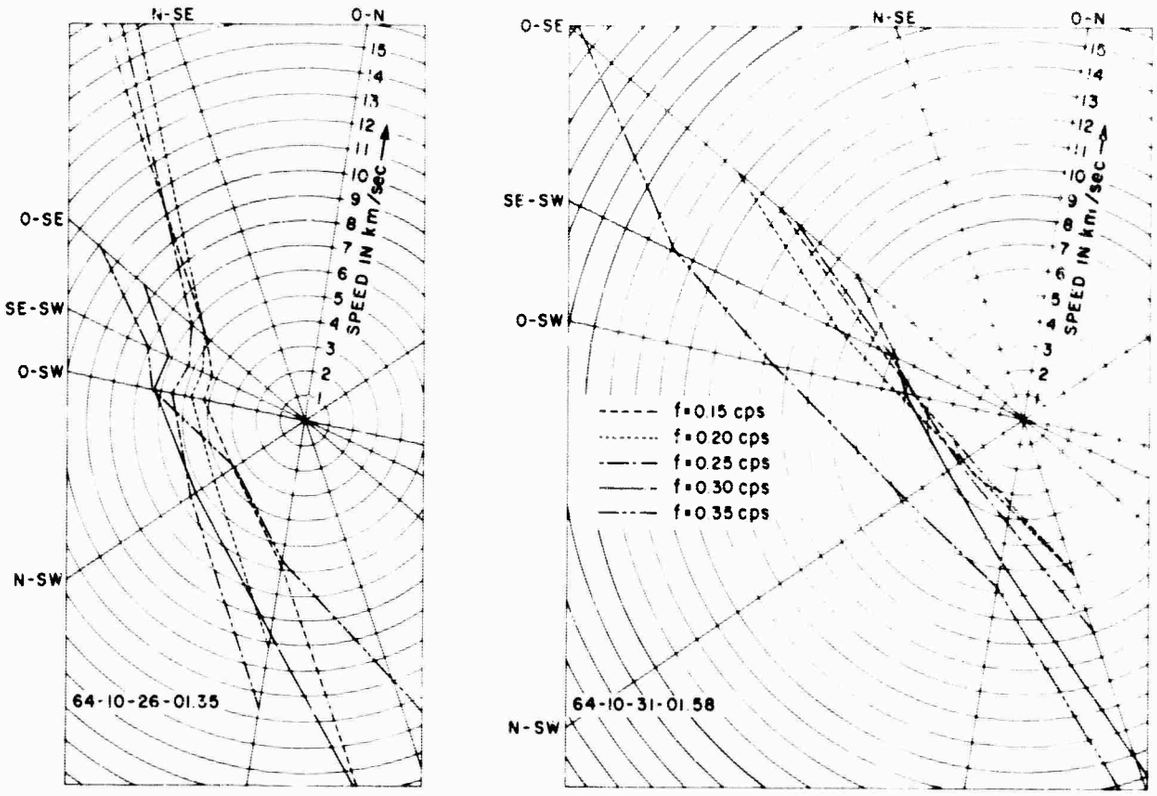

Fig. 19 - Horizontal propagation velocity computations for unidirectional noise. Vertical is north. Data from cross-correlation phase spectra are used. Results are shown for two noise samples. For each sample computations at several frequencies are given. Vector from origin to wave front gives direction of propagation.

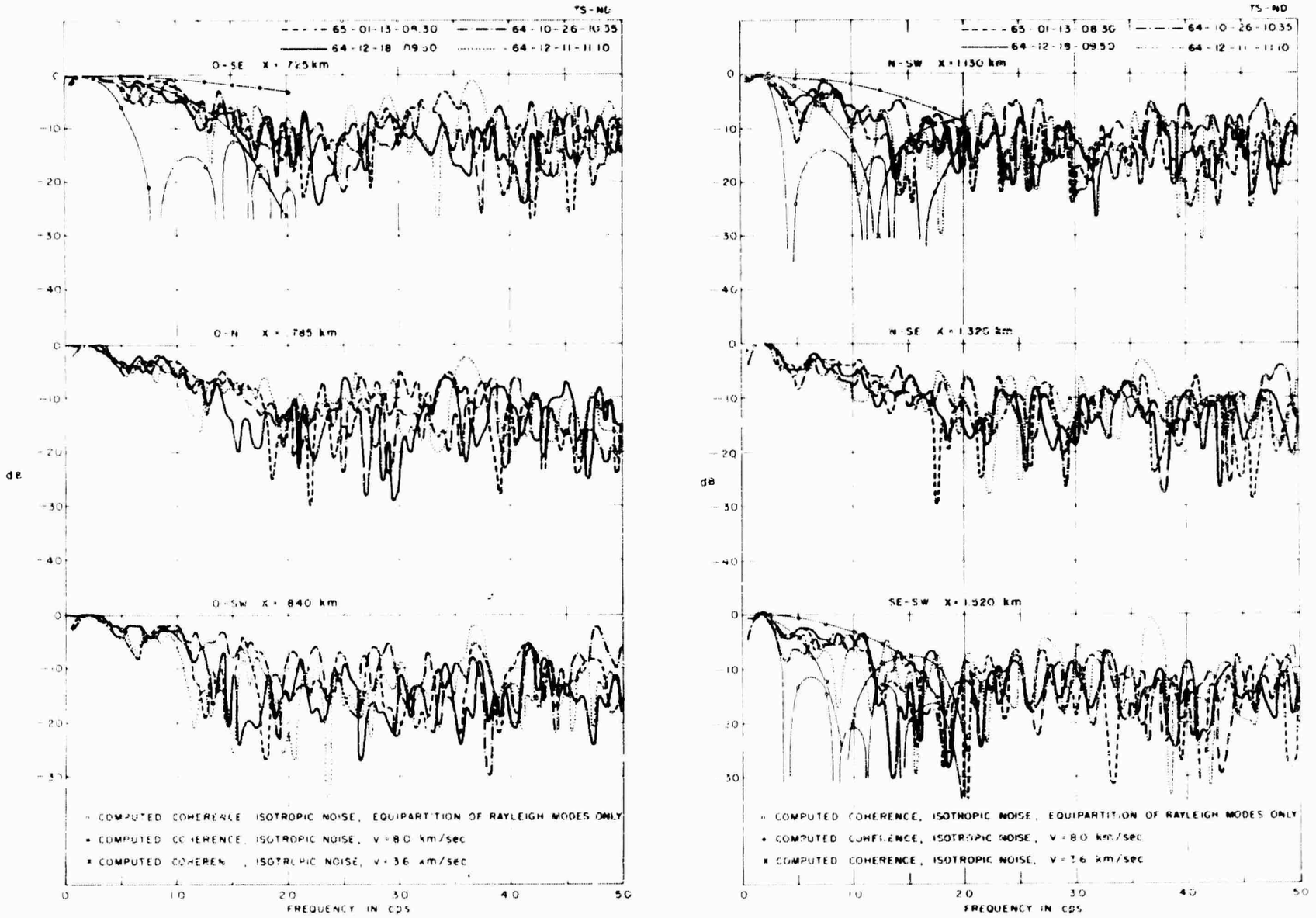

Fig. 20 - Coherence versus frequency for noise from pairs of seismometers in the surface array. Results for four different noise samples are shown. Theoretical coherence is shown for three noise models.

THEORETICAL STUDIES

During the final five months of this project, since the writing of the third semi-annual technical report,[3] our analysis has been concerned mainly with a plane-layered elastic model of the Trotters well site in North Dakota. The response of the model to trapped surface waves as well as to plane P, SV, and SH waves incident from below was investigated by means of the numerical techniques and computer programs described in the first,[1] second,[2], and third[3] semi-annual technical reports. In addition, a new computer program was written for use in the calculation of statistical response parameters for a plane-layered elastic half-space subject to plane P, SV, and SH waves incident from below equally at all angles of incidence.

More specifically, these calculations are based on the assumption that in the homogeneous half-space below the layers, plane P, SV, and SH waves are incident on the layers from below and that these waves all have equal energy flux in the direction of propagation, independent of the wave type and of the angle of incidence. At a given frequency, we consider the phase of each incident plane wave to be statistically independent of the phase of every other wave. We assume that the final response is to an input for which waves for all angles of incidence are given equal weight. The program then permits us to calculate at a given frequency the ratio of total horizontal component to vertical component power level at the free surface, the vertical component power level as a function of depth, and the vertical velocity component coherence as a function of depth with respect to a detector at the surface and at a given reference depth.

TABLE 2

MODEL 1 OF THE TROTTERS WELL SITE

Layer Thickness (km)	Compressional Wave Velocity (km/s)	Shear Wave Velocity (km/s)	Density (g/cc)
0.006	0.50	0.13	2.0
0.032	1.22	0.31	2.1
0.062	1.55	0.52	2.1
0.130	1.84	0.92	2.1
0.210	2.12	1.25	2.2
0.140	2.40	1.41	2.2
0.120	2.05	1.03	2.2
0.200	2.22	1.11	2.3
0.290	2.55	1.28	2.3
0.500	2.82	1.41	2.4
0.340	3.47	1.93	2.4
0.230	4.25	2.50	2.5
0.400	4.52	2.51	2.5
0.080	4.75	2.50	2.2
0.080	4.75	2.50	2.5
0.180	6.00	3.16	2.6
1.300	6.00	3.16	2.7
∞	6.90	3.63	2.8

Model 1 of the Trotters well site is described in Table 2. Figures 21a-c show plots of horizontal phase and group velocities as functions of frequency for the 11 Rayleigh modes that are present in the interval 0.125 - 2.00 cps. Figure 22 shows the ratio of the horizontal to the vertical velocity component at the surface as a function of frequency for each of these Rayleigh modes. Figures 23 a and b present horizontal phase and group velocities as functions of frequency for the 9 Love modes present in the interval 0.125 - 2.00 cps. Figures 24 a and b are plots of the vertical velocity component as a function of depth for Rayleigh wave motion at 0.5 and at 1.0 cps. The amplitudes plotted in Figure 24 correspond to an assumption of equal energy density for the motion in each trapped mode at a given grequency.

The response of Model 1 of the Trotters well site to trapped surface waves, as illustrated in Figures 21-24, can be compared with similar response curves for various models of the Juno and of the Hempstead well sites, which were presented in the two preceding semi-annual technical reports.[2,3] Loosely speaking, we may say that the computed response at the Trotters well site is considerably more complicated than the response for the Juno models but somewhat less complicated than the response for the Hempstead models. This is understandable when we consider that on the average the shear wave velocity as a function of depth for the Trotters well site is greater than that for the Hempstead well site but less than that for the Juno well site.* Our Trotters model has no low-velocity channel at great depth, as did the Hempstead model, but it does exhibit a velocity reversal at relatively shallow depth, not unlike that for the Juno model. Much of the unusual behavior of the surface waves for the Trotters model can probably be ascribed to the presence of this 350-meter-thick higher-velocity interval, which starts at a depth of 230 meters. Particularly noteworthy in this connection is the behavior of the first and second Rayleigh modes. We note, for example, that in Figure 24b the vertical velocity component at the surface for mode 1 is shown to be about one-third

---

*Shear wave velocities at the Hempstead and Trotters well sites are comparable to a depth of around 1.5 km. The high velocity half-space starts at much greater depth at Hempstead.

that for mode 2. Figure 22 shows that at 1 cps the ratio of horizontal to vertical velocity component at the surface is about two and one half times greater for mode 1 than for mode 2. Indeed, from about 1.40 to 1.75 cps, the ratio of horizontal to vertical velocity component at the surface for mode 1 is very large, indicating that there is very little vertical motion at the surface due to this mode. Although we have not shown it in any of the figures, at 1.5 cps the vertical velocity components for mode 1 as well as for mode 2 are in phase at all depths; the horizontal component has one zero crossing with depth for mode 1 but has none for mode 2. The frequency interval for which the vertical component of the second Rayleigh mode has no zero crossing corresponds precisely to the interval for which the horizontal group velocity of mode 2 is less than that of mode 1 (see Figure 21a). The fact that the Rayleigh modes often cannot be put in the right order when we count the number of zero crossings of the vertical (or of the horizontal) component with depth has been discussed in previous reports[2,3] and is again evident from Figure 24b. Similarly, we have discussed the effect of interlacing of horizontal phase velocity curves for simpler models on the horizontal group velocity curves for a more complicated model, which can be considered to be made up of two or more such simpler models.[2,3]

We next turn to a consideration of the response of Trotters Model 1 to plane waves incident from the lower elastic half-space. In Figure 25 we have plotted vertical component power levels, normalized with respect to values at the surface, as functions of depth for 1.00 and 1.25 cps. The solid curves give the response to P-waves incident vertically from below. The lines give the response to P, SV, and SH* waves incident from below equally at all angles of incidence. We shall call this the isotropic plane wave noise model. As was mentioned earlier in the description of the computer program, we assume that the P, SV, and SH waves all have equal energy flux in the direction of propagation, and that the phase of each plane wave is statistically independent of the phase of every other wave. Such a model for noise in an infinite isotropic homogeneous medium is not unlike the energy density equipartition noise model which we have used for surface waves, and it can be justified by similar qualitative arguments about far-field scatterers and sources.

---

*Evidently the SH waves do not contribute to the vertical component power level.

We note from Figure 25 that the vertical velocity component of the response of the medium to isotropic plane wave noise is quite similar to the response to vertically incident plane P-waves, especially at the shallower depths. This is not an unexpected result, since plane waves incident at depth even at large angles of incidence will generate plane waves at much smaller angles of incidence in the lower-velocity shallow layers. The zeros present in the curve of power level versus depth for the vertically incident P-waves are of course no longer present for the isotropic plane wave noise input. The vertical velocity component coherence is still high for the isotropic plane wave noise input, as shown by the curve in Figure 26. We note that an additional "smearing out" of the response will be observed when we take into account the fact that actual data processing must view the response through a frequency window of finite width. The effect of small changes of frequency on the response to plane P-waves incident vertically from below was illustrated for the Hempstead Model 4F in Figures 17 a and 18 a of the third semi-annual technical report.[3] The effect of small frequency changes on vertical velocity component resonances excited by plane SV waves incident from below was illustrated in Figures 17c, d and 18c, d, e of the same report.[3] Numerical work has shown that such resonances do not have an overwhelming effect on the response of the medium to isotropic plane wave noise.

In Figure 26, we compare the vertical velocity component coherence for Trotters Model 1 as a function of depth for three types of noise excitation. The reference detector is at a depth of 145 m. As was mentioned in the preceding paragraph, the solid curve refers to isotropic plane wave noise incident from below. The cross bars refer to a noise model based on the assumption that at a given frequency the average energy density is the same for each trapped surface mode and that the motion due to each mode is statistically independent of the motion due to every other mode. This noise model has been discussed in our previous semi-annual technical reports.[1,2,3] Finally, the lines refer to a situation where there is both surface wave and plane wave type of noise input; these inputs are assumed to be in such proportion that the vertical component power level at the surface is the same for both. This last assumption of equal power level at the surface due to each type of noise input has no rational basis,

and the calculations based on it serve merely to illustrate the general nature of the response that may be expected when both types of noise input are present. Since the two noise models are independent, a proper description of their relative excitation either requires additional assumptions about the distribution of scatterers and sources, or should be derived as a parameter from the statistical analysis of experimental data. Coupling of the two noise excitations by scatterers in the layers may not be entirely consistent with the energy density equipartition assumption for trapped modes. In any event, it may require that the average energy density in the layers (excluding the lower half-space) due to isotropic plane wave noise input from below be in a given proportion to the average energy density in the medium due to trapped surface wave noise. This proportion can in turn be frequency-dependent. Lack of time has prevented us so far from investigating such a hypothesis numerically.

A plot of the vertical component power level as a function of depth for Trotters Model 1 is shown in Figure 27 for frequencies in the interval 0.25 - 2.00 cps. All curves are normalized to a value of unity at the surface. The curves in Figure 27a are calculated on the basis of energy equipartition and statistical independence of the motion in all trapped modes. The curves in Figure 27b are calculated on the basis of isotropic plane wave input from below. The curves in Figure 27c are calculated on the basis that both of the above types of noise input produce equal vertical component power levels at the surface. Thus the curves in Figure 27c are averages of the corresponding curves in Figures 27a and b. The influence of the isotropic plane wave noise on the power level curves in Figure 27c is must less pronounced than its influence on the coherence curve, shown in Figure 26, and especially on the polarity of the coherence curve.

Figures 28a-c present the ratio of total horizontal component to vertical component power level at the surface as a function of frequency for Trotters Model 1, Juno Model 2, and Hempstead Model 4F. Total horizontal component power level includes the motion in all horizontal directions; for the horizontally isotropic distribution of wave motion, which we assume, the power level measured for a single horizontal component is one-half of this total horizontal component power level. The lines in Figure 28 refer to calculations based on the surface wave energy equipartition assumption;

the cross bars refer to the assumption of isotropic plane wave noise. The ratios of horizontal to vertical power level at the surface for the two types of noise input are of the same order of magnitude but are generally higher for the isotropic plane wave input. For Juno Model 2, for example, the ratio of horizontal to vertical power level for isotropic plane wave noise input is just about twice that for equipartitioned surface wave noise input. For the Trotters and Hempstead models, the horizontal-to-vertical power ratios for the two noise inputs differ by less than a factor of 2. The ratios themselves are greatest for Trotters Model 1 and least for Juno Model 2. Since the ratios of horizontal component to vertical component power level at the surface are of the same order of magnitude for the two types of noise input considered by us, this ratio will not be greatly affected if we consider both types of noise input to be present in varying proportions.

Figures 29a-n present the vertical component power level at various detector depths as a function of frequency for Trotters Model 1. Values are normalized to unity at the surface. Figures 30a-n present the vertical velocity component coherence at various depths with respect to a reference detector at 145 m as a function of frequency for the same model. In both Figure 29 and Figure 30 the lines refer to the noise model of energy density equipartition between all trapped modes; the cross bars refer to the assumption of equal vertical component power level at the surface due both to equipartitioned trapped mode and to isotropic plane wave noise inputs. Again we mention that this latter assumption is completely arbitrary; there is no reason to believe that the relative weights to be assigned to each of these noise inputs should depend only on the vertical component power levels at the surface or be independent of frequency.

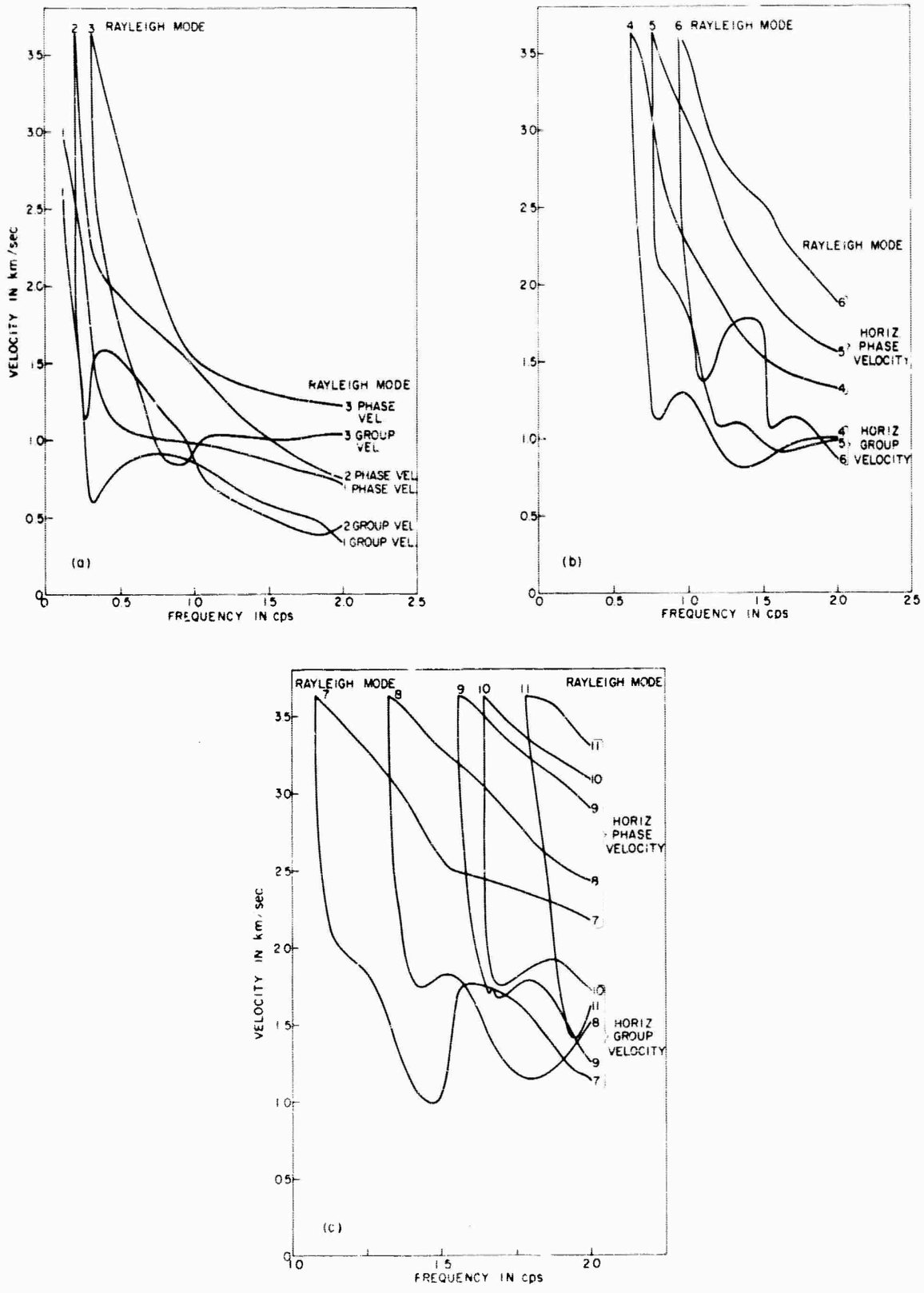

Fig. 21 - Horizontal phase and group velocities as a function of frequency for all Rayleigh modes of Trotters Model 1 in the interval 0.125-2.00 cps.

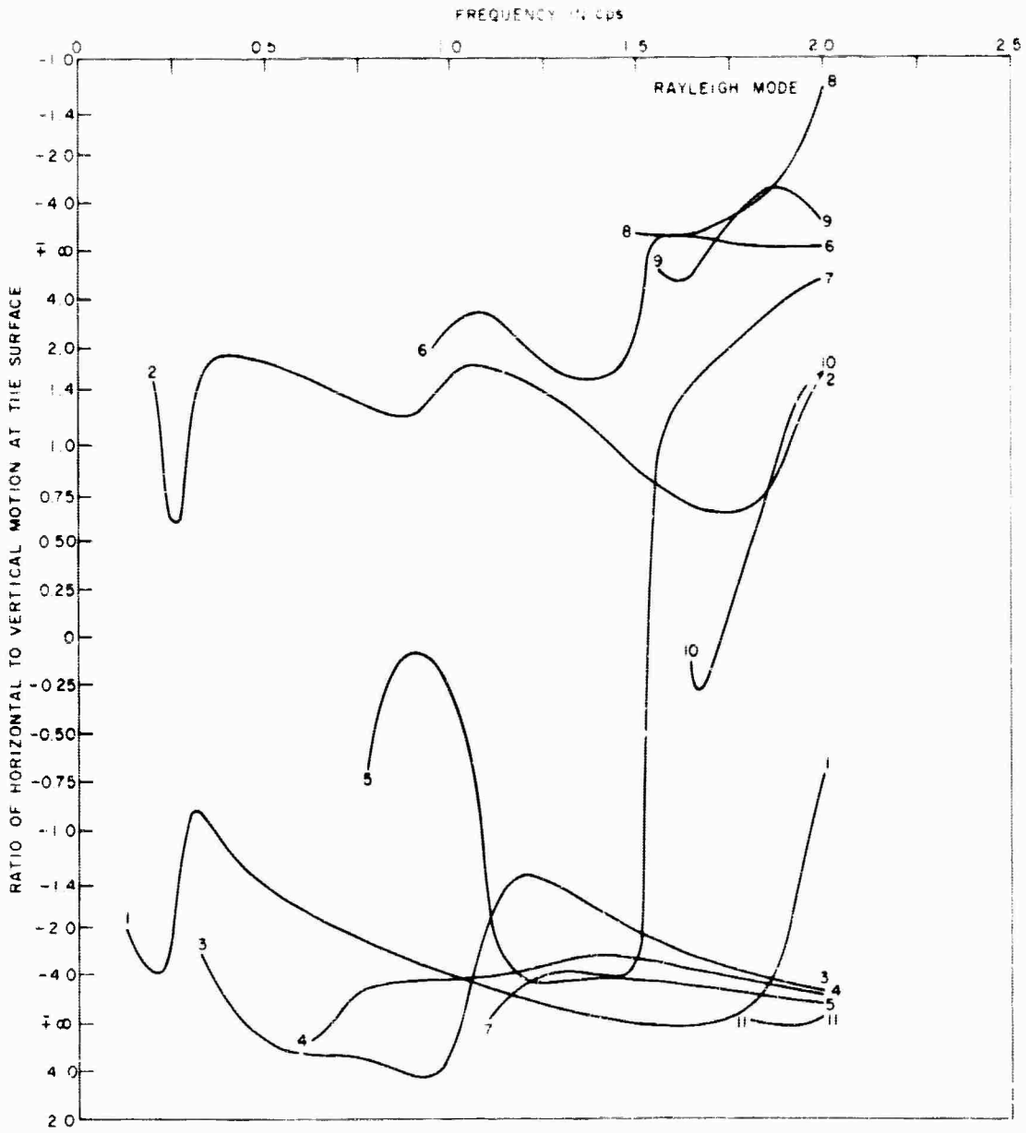

Fig. 22 - Ratio of horizontal to vertical particle velocity at the surface as a function of frequency for all Rayleigh modes of Trotters Model 1 in the interval 0.125-2.00 cps.

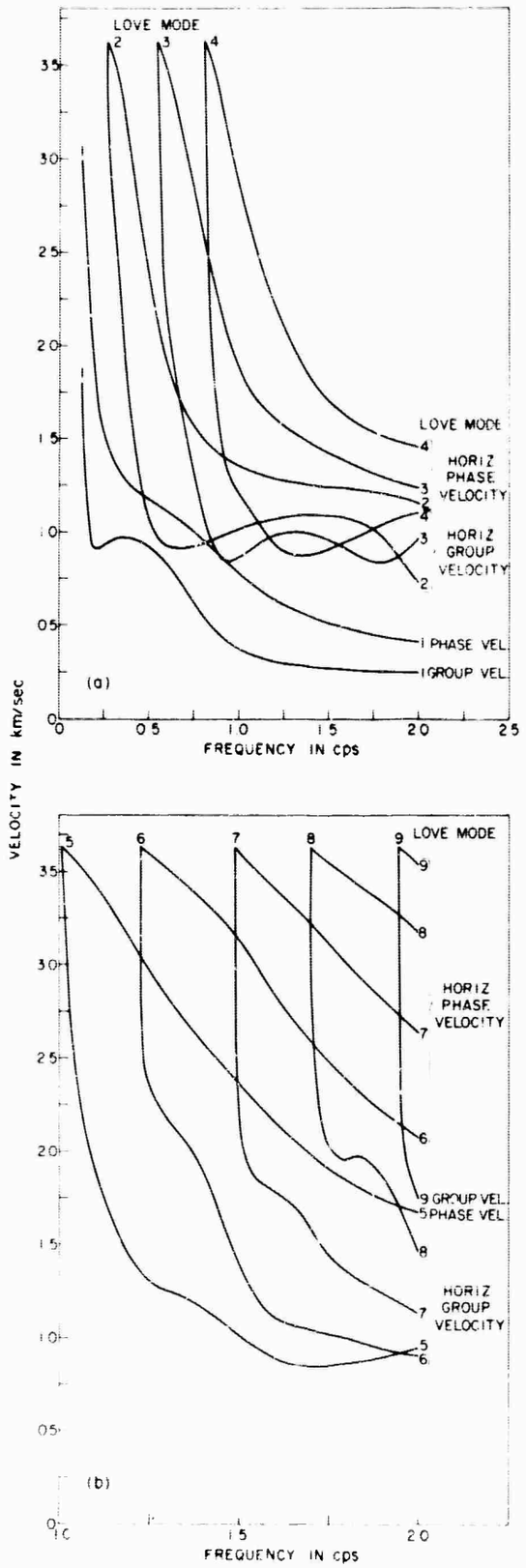

Fig. 23 - Horizontal phase and group velocities as a function of frequency for all Love modes of Trotters Model 1 in the interval 0.125-2.00 cps.

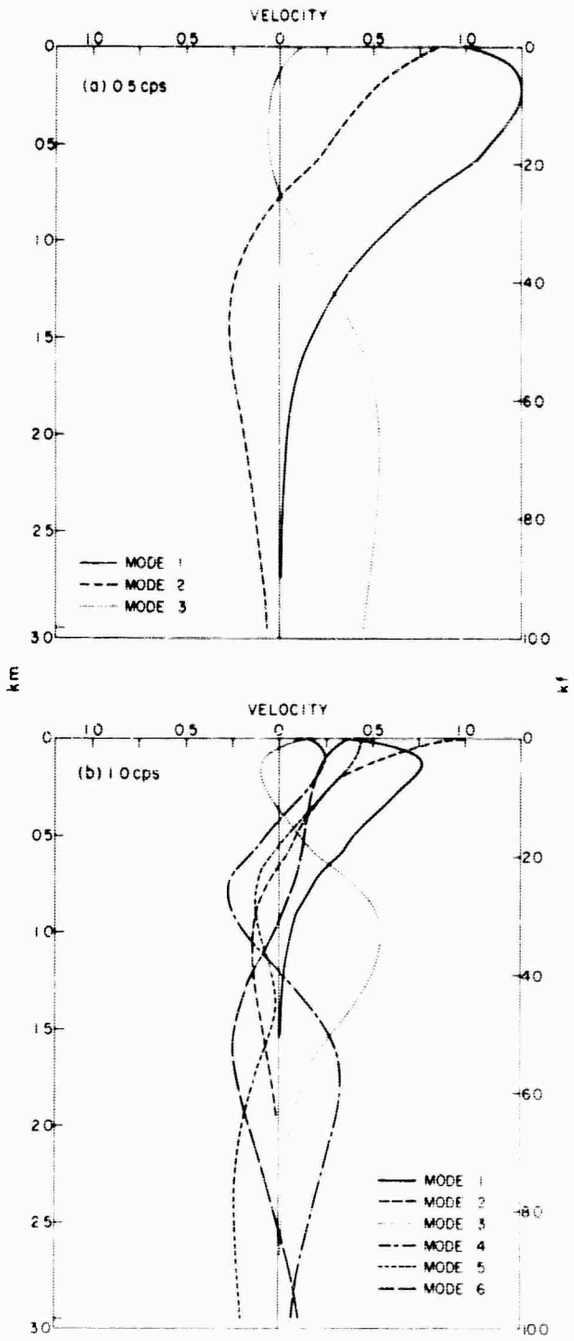

Fig. 24 - Vertical velocity component as a function of depth for Rayleigh-wave motion of Trotters Model 1. Energy equipartition between all trapped modes assumed.

A frequent source of noise near the Trotters well was the local winds. The wind conditions are described above. Fortunately, these winds were intermittent so that relatively quiet data could be obtained during most 24-hour periods. The effectiveness of these winds in producing noise varied considerably over distances of the order of a few tenths of a kilometer and seemed to be closely associated with the local topography. Results from the five surface stations occupied suggested that sites in valleys protected from the local winds were quieter than the high exposed sites. The SPZsw seismometer which was originally in a position on the edge of a rather high plateau and near a fence post, was much noisier than the other seismometer locations which were situated in or near valleys. The noise of the former site was of a high frequency character and strongly wind dependent and only during periods of little or no wind did the seismometer output resemble in level and appearance the noise of the other stations. As mentioned above, the SPZsw location was shifted into a valley some

All spectra were computed from auto- or cross-correlations of 150-second long noise samples. These correlations were truncated with a triangular weighting function 20-seconds long before Fourier analysis.

Experimental Results

Signal amplitudes - seismometer coupling. Except for the very near surface, the Trotters well was protected over its entire length by a single string of completely cemented casing so that good coupling of the seismometer to the formation was expected. The first 714 feet contained two strings of casing, but both were cemented. Direct comparisons of noise recorded at 470 feet in the deep well and in the 500-foot reference hole gave identical results for all frequencies below 3.0 cps.

Seismometer coupling at deeper depths was investigated by comparing the levels of clearly defined earthquake P-waves recorded at depth and at the surface and near surface stations. The observed signal levels agreed with the levels predicted for plane P-waves arriving vertically from below the well within the expected error of measurement. The results obtained at Trotters. The power levels at the maximum depth of observation are between 10 and 20 db below those observed at 500 feet. This decrease, corresponding to a decrease in amplitude by a factor ranging from about 1.7 to 3.0, is of the same order as the observed decrease in earthquake signal levels. Thus, only a slight improvement in general signal-to-noise ratio is to be expected at depths below 500 feet at the Trotters site. At frequencies above 1.0 cps, however, a definite gain can be obtained by shallow burial of the seismometer.

Noise stationarity. The noise observed at Trotters during preselected "typical quiet" periods was quite stable in its general characteristics. Surface power spectra for a number of different quiet periods are shown in Figures 7, 10, 11 and 12. These were periods of low wind which showed no unusual noise conditions on the developcorder records. In general, these spectra fall within a few db of each other for frequencies of the order of 2.0 cps and lower. At Trotters occasional variations were visible, however, in the amplitudes of fairly well defined by as much as 40 db between 1.0 and 2.0 cps. In the same frequency range the noise at 500 feet increased by only 10 to 15 db. The increase at 5000 feet was such that the power ratio of the 5000-foot and 500-foot data is almost the same as the ratio observed during quiet periods. Clearly the increased noise seen at the surface contains a component which decreases with depth in approximately the same fashion as typical quiet noise and a much larger component which is confined to depths shallower than 500 feet.

Figure 11 contains a comparison of surface, 500-foot, and 6000-foot observations for a quiet period and a period during which extreme noise from an eastbound train is visible at all three depths. The train is at a distance of approximately 15 miles. The increase in surface noise is almost as great as that observed during the blizzard, however, it begins at a higher frequency (about 1.0 cps) and is obviously of a different nature. The large increase from this distant source is present at all depths at levels such that the ratio of surface to 500-foot power as well 500-foot for typical quiet noise.

2) During windy periods much of the large increase in surface noise above 0.5 cps is not present at 500 feet. Comparing the upper and middle curves we can see that almost none of the increase on 64-12-18 and only about one half of the increase on 65-01-13 are present at 560 feet.

3) During windy periods the ratios of noise power at 100 feet and 500 feet or 200 feet and 500 feet do not change. Since the largest part of the surface noise increase is not present at 500 feet, we can conclude that it does not extend even to a depth of 100 feet.

These observations are consistent with the conclusion that a large fraction of the surface noise increase observed during windy periods does not behave like typical quiet noise and is confined to depths shallower than 100 feet. It is our present belief that much of this noise is generated at or very near the seismometer vaults.

The horizontal components. In Figure 12 we have plotted the ratio of radial-to-vertical power as a function of frequency for several

noise data; though the use of plane waves enhances the fit somewhat, the improvement is not such as to demonstrate unequivocally the presence of this type of noise at the Trotters site.

Horizontal propagation velocities - the surface array. A representative sample of the basic data from the surface array at Trotters is given in Figures 18, 19 and 20. These are the data from which inferences may be drawn concerning the propagation directions and velocities of the near surface noise.

Cross-correlation phases between all pairs of surface seismometers are shown in Figure 18 for two different noise samples. The data for the short distances (≈ .8 km) and the long distances (≈ 1.3 km) are separated. At numerous frequencies below about 1.5 cps a number of the noise observations at Trotters have phases which can be interpreted in terms of approximately unidirectional noises propagating from a generally NE direction with velocities ranging from about 3.0 km/sec to 6.0 km/sec and greater; velocities of the order of 4.0 to 6.0 km/sec are most common. Such observations were quite rare at our other sites. Both of the samples shown in Figure 18 are of this type. The very low phases consistent with a more isotropic noise distribution which are usually observed at low fre-

TABLE 1

RELATIVE SURFACE VERTICAL AMPLITUDE FOR LEAST SQUARE ERROR

f = 1.0 cps

R_1	R_2	R_3	R_4	R_5	R_6	$P_{vert.}$	σ
1.0	2.8	0.4	0.4	1.2	1.0	–	*

0.7 cps where all phases are low suggesting interference of noises from various directions. Near 1.0 cps the phases give a picture very roughly consistent with unidirectional propagation from the NW with velocities of the order of 7.0 km/sec. Above about 1.5 cps the phase curves become very erratic suggesting the presence of numerous phases 2π; no well defined zones of phase reversal, such as might be expected for very uniform isotropic noise, are observed, however.

The surface array phase data at Trotters have not provided a clear picture of the nature of the horizontal propagation velocities of the near surface noise. There seems to be fair evidence at frequencies below 0.5 cps for measurable unidirectional velocities above the theoretical velocities computed for Rayleigh waves. At higher frequencies much less reliable measurements occasionally suggest even higher velocities. Phases consistent with a picture of a very uniform isotropic noise are not often observed.

In Figure 18 we have also shown the coherence for all the seismometer pairs in the surface array. In addition, Figure 20 shows similar results for four additional noise samples. The coherence plots

the frequency of a predicted minimum for the equipartition mixture. Isotropic noises with velocities somewhat higher than those expected for the Rayleigh waves would give coherence values more nearly in agreement with the observations. Curves for constant velocities of 3.6 km/sec and 8.0 km/sec are shown for reference. Of course, high coherence values can also be obtained with a strong unidirectional noise and it may be possible to explain both the phase and coherence data with a mixture of fairly isotropic Rayleigh waves and a more unidirectional component of somewhat higher velocity.

Fig. 1 - Location and geological environment of the three deep wells surveyed.

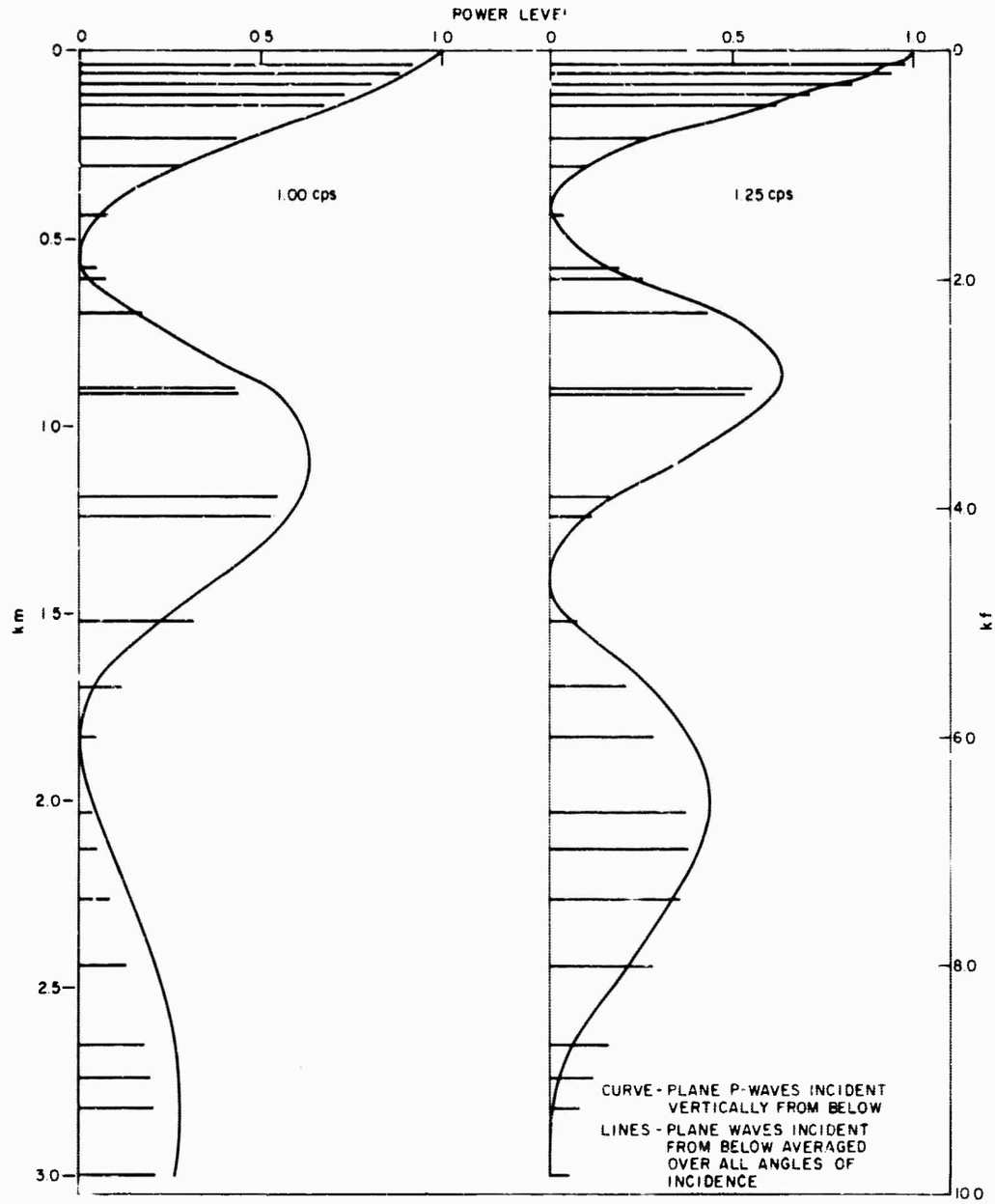

Fig. 25 - Vertical component power level as a function of depth at 1.00 and 1.25 cps for Trotters Model 1. Comparison of response for two different plane wave excitations from below.

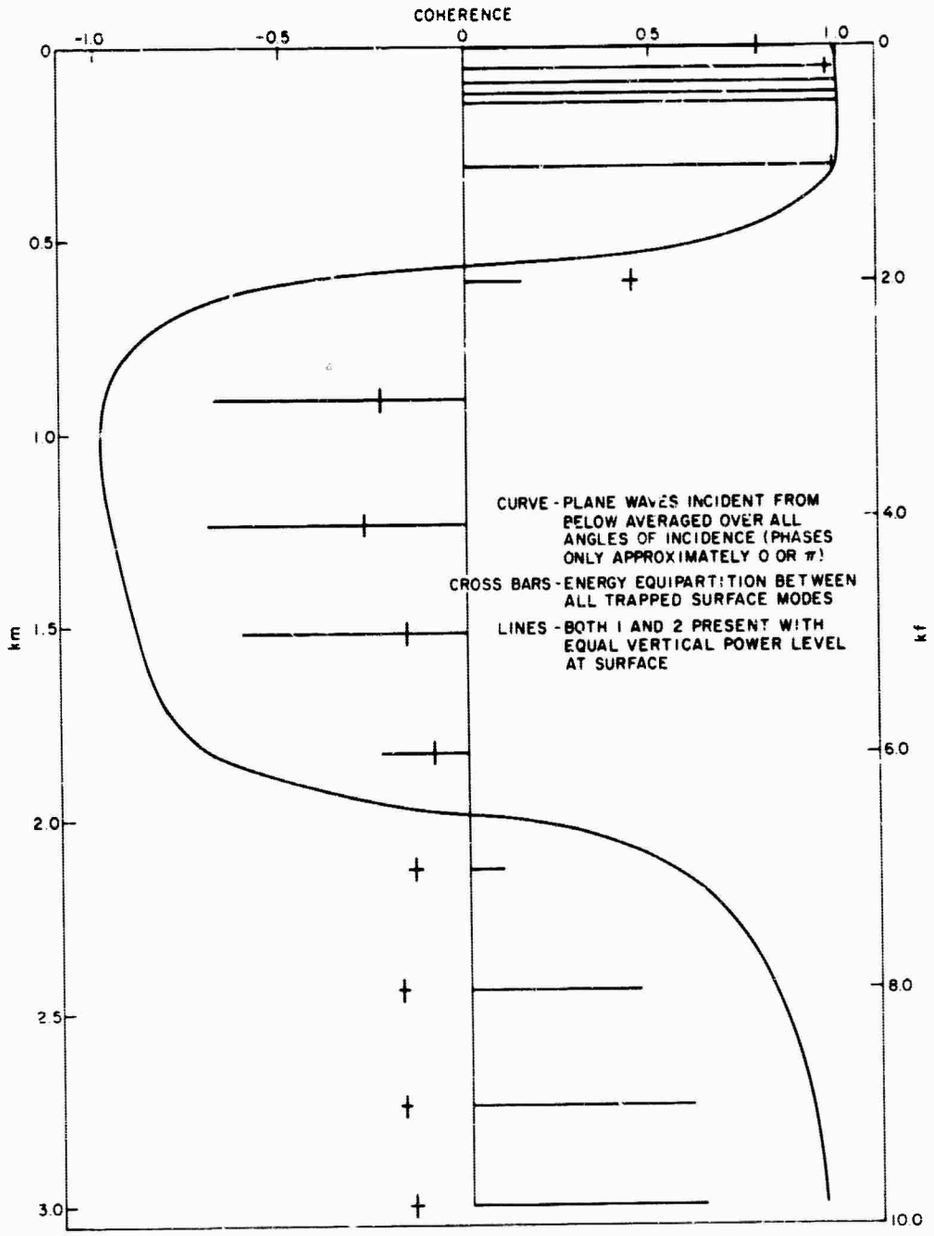

Fig. 26 - Vertical velocity component coherence as a function of depth at 1.00 cps with respect to detector at 145 m for Trotters Model 1.

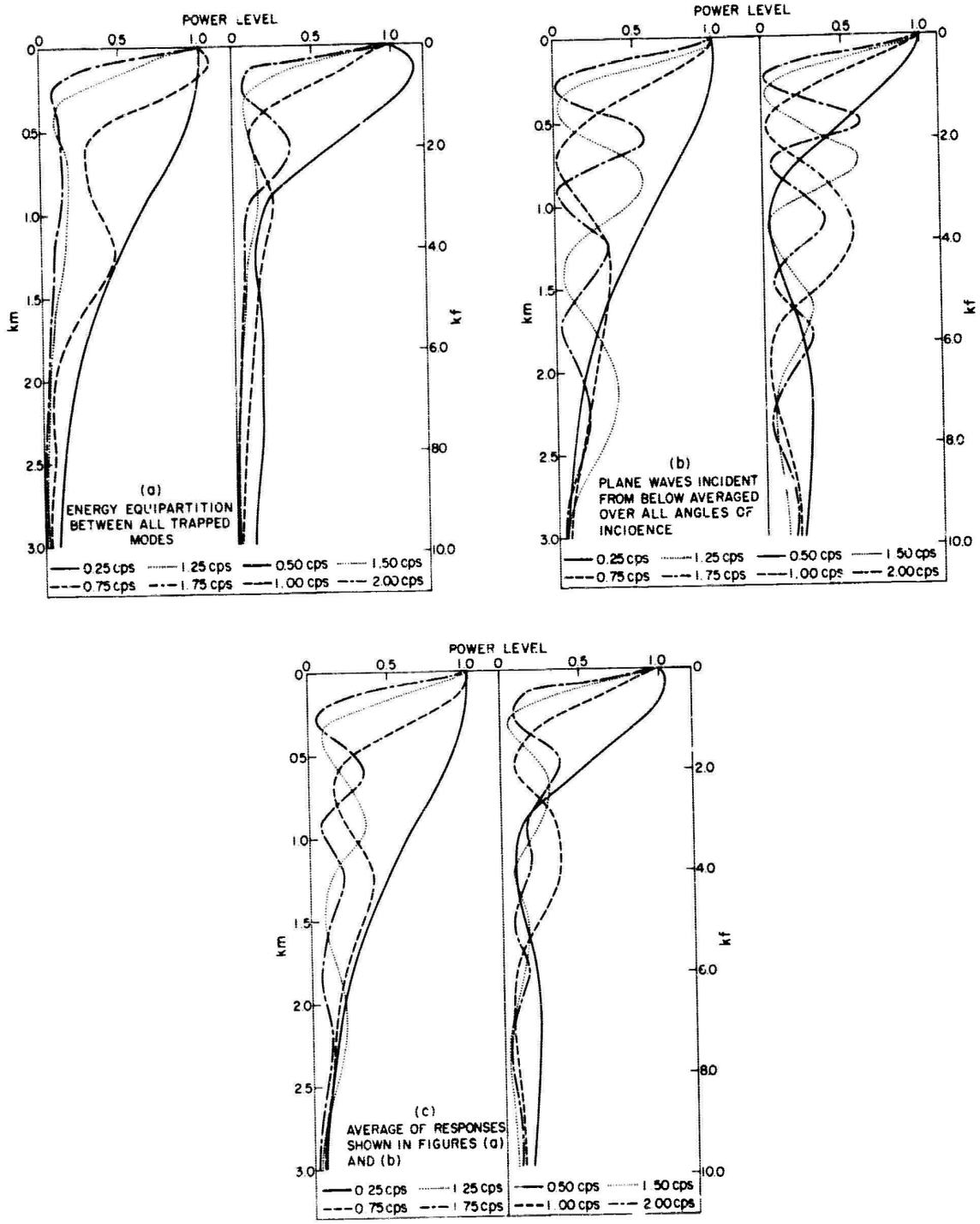

Fig. 27 - Vertical component power level as a function of depth at various frequencies for Trotters Model 1. Level at surface is 1.

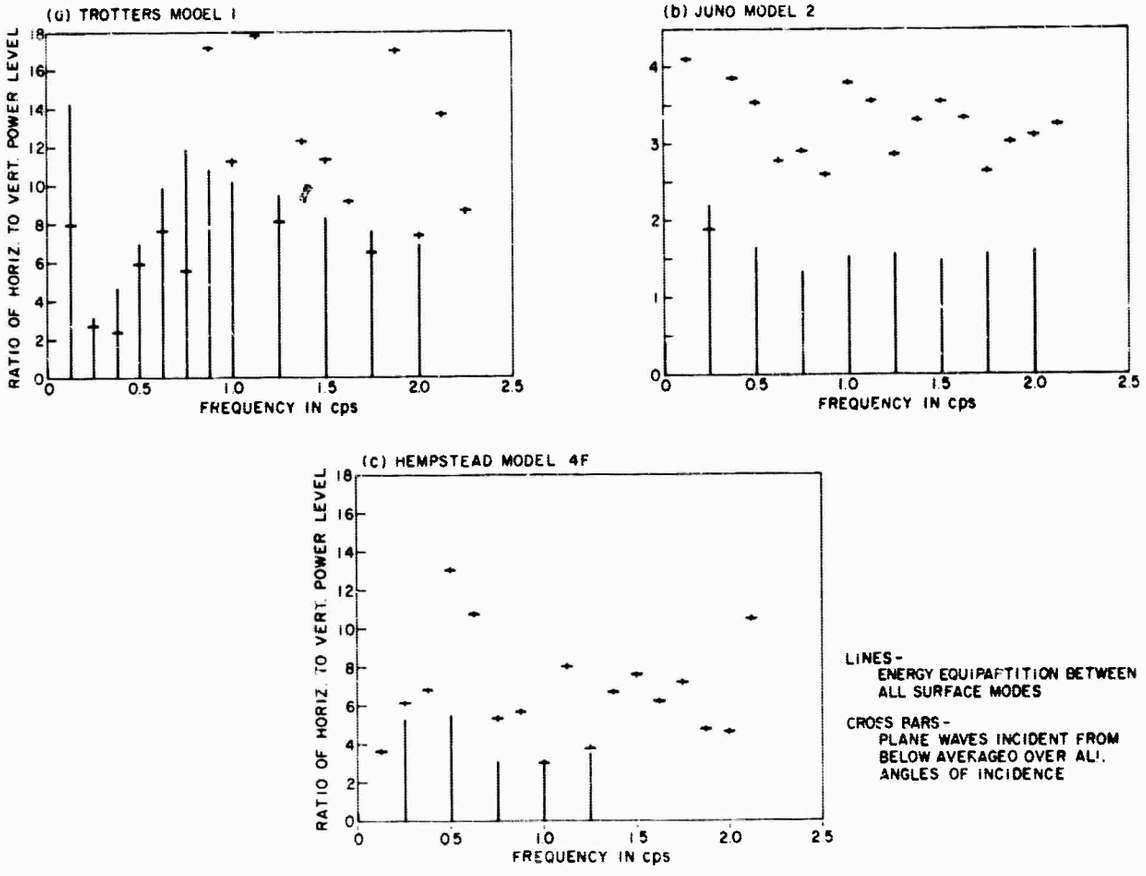

Fig. 28 - Ratio of total horizontal to vertical power level at surface as a function of frequency for models of 3 well sites.

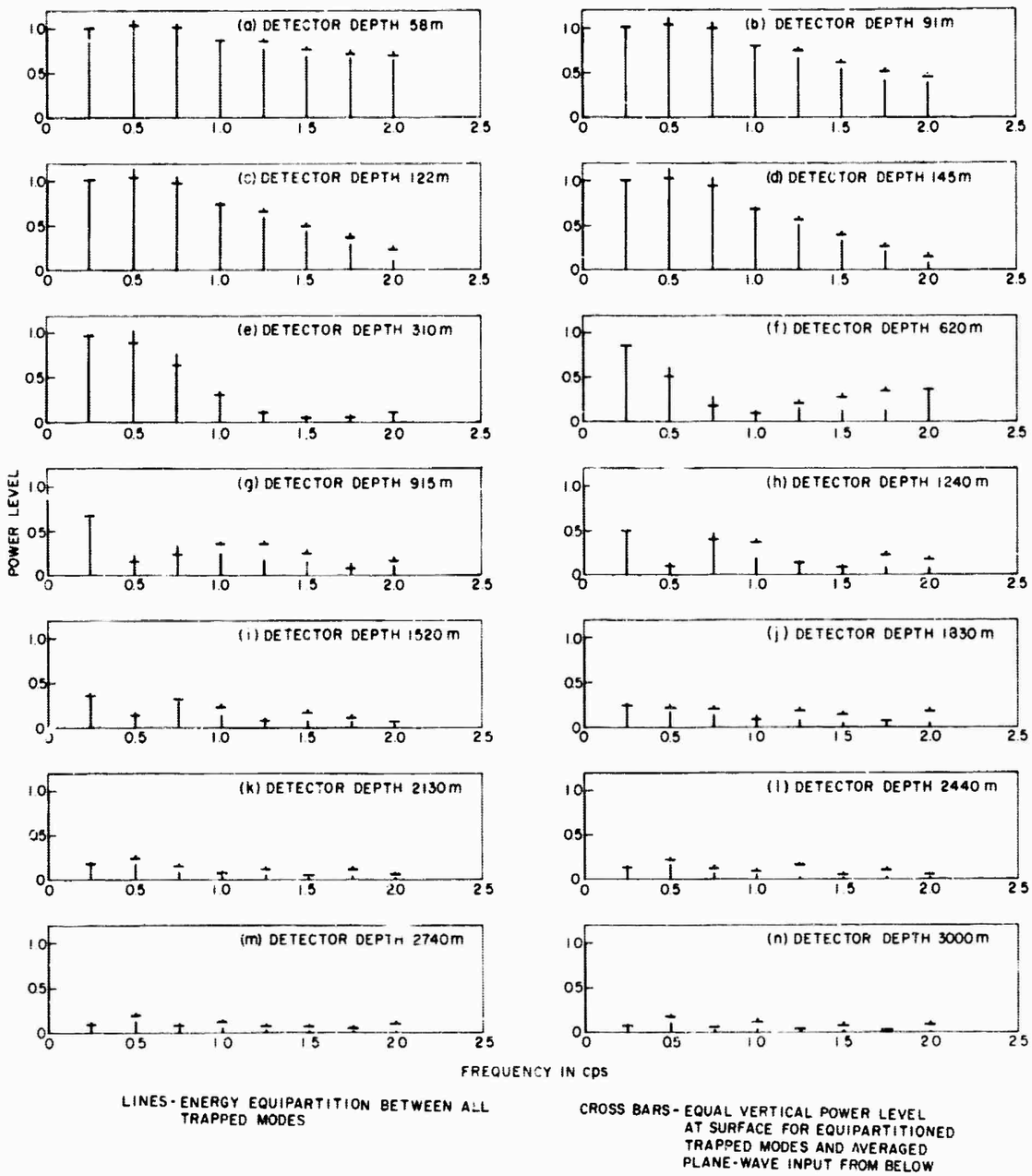

Fig. 29 - Vertical component power level at various depths as a function of frequency for Trotters Model 1. Level at surface is 1.

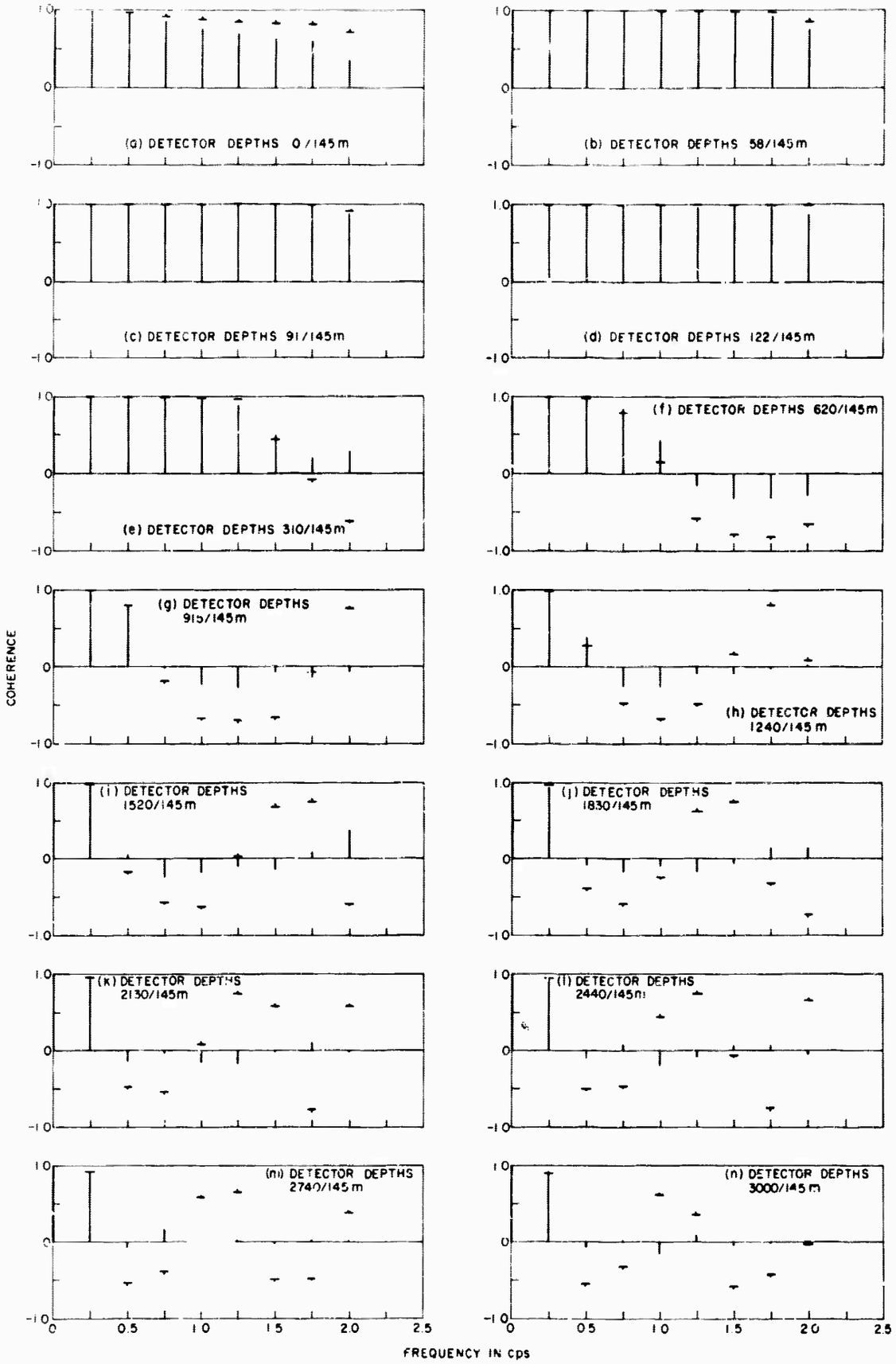

Fig. 30 - Vertical velocity component coherence at various depths with respect to detector at 145 m as a function of frequency. Trotters Model 1.

SUMMARY - THEORETICAL STUDIES

The theoretical work done in conjunction with the borehole noise project was based on the assumption that the earth in the vicinity of the borehole can be satisfactorily described in terms of a plane-layered elastic half-space. The response of appropriate plane-layered elastic models to trapped Rayleigh and Love waves as well as to plane P, SV, and SH waves incident from below was investigated in detail over the applicable frequency range. A number of interesting features of surface wave propagation were presented and discussed; these arose because of the presence in the model of deep low-velocity channel, or of a shallow high-velocity layer, or of a weathered layer of very low shear wave velocity, etc. Similarly, some interesting resonance phenomena in the vertical component of the response of layered media to plane SV waves incident from below were presented.

Two essentially independent models for "noise" in the plane layered elastic half-space were investigated. One is based on the assumption that at a given frequency the average energy density is the same for each trapped surface mode (Rayleigh and Love) and that the motion due to each mode is statistically independent of the motion due to every other mode. The other is based on the assumption that at a given frequency, plane P, SV, and SH waves are incident from the lower elastic half-space equally at all angles of incidence. All waves have equal energy flux in the direction of propagation, and their phases are statistically independent. Although the statistical response parameters for the two noise models applied to a given plane-layered elastic medium have many similar features, a better fit to experimental data seems to be obtained when noise due to both types of input is considered. The relative input due to each type of noise source should perhaps be based on total average energy density in the layers (excluding the half-space for incident plane waves); however, this input ratio can also be treated as a parameter to be fitted to the experimental data.

Numerical investigations were carried out on various plane-layered elastic models pertaining to the three well sites where measurements were made during the course of the contract. Statistical response parameters corresponding to both noise models described above were evaluated. (Although computations for the averaged plane wave noise input model were carried out for models of all three well sites, most results were

presented graphically only for the Trotters model.) All of our analysis was carried out with the aid of three computer programs, for which descriptions and Fortran Decks are available. A modification of the usual procedure for calculating the response of a layered medium to the higher Rayleigh modes at relatively high frequencies has enabled us to effect such calculations for very deep and complicated models.

The author of the theoretical sections of the semi-annual reports wishes to express his sincere gratitude to Dr. A. S. Ginzbarg of the Shell Development Company for help, encouragement, and advice, without which the work reported here would not have been possible.

SUMMARY - EXPERIMENTAL OBSERVATIONS

Introduction

In this summary of the experimental results we shall not attempt to reiterate all of the material previously given in the reports of the data from the individual sites. Those detailed analyses of the evidence for various types of waves are of fundamental importance but repeating them in this summary would be impractical. We shall emphasize here certain results which were originally open to considerable question or were unsuspected and results which bear directly on particular parts of the work statement of this contract. We shall place special emphasis on comparisons of the results from the different environments. In this connection some of the theoretical predictions for the different sites will also be compared to indicate the type of environmental variations predicted by the noise models.

The Sites - Environmental Factors

Three deepwell sites have been investigated - Hempstead, Texas (HE-TX); Juno, Texas (JU-TX); and Trotters, North Dakota (TS-ND). Their locations are shown on Figure 1. The Hempstead well is located in typical sediments of the gently dipping Gulf coastal plain. The Juno site is further inland near a region of considerable orogeny. It lies in a narrow basin of complicated structure with steeply dipping sedimentary beds of much greater geologic age than those of the Gulf Coast. The Trotters well is in the Williston Basin near the center of the continent. The Williston Basin is a fairly large basin with very simple structure and a gently dipping sedimentary section. Thus, geographically and geologically the sites are in quite different environments. The relation of these factors to possible seismic noise sources in the short period range are not known however.

At the outset of this research, the factor presumed to be of most probable importance in determining the local characteristics of seismic noise was the distribution of seismic velocities and densities in the general area of the well. Both the vertical distribution of these parameters and the rapidity with which this distribution changes laterally were considered. For the case of an earth approximated by plane horizontal layers with constant elastic parameters over a large area near the well, one can compute many properties of propagating seismic signals for comparison with the observations. These computations utilize the compressional and shear wave velocities of the layers and the layer densities.

The wells chosen sample fairly different types of velocity environment. The Hempstead and Trotters wells are most similar. They penetrate rather low speed sediments (2.0 to 3.0 km/sec for compressional waves) with similar vertical distributions down to about 2.0 km. Below this depth the velocity at Trotters rises rapidly to 6.0 km/sec while at Hempstead velocities between 3.5 and 4.0 km/sec predominate down to about 6.0 km. Both well sites have very low velocity sediments (1.0 to 2.0 km/sec) and P to S velocity ratios probably considerably greater than 2.0 in the first few hundred feet below the surface. The Juno well penetrates rocks of much higher velocity. Velocities between 3.8 and 4.8 km/sec are encountered for the first 4.0 km with 6.0 km/sec material being present at greater depth. The near surface at Juno, except for the first few feet, also has velocities well above 2.0 km/sec. Figure 31 is a plot of vertical travel time versus depth for compressional waves at the three sites. Some of the features described above are visible on these plots. These times have been used in comparing the noise data from the different wells.

In the previous paragraph we have discussed only the compressional wave velocities at the three sites. In fact, the shear wave velocities may be even more pertinent in any comparisons involving trapped waves. Unfortunately very few field measurements of shear velocities are available. P-wave data is quite plentiful, however, and we have been forced to estimate shear velocities from the rather poorly known ratios of P to S velocities for various rock types. Under the circumstances we have based our comparisons among wells on compressional wave travel times. In general, however, the shear velocity variation with depth for each of the three wells has very nearly the same shape as the variation of compressional velocity.

The densities used in our theoretical calculations are also poorly known. In general, estimated regional values were used. For both Trotters and Hempstead these estimates increase with depth from about 2.0 gm/cm^3 to 2.7 gm/cm^3. At Juno the estimated density starts at 2.6 gm/cm^3.

Juno differs from Trotters and Hempstead in still another possibly important fashion. Velocity logs taken in several holes near the Juno well show a rapid lateral variation of velocity and layering. Major changes occur within a distance of a few miles so that no detailed model of the layering can be expected to hold over distances of the order of tens of miles. On the other hand, both Hempstead and Trotters are in areas of slow lateral variation. For those two wells, a model of horizontal layers might fit quite well over distances much greater than ten miles.

As will be seen below, the noise behavior with depth and frequency does appear to be related to the observed vertical velocity distribution. While both theory and experiment for vertical component noise as a function of depth seem to be fairly insensitive to the details of the velocity variation with depth, both show a considerable difference between the low velocity locations, HE-TX and TS-ND, and the high velocity section at JU-TX. This is true both for the very near surface behavior of the noise and for the behavior below say 500 feet.

Although the data at hand are not sufficient to establish any relationship between the observed noise and the occurrence of rapid horizontal variations of the velocity layering, one might expect such a dependence to be weak in cases, such as Juno, where the variation is still small compared with the differences between, say Juno and Hempstead.

Seismometer Coupling

For operational ease it was decided to attempt to use the deepwell seismometers in cased holes. The design of the seismometer is such that good coupling of the seismometer and the casing is to be expected. In any particular hole however, the coupling of the casing and the earth is an unknown, particularly where the casing is uncemented or improperly cemented or where the seismometer is clamped in an uncemented liner within another casing. All of these conditions were encountered in the Hempstead hole. The Juno well was cased and completely cemented during its original completion. Only a single casing was present at each depth. The Trotters hole was cased by us with a single string of casing cemented completely from three injection points.

At each well the coupling of the seismometer to the earth was investigated by studying the relative amplitudes of clearly defined earthquake P-waves observed on the deepwell seismometer and also on the 500-foot reference seismometer and on the surface array. These measurements were compared to the theoretically predicted amplitudes for P waves travelling upward in a layered elastic medium and perfectly reflected at the surface. Figure 32 shows such a set of measurements and predictions for the Juno well. It is taken directly from our Third Semi-Annual Report. Similar agreement between theory and experiment was obtained at the other two wells.

It should be noted that the quality of the results depended on several factors. (1) Only events with a signal to noise ratio definitely greater than one at all the surface seismometers were considered. (2) Only phases with a clear onset at depth were used, i. e., phases in which interference due to the surface reflection of earlier loops could be discounted.

(3) Data were used only if reliable calibrations of seismometer period, damping and sensitivity were available for the same twenty-four-hour period and seismometer calibration drift was known to be negligible. The results obtained testify to the fact that seismometer calibration accuracy was limited to about 15% and even the achievement of this accuracy required constant care.

We have concluded that in every case where careful observations have been made the seismometer coupling for P-waves was excellent. This result is especially interesting for those depths of the Hempstead well where the seismometer was within two uncemented casings. Of course, the agreement between the observed and predicted amplitudes also serves to verify the theoretical model used for the P-waves.

Time Stationarity of the Noise - Simultaneous Observations at Depth

The procedure used in these experiments for studying the variation of noise with depth depends for its validity on the time stationarity of the noise, since simultaneous observations were made only at the surface, at 500 feet and at one depth in the deep well. All of the results obtained during the investigations of all three wells demonstrate that properly selected noise samples are quite reproducible at any given depth and that the observations at different depths vary so systematically as to eliminate all doubt as to their reliability. This conclusion is particularly strong if one refers to results obtained from deepwell data normalized with respect to the reference seismometer in the 500-foot hole.

The discovery of this feature of the data, which was already clearly evident at Hempstead, led to the abandonment of all efforts to design instrumentation for simultaneous observations at more than one depth in the deep well. It appeared that such observations were not essential to the success of the experiments and would not justify the additional experimental difficulties anticipated.

The preselection of the noise samples referred to above has been discussed in considerable detail in previous reports. At all three sites the noise appeared to consist of a "normal" background to which was added occasional components from numerous local sources. Many of these sources were readily identifiable, e. g., trains, automobiles, farming activity, shots fired by geophysical exploration crews, local winds, wind-induced movements of seismometer vaults, tube waves in the deep well, etc. Other sources could not be identified but the noises they added were so atypical of the normal background as to be easily recognized by inspection of develocorder

records. The develocorder records were visually inspected to exclude all of these noises as well as recognizable earthquakes. The remaining normal noise from periods of low wind made up the relatively stationary samples from which all the following results were taken.

Noise Power Spectra

Shapes and levels. Figure 33 shows a comparison of typical power spectra from the three wells. Simultaneous spectra for the surface vertical component, the 500-foot reference and the deep well seismometer are shown. The deep well observations are for depths of equal vertical travel time for P-waves. In each case the depth shown is near the bottom of the well. The spectra shown are corrected to absolute ground motion only at 1.0 cps. The system response characteristics as a function of frequency have not been removed, but they are the same for all the spectra shown.

As can be seen from Figure 33 the shapes of the noise power spectra are very similar at the three sites for the 500-foot and deep well locations. At the surface the TS-ND and HE-TX spectra are most nearly alike while the JU-TX surface spectrum drops a little more rapidly with frequency than the other two. These observations suggest that except for the near surface behavior, gross spectrum shape does not seem to depend critically on the environment.

The overall noise levels at HE-TX and TS-ND are similar and the surface noise levels are well above average for the continental United States. The level at JU-TX is considerably lower at all depths and at all frequencies; surface noise at JU-TX is below average for the United States. The data available here suggest a relationship between the high velocities and densities at Junio and the generally low noise level; they are not conclusive, however, particularly since the distribution of sources for the short period noise is unknown.

Near surface noise. Figure 33 also shows the power ratios 500-foot/surface and deep well/500-foot. The rapid decrease with depth seen above 1.0 cps in "typical quiet" near surface noise at HE-TX and TS-ND seems to be related to the very low near surface P and S velocities present there.

At these sites the increased surface noise observed during windy periods decays with depth even more rapidly than the noise shown in Figure 33. As mentioned in the report on TS-ND much of this increased noise is confined to depths less than 100 feet and may originate at or very near the seismometer vault. In this regard it is interesting to note the previously reported fact,[3] that compared

with the HE-TX and TS-ND the high velocity surface rocks at Juno seems very insensitive to surface noise sources (autos, etc.).

Overall decrease with depth - signal to noise improvement. The deep well/500-foot power ratios of Figure 33 and Figure 34 show that the frequency dependent decrease in noise level below 500 feet is very similar at the three sites for depths with equal vertical travel time. At the greatest depths achieved the average decrease is not large, ranging from 10 to 20 db in power (a factor of 1.7 to 3.0 in amplitude).

A striking fact about this decrease is that it is very similar to the general drop in the amplitude of earthquake P-wave signals (cf Figure 32), so that the average signal to noise ratio for "typical quiet" noise does not increase appreciably with depth below a few hundred feet. For many of the local noises occasionally present on the seismograms, however, the noise decays more rapidly with depth than normal and the signal-to-noise ratio improves continuously with depth. Even for these noises, however, the improvement is greatest in the first few hundred feet.

The 2.0 cps peak. The noise peak near 2.0 cps frequently reported by other observers is seen at all three of these sites. It is visible on all spectra at JU-TX and HE-TX but is less pronounced at TS-ND than at the other two sites. At HE-TX this peak had a clearly evident doublet character which was not noticed at the other two sites. At HE-TX and JU-TX, where the 2.0 cps was strong, it was present with almost undiminished strength at most depths.

The source of this 2.0 cps noise has not been identified.

Noise Variation With Depth

Power ratio. The ratio of the deep well and 500-foot power spectra shows the depth variation of the noise without including effects of the source spectra. Complete data for power ratio as a function of frequency at various depths have been given in the reports of the three sites (cf Figures 14, A-1 and A-4). These data are summarized in Figure 35 where power ratio versus vertical travel time for P-waves is shown for several frequencies. The characteristic shape of these curves has been discussed previously for each site. In particular we have noted the presence of a clearly marked first minimum at a frequency $f_1 \approx 1/4T$, where T is the one way vertical travel time for P-waves, and occasional subsidiary maxima and minima near multiples of this frequency.

The similarity of the power ratio curves for the three sites is clearly visible on Figure 35 and on Figure 34 where we have superimposed power spectra from all three sites for depths of equal T. For frequencies below

about 2.0 cps and for depths below 500 feet, the experimental data from the three sites agree sufficiently well that the apparent data scatter from each site is almost as great as the separations of the data from different sites. The second minimum is usually more clearly defined at HE-TX and JU-TX than at TS-ND but the general levels are similar.

Coherence and phase. Figures 34 and 36 contain comparisons of coherence of the deep well and 500-foot seismometers at the three sites. Cross-correlation phase comparisons are also shown. Here again the similarities of the data from the three sites are much more striking than their differences if data from depths of equal T are compared. The data shown for $T \approx .7$ sec and $T \approx 1.0$ sec are especially close.

The alternating coherence minima and maxima and the associated 0 and π phases discussed in the individual site reports are clearly seen on these data. The existence of several phase transitions and at least two coherence minima is clear at all three sites and one can infer the existence of noise modes with several sign changes with depth. The breadth of some of the coherence minima suggests in addition that several modes are present simultaneously near the transition frequency. The slight difference in frequency between the first coherence minimum and the first power ratio minimum is visible at many depths at all three sites. Such a shift would be expected where the noise consists of mixture of modes since the coherence should reach its first minimum at a frequency somewhat above the frequency for which the first sign change of a strong mode produces a power ratio minimum.

Comparison of Deep Well Observations With Theory

Energy equipartition of trapped modes. Figures 35 and 36 show succinctly the predictions of power ratio and coherence versus depth for the case of an energy equipartition among the trapped modes only, i.e., Rayleigh and Love waves. Of course, only the Rayleigh waves contribute to these vertical component results.

When plotted as a function of vertical travel time, T, the predictions for the three sites are remarkably similar at depths below 500 feet. The shallower predictions for the low velocity near surface sites, HE-TX and TS-ND, differ from the JU-TX theoretical results: all three predictions seem to fit their own shallow experimental data reasonably well. Except near the surface the predictions of these three models plotted as functions of T are probably not distinguishable with experimental data of the present accuracy. Indeed,

the three sets of experimental observations lie closer to each other than to the predicted curves. If depth is used as the coordinate, however, the high speed model JU-TX would separate from the other two, so that the high average velocity is distinguishable even if the details of the distribution are not.

The trapped mode model clearly predicts many of the general features of the noise visible on these curves and discussed in the previous section. The general shape and level of the power ratio data, the locations of the first power ratio and coherence minima, the 0 and π phases and at least the first transition frequency are all fairly well predicted.

Some quantitative features at frequencies above the first power ratio minimum are not predicted by this model, however. The power ratio curves frequently show higher maxima and more pronounced minima at the higher frequencies than would be predicted by the theory. The high values of coherence observed at depth and at higher frequencies and the clearly marked second and third phase transition frequencies are also poorly predicted by the trapped mode theory.

Vertical P-waves. The possible presence in the typical quiet noise of strong nearly vertical P-waves was unsuspected at the outset of these experiments. Clearly, however, all of the general features of the observed noise predicted by mixtures of trapped modes would also be given by surface reflected P-waves. The 0 and π phases and the alternating maxima and minima in the power ratio near frequencies which are multiples of $f_1 = 1/4T$ are cases in point. The coherence behavior probably requires the addition of some other type of noise to the P-waves, e.g., the presence of lowest mode Rayleigh waves would explain the broadening and frequency shift of the coherence minima.

In addition to the general features which can also be explained by the trapped modes the presence in the noise of vertical P-waves would explain the high coherence and power ratio values at great depths and higher frequencies. The frequencies of the clearly marked secondary phase transitions are also better explained by P-waves. P-waves alone, however, would exaggerate these effects beyond the levels observed and would leave other phenomena which seem to require a mixture of modes unexplained.

Striking evidence for the existence of near vertical P-waves in the noise at JU-TX was found in the synthetic deep well seismograms computed on the assumption that the deep well trace consisted of upward and downward travelling copies of the surface noise. These seismograms showed[3] almost

perfect agreement with the actual deep well traces over many long segments. This evidence is particularly notworthy because the conclusions drawn referred to individual pulses rather than results averaged over the 150 second noise samples used for computing spectra. While the time average behavior of P-waves and a mixture of Rayleigh waves show many similar features, it is less likely that they would be alike at almost every instant.

Isotropic plane waves. The isotropic plane wave noise model discussed in this report also shows promise of fitting the observed data. As pointed out in the sections on the Trotters well, however, the predictions for the isotropic plane waves and for near vertical P-waves are so similar that they could hardly be distinguished with the available data. As noted previously, however, these two noise models could result from quite different mechanisms and yield quite different world-wide results. Thus it will be well to keep both in mind for future investigations.

Least square fits - conclusion. In our previous reports we have described techniques for obtaining an objective estimate of the amount of each of the various types of energy present in the observed data by simultaneous least sqaure error fitting of the power ratio and signed coherence data. Some least square fits were given for Juno and Trotters. Interestingly enough these fits suggest the same model already implied by some of the results discussed above. At 1.0 cps and below the data appear to be consistent with a roughly equipartition mixture of trapped modes mixed with a strong component which behaves like vertical P-waves. At the surface, for these frequencies, the vertical component energy may be equally divided between P-waves and Rayleigh waves.

Horizontal Propagation Velocity - The Surface Array

Data from the horizontal array have been analyzed in three ways in an attempt to determine horizontal propagation velocities of the surface noise.

1) Direct observation of the filtered seismograms seemed to produce useable results only at JU-TX, where numerous pulses travelling with apparent velocities above 5.0 km/sec were observed. This result suggests the presence in the noise of signals other than trapped waves. At the other sites such clear arrivals were not visible, the seismograms appeared to consist of an interference of arrivals from many directions. Even at Juno, however, well defined pulses did not predominate in the records.

2) Cross-correlation phases of the surface array seismometer pairs yielded results most difficult to interpret. At TC-ND and to a lesser extent at HE-TX some evidence of unidirectional arrivals with measurable phase velocity was found at frequencies of 0.5 cps or less. These velocities generally seemed greater than the velocities predicted for Rayleigh waves. JU-TX also showed some evidence of directionality in the noise spectra. On the other hand, all three sites showed a more or less well defined frequency in the phase spectra at which a transition from phases near zero to phases nearer π takes place. Such transitions would be expected for more or less isotropic noise, but they could also result from a noise which changes composition drastically at a frequency near the transition. Unfortunately we have not been able to draw general conclusions from the phase information which would clarify further the discussions given in the individual site reports.

3) The coherences between seismometer pairs of the surface array seem to give a simpler picture than the phase data. At all three sites the coherences are fairly consistent with an isotropic azimuthal distribution of noise of fairly high velocity. Figure 37 shows a comparison of coherences from the three sites. The results for different X-distances seem to scale almost as expected for noise with an apparent velocity which is nearly independent of frequency. For frequencies below 0.5 cps the coherence plots are not very diagnostic of velocity. At higher frequencies, however, (up to 1.5 or 2.0 cps) the observed coherences seem to be definitely higher than the prediction for an isotropic distribution of Rayleigh waves with an equipartition of energy. These time average results seem to suggest a fairly isotropic noise of apparent velocity somewhat above the maximum predicted for Rayleigh waves.

Combining all three types of analysis there seems to be definite evidence in the surface array data for velocities above those predicted for trapped waves. In addition, the data seem to preclude interpretation by a simple isotropic mixture of surface waves and probably require both unidirectional components and mixtures with proportions which vary with frequency.

The Horizontal Components

Horizontal-to-vertical power ratio. Figure 38 shows the ratio of radial to vertical power at the surface as a function of frequency for the three sites. This ratio is closely related to the ratio of total horizontal to vertical component. The theoretical values computed for an equipartition mixture of trapped waves are shown for all three sites. The results of Figure 38 are striking for two reasons. First, the experimental results for the three

sites seem different in general shape or level. Second, the experimental results at each site are in rough agreement with the theoretical results for trapped Rayleigh and Love modes. In all three cases the theoretical ratio is strongly affected by a large Love wave component in the horizontal motion. The theoretical results shown at TS-ND for isotropic plane waves suggest that this noise model will also fit the observation at that site. From Figure 28 we see that a sizeable admixture of isotropic plane waves would not upset the agreement of theory and experiment at the other sites. Similarly a significant admixture of vertical P-waves would lower the theoretical ratios but would not completely destroy the rough agreement of theory and experiment. Clearly, the apparent usefulness of this ratio in distinguishing between these three sites should be investigated further.

Coherence and phase. The coherences and phases involving horizontal components provided no detailed information at any of the three sites. All coherences were low and all phases appeared to be random. These results are, of course, compatible with the conclusion that the horizontal component contains a sizeable Love wave contribution which is statistically independent of the modes which contribute to the vertical motion.

Usefulness of deep well horizontal component detectors. At the beginning of this research some consideration was given to the possible usefulness of simultaneous observations of horizontal and vertical components in the noise in the deep well. The early results at Hempstead showed no useable correlations between the surface horizontal and vertical components. Moreover, theoretical calculations of Love and Rayleigh wave motions as a function of depth suggested that this situation was not likely to improve with depth if the surface results were due to the presence of strong Love waves in the noise. These same results also suggested that no improvement in signal to noise ratio for earthquakes or similar events would be obtained at reasonable depths by using horizontal component detectors. Under the circumstances it was decided to concentrate our available efforts on a better understanding of the vertical component motion.

Conclusion

Many detailed conclusions concerning the composition of the short period noise and its behavior as a function of depth have been given above. The salient results of all of these different types of observation and analysis

can be summarized as follows. The observed noise at all three sites varies quite systematically with depth for frequencies below 2.0 cps and exhibits a behavior roughly predicted by an average of two noise models (1) an energy equipartition of trapped waves and (2) a mixture of plane waves arriving from below the wells. The most striking experimental consistencies are almost equally well explained by either noise model, but there is some evidence that both types of noise are important.

ACKNOWLEDGMENTS

It is a pleasure to acknowledge the work of a number of individuals whose specific contributions to this research were essential.

Mr. C. W. Cowan's tireless and conscientious efforts in preparing the sites and acquiring the data and the friendly and willing cooperation of all members of the Geotech crew in installing and operating the seismometers and the LRSM recording van were fundamental to the success of our field program.

The excellent equipment and data handling programs which were used in digitizing the original recordings were designed by Mr. D. L. Faass and carefully operated by Mr. R. L. Guest. The facile system of digital computer programs for spectral analysis was facilely prepared by Mr. D. J. Vanderschell.

Mrs. Gail Rother and Mrs. Sharon White ably assisted in the theoretical work of the project.

Many other persons suffered uncomplainingly through the preparation of the figures and texts of the several reports of this project. Their patience and skill are herewith gratefully acknowledged.

REFERENCES

1. Semi-Annual Technical Report No. 1, Contract No. AF19(628)-2785, Seismic Noise in Deep Boreholes, Shell Development Company, Houston, Texas, October 20, 1963.

2. Semi-Annual Technical Report No. 2, Contract No. AF19(628)-2785, Seismic Noise in Deep Boreholes, Shell Development Company, Houston, Texas, August 15, 1963.

3. Semi-Annual Technical Report No. 3, Contract No. AF19(628)-2785, Seismic Noise in Deep Boreholes, Shell Development Company, Houston, Texas, May 1, 1965.

4. Pye, Willard D., Habitat of Oil in Northern Great Plains and Rocky Mountains, Habitat of Oil - A Symposium, The American Association of Petroleum Geologists, p. 178 (1958).

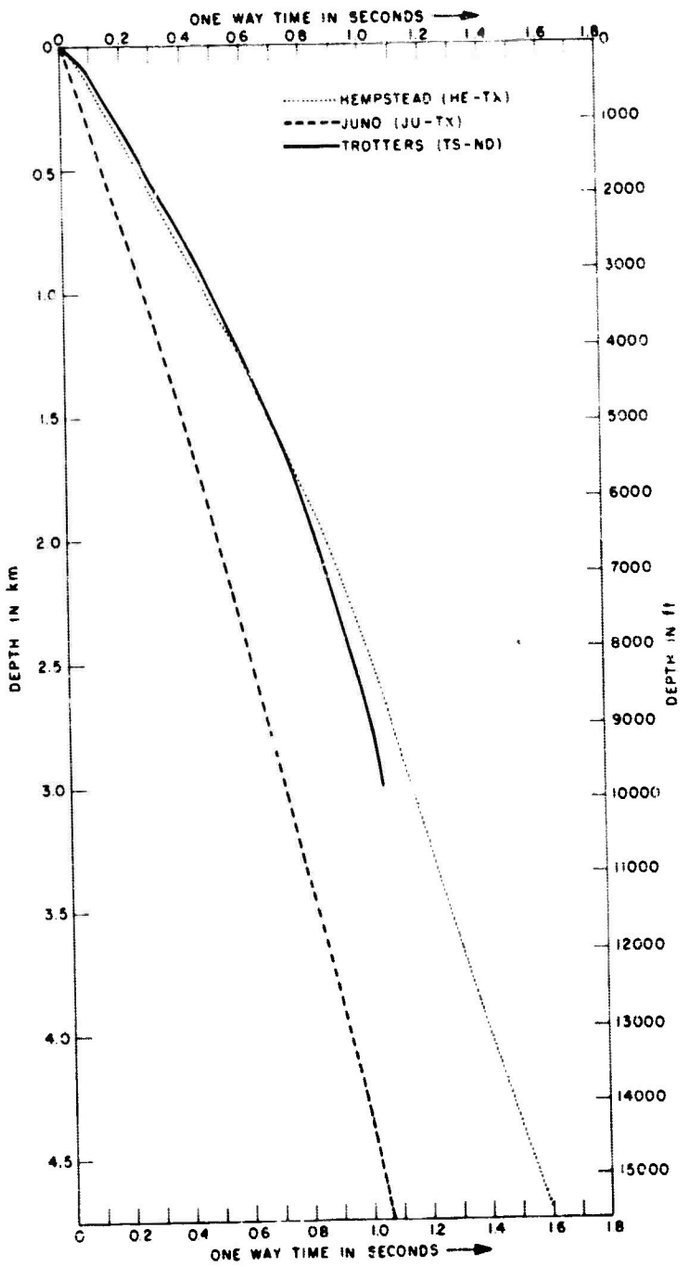

Fig. 31 - Measured time depth curves for compressional waves at the three deep well sites.

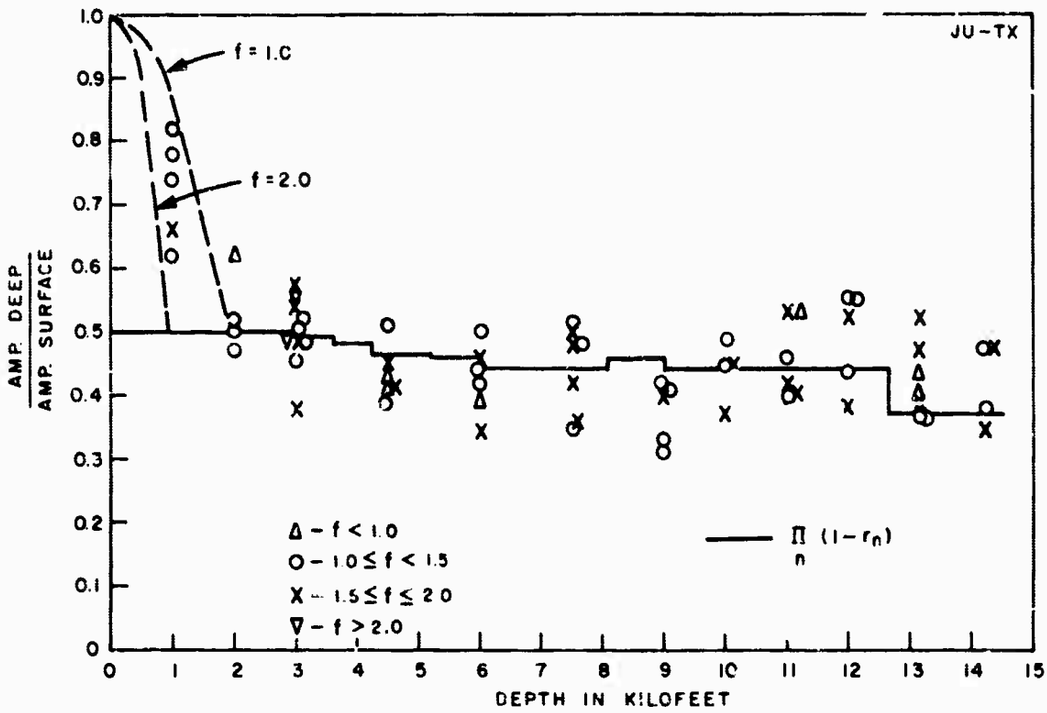

Fig. 32 - Relative amplitude of earthquake P-waves observed at the surface and in the deep well at Juno. The points show the experimental data. Approximate theoretical curves are given for vertical incidence in a plane layered model. The dashed curves show the effect of interference between incident and surface reflected signals assuming perfect reflection. f is the approximate peak frequency of the pulse in cycles per second. r_n is the reflection coefficient at the n^{th} interface.

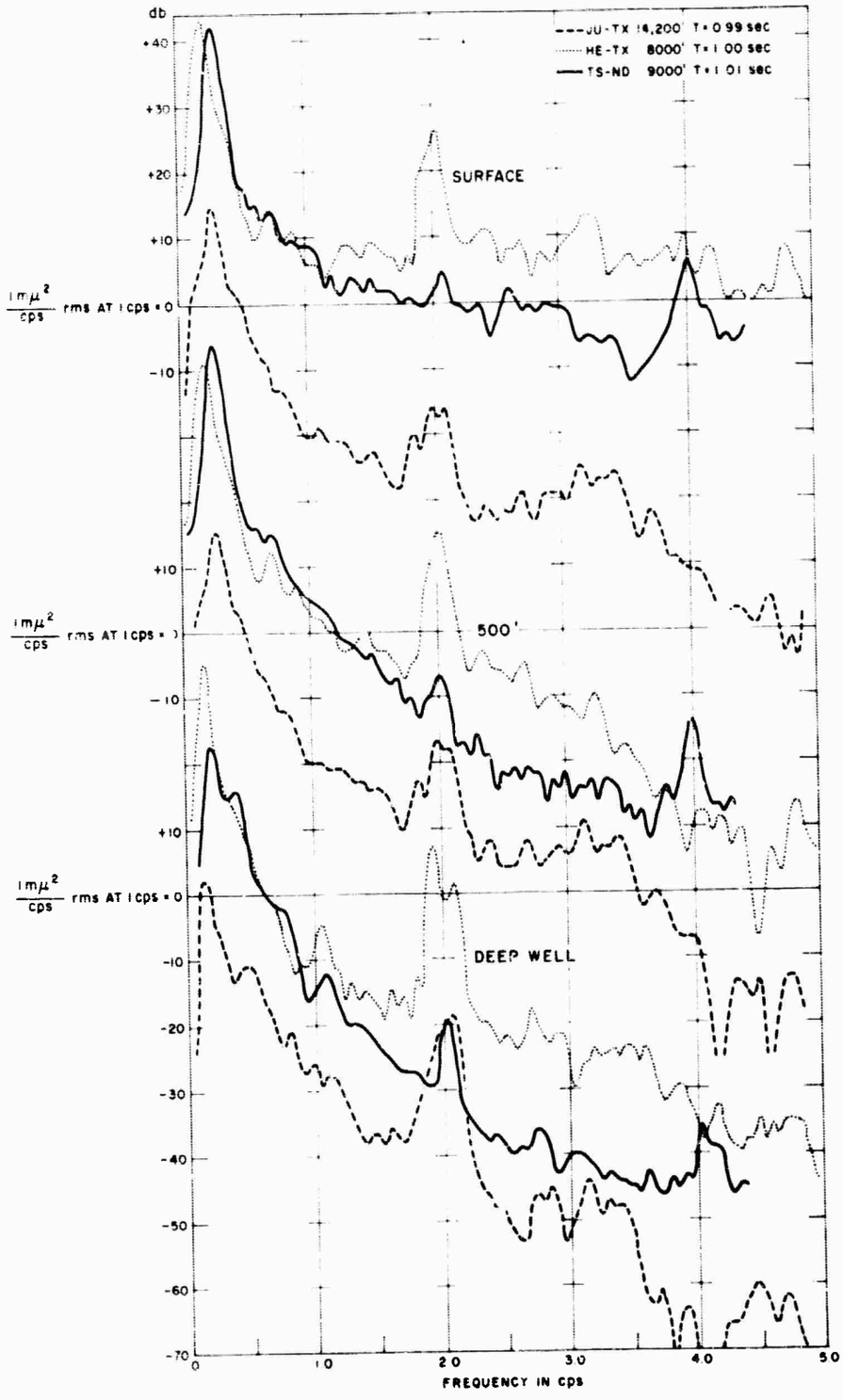

Fig. 33a - Typical power spectra for simultaneous noise observations at the surface, 500 feet and in the deep well. Data for the three deep well sites are compared. Deep well depths are chosen to give equal values of T, the one-way vertical travel time for P-waves.

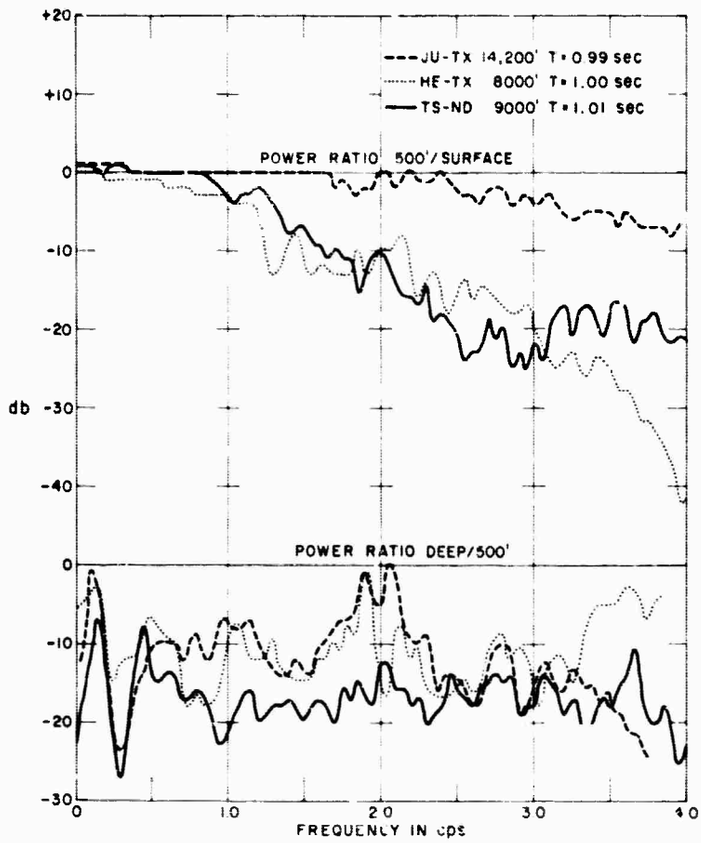

Fig. 33b - Power ratios for the noise samples of Figure 33a.

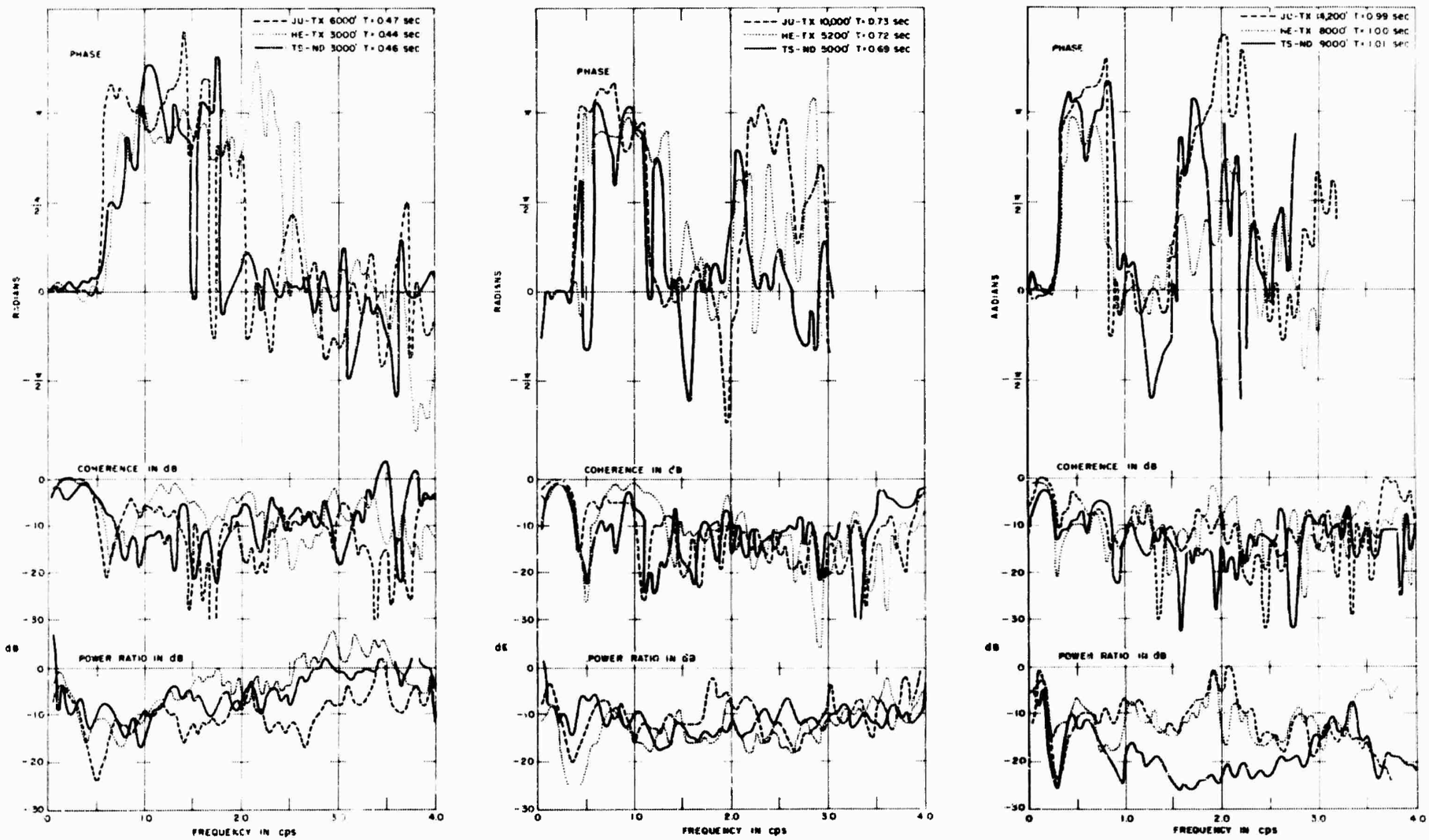

Fig. 34 - Comparison of deep well/500-foot power ratio, coherence and cross-correlation phase versus frequency for noise samples from the three sites. Samples taken at depths with equal P-wave travel times are compared. Results for one-way travel times, T, of approximately 0.5 sec, 0.7 sec and 1.0 sec are shown.

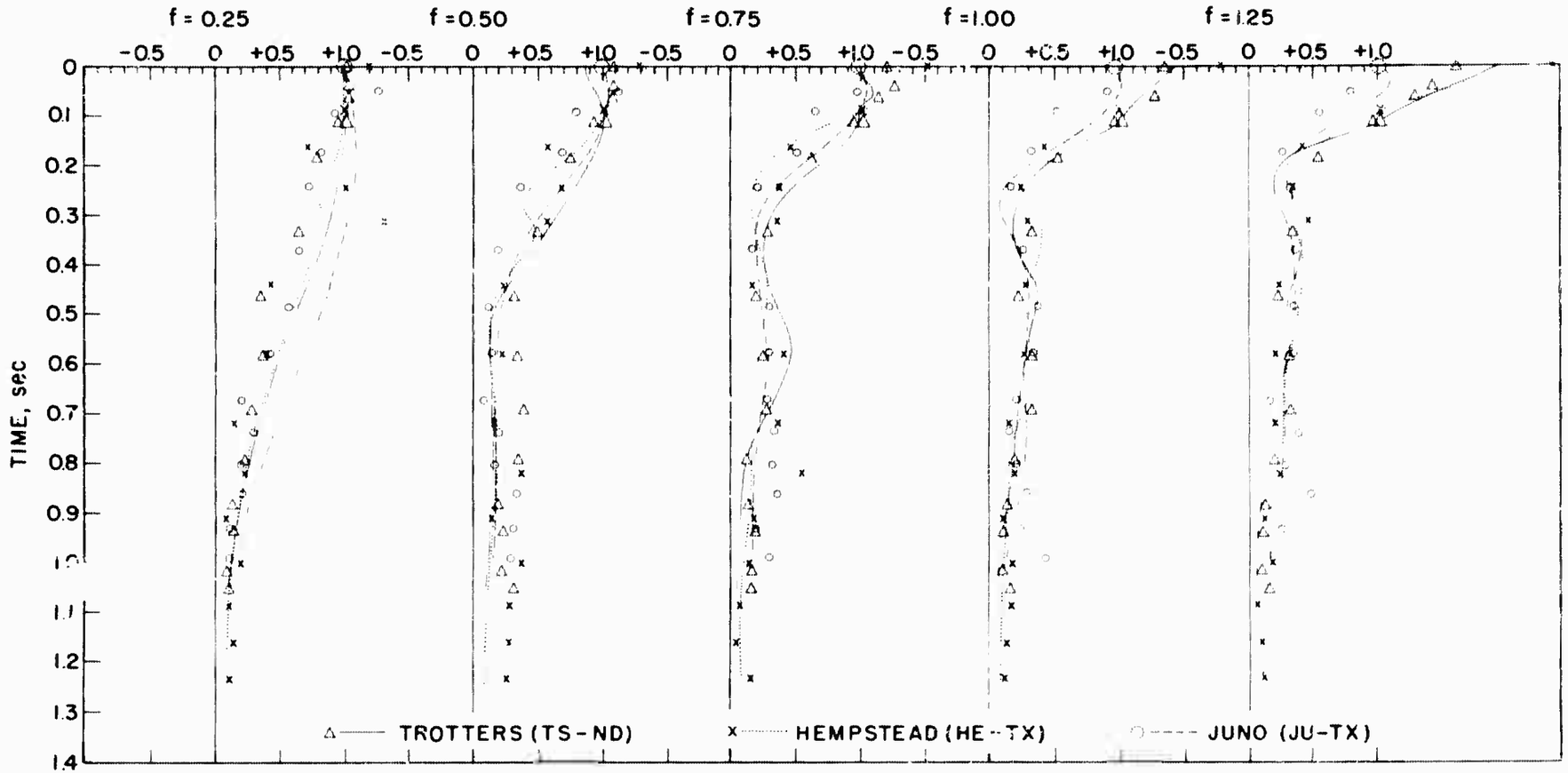

Fig. 35 - Noise power ratio, deep well/500-foot, versus vertical travel time of P-waves; experimental and theoretical results for the three sites are compared. Results for several frequencies are shown. The points indicate averages of the experimental data at each site. Theoretical results for an energy equipartition of trapped waves only are shown by the curves. For all three sites the first minimum for noise consisting of vertical P-waves would occur approximately at the time 0.25/f seconds, where f is the frequency in cps.

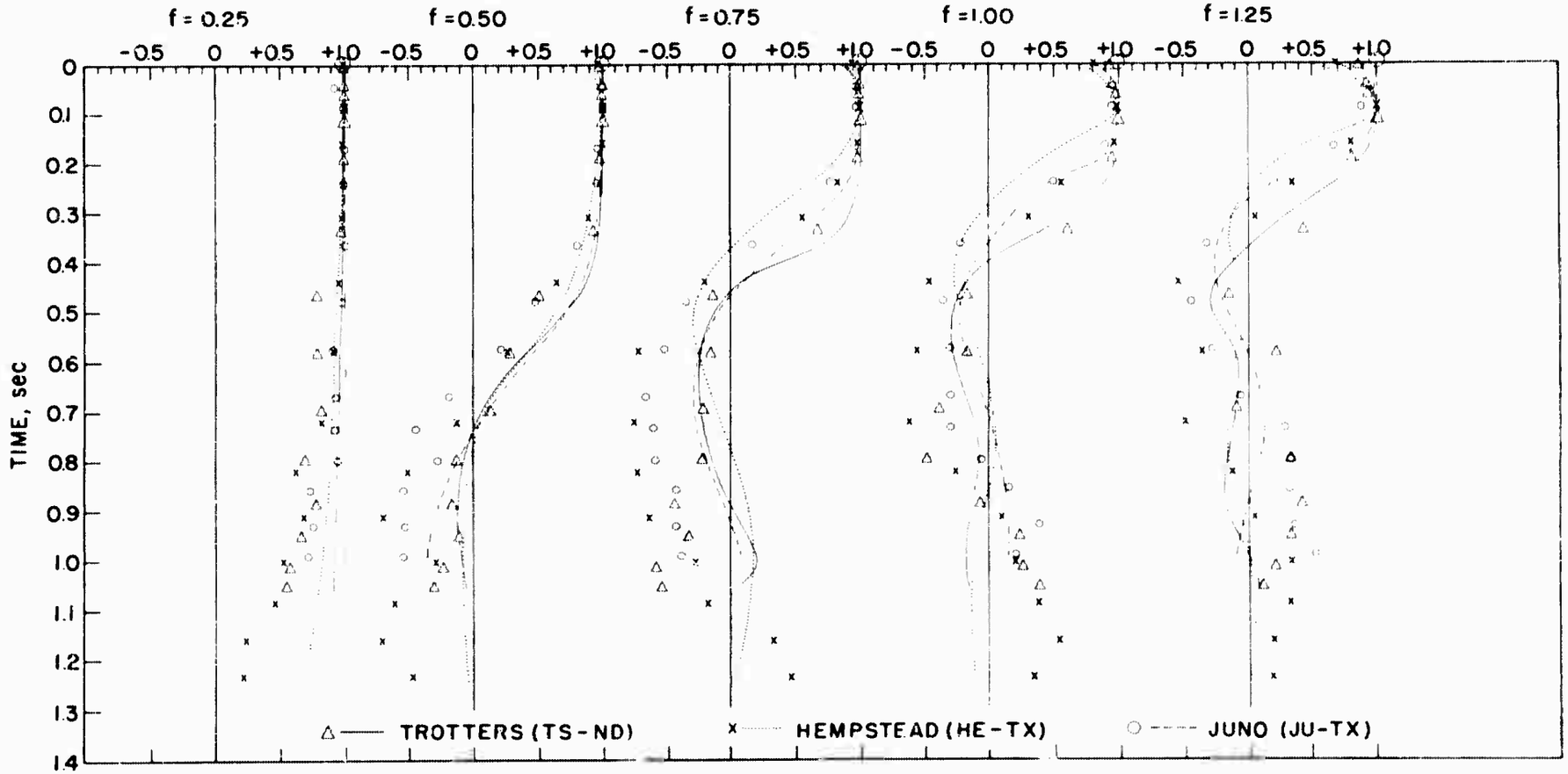

Fig. 36 - Coherence between deep well and 500-foot noise versus vertical travel time of P-waves; experimental and theoretical results for the three sites are compared as in Figure 35. Results for several frequencies are shown. For all three sites the first zero crossing for noise consisting of vertical P-waves would occur approximately at 0.25/f seconds, where f is the frequency in cycles per second.

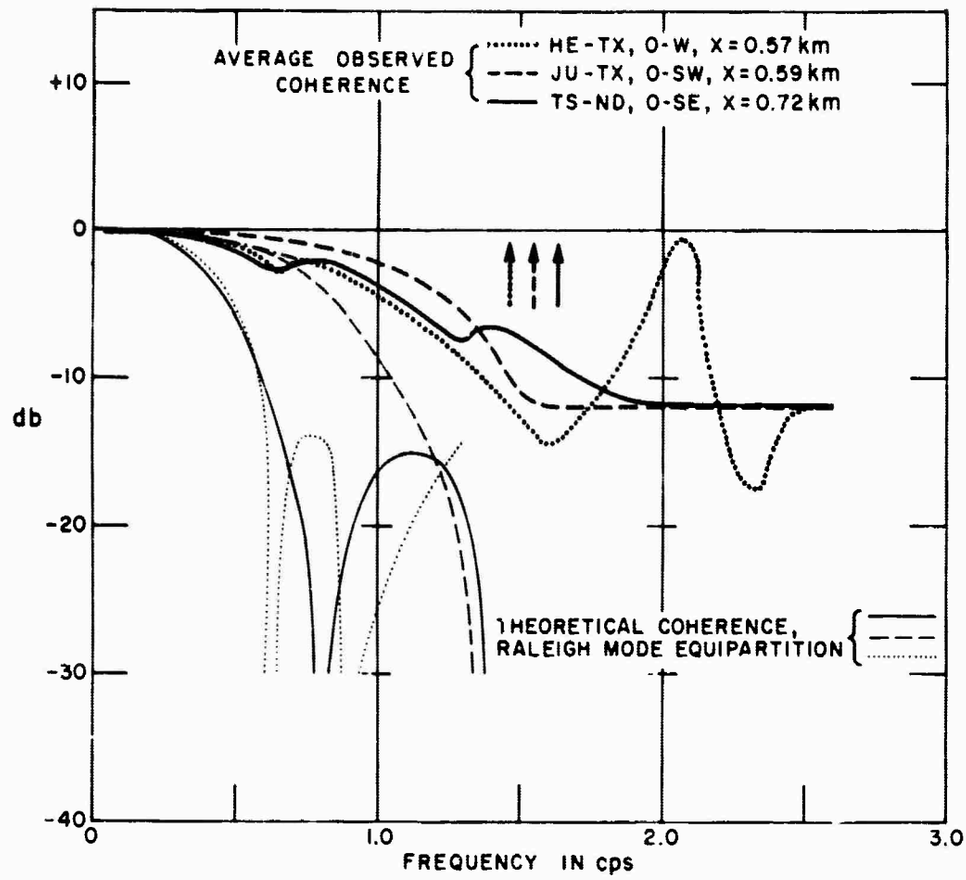

Fig. 37 - Coherence versus frequency for noise from pairs of seismometers in the surface array; experimental and theoretical results for the three sites are shown. The experimental results are averages for a number of noise samples. The seismometer separations, x, are shown on the figure. The arrows indicate the frequency above which observed phases near π are common.

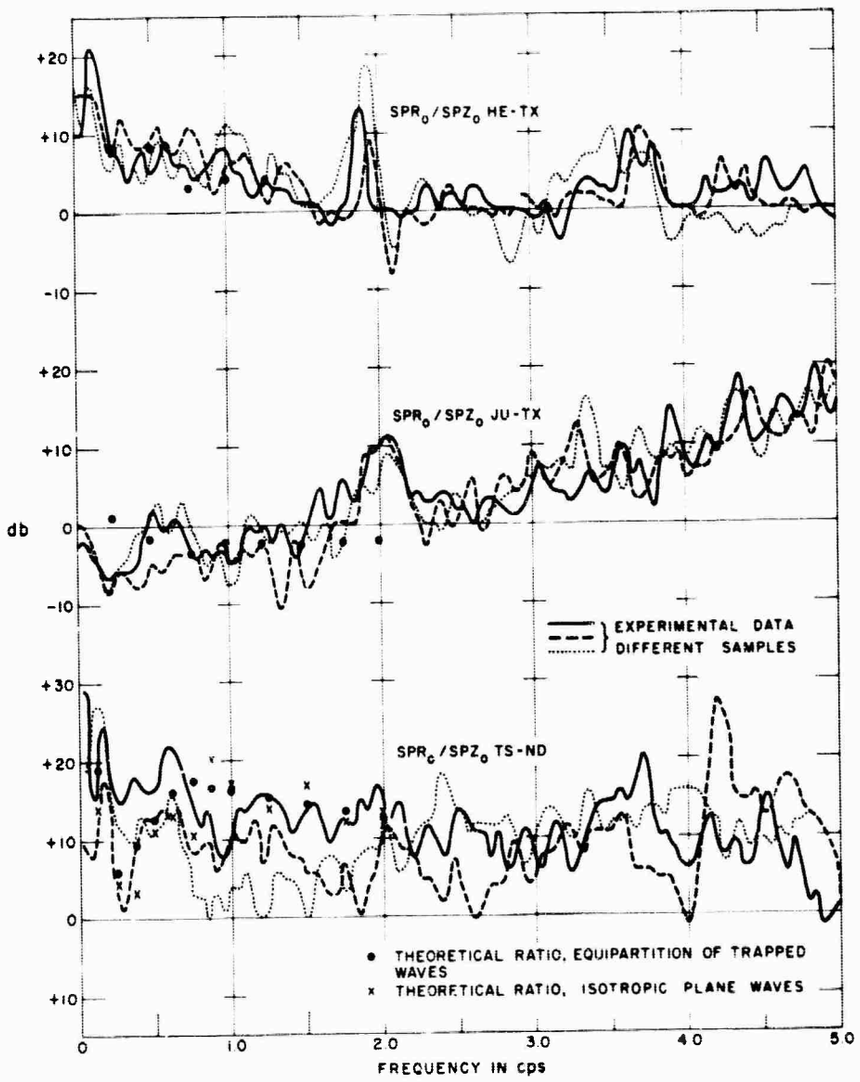

Fig. 38 - Comparison of horizontal-to-vertical power ratios for surface noise at the three sites. Experimental and theoretical values are given. Experimental results for three different noise samples are shown for each site.

APPENDIX A

DEEPWELL DATA FOR JUNO, TEXAS AND HEMPSTEAD, TEXAS

The data shown in the figures of this appendix are taken directly from Semi-Annual Reports 2 and 3 of this project. Minor additions have been made. The reader is referred to those reports for further details.

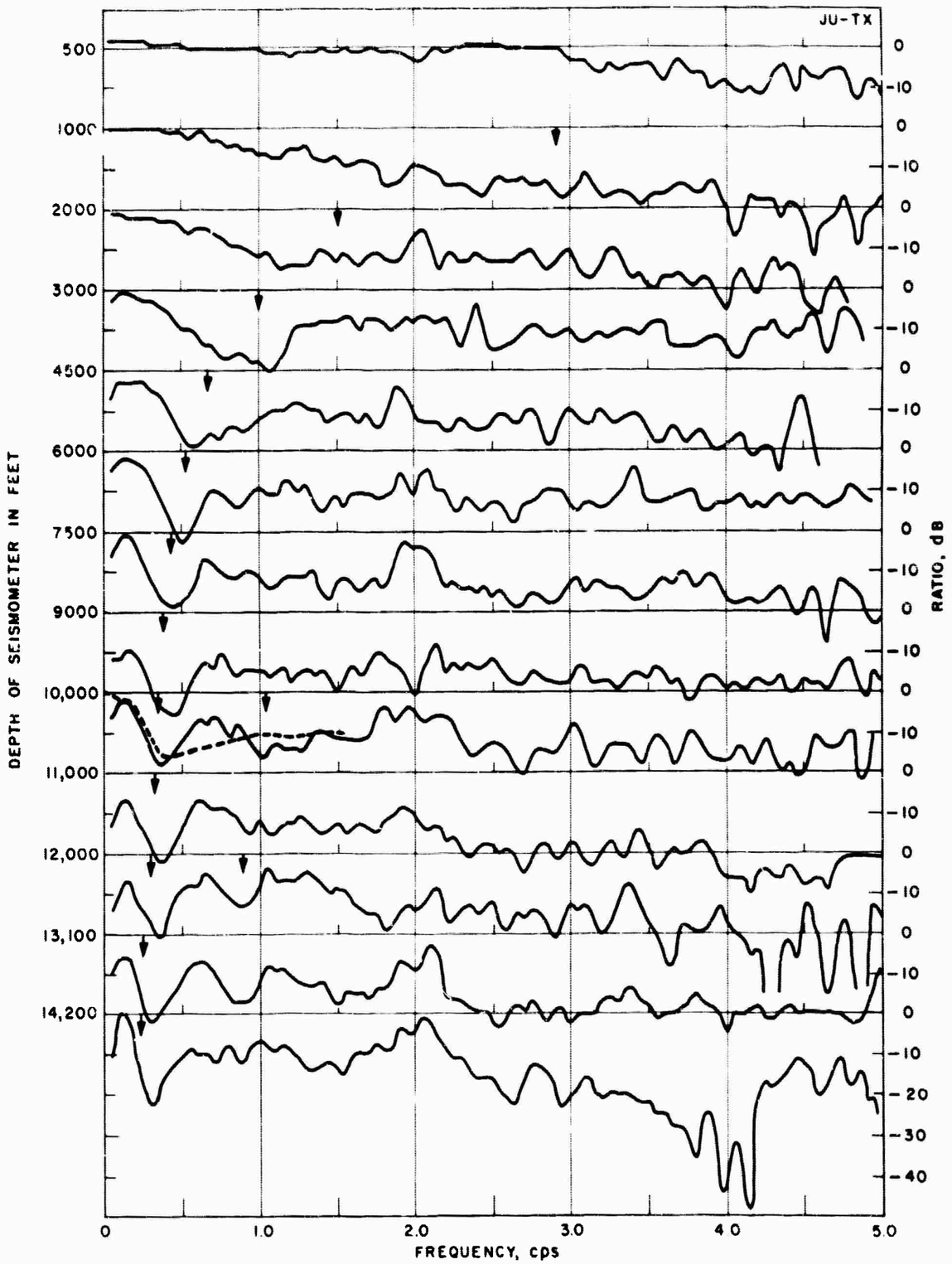

Fig. A1 - Noise power ratio deep well/surface as a function of frequency for various depths at Junc, Texas. All samples are for "typical quiet" noise. The arrows are at frequencies $f_1 = 1/4$, where τ is the vertical travel time for P-waves. The dashed curve is the theoretical result for energy equipartition of all trapped modes at 10,000 feet.

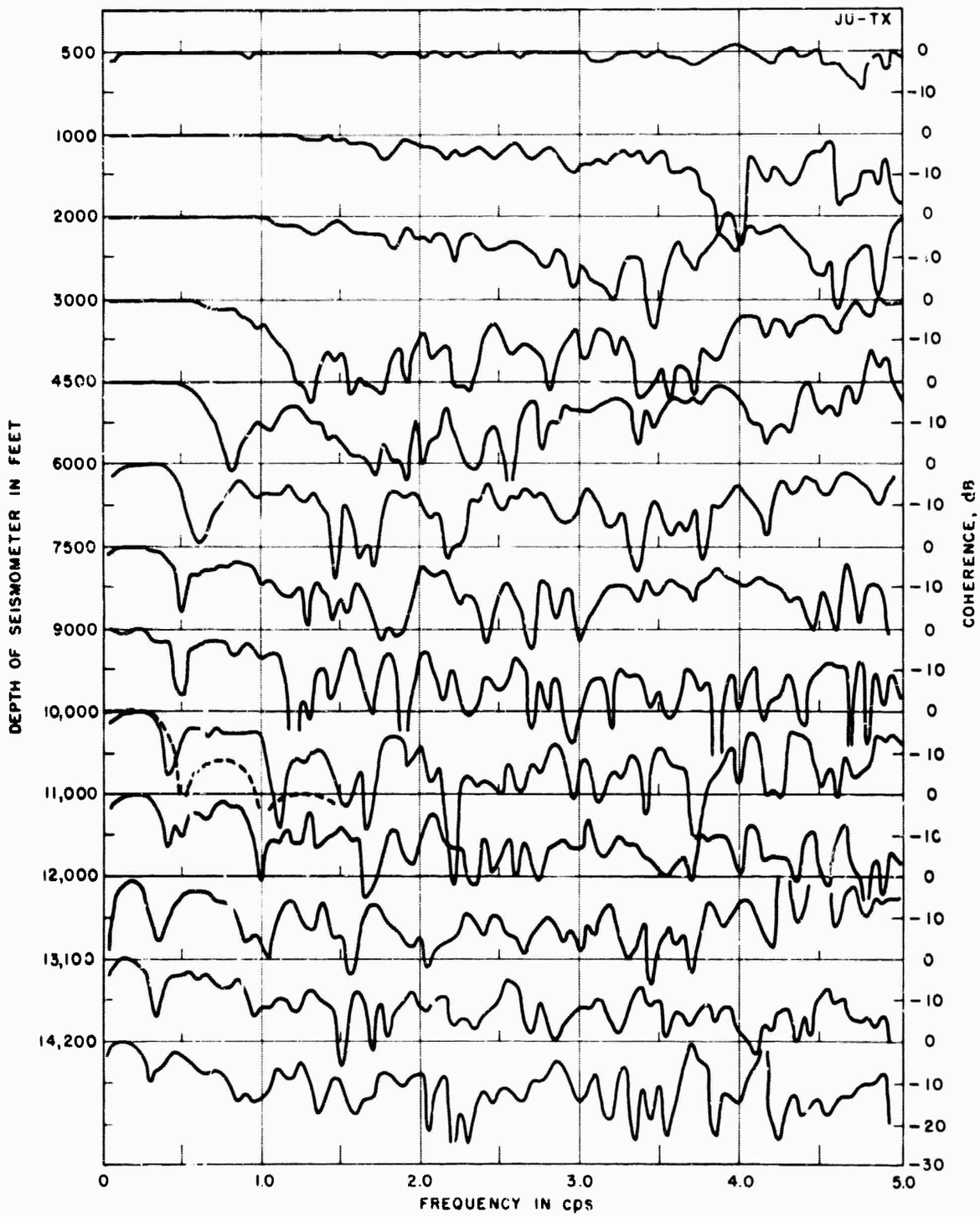

Fig. A2 - Coherence of deep well and surface noise as a function of frequency for various depths at Juno, Texas. Same samples as Figure A1. The dashed curve is the theoretical result for energy equipartition of trapped waves at 10,000 feet.

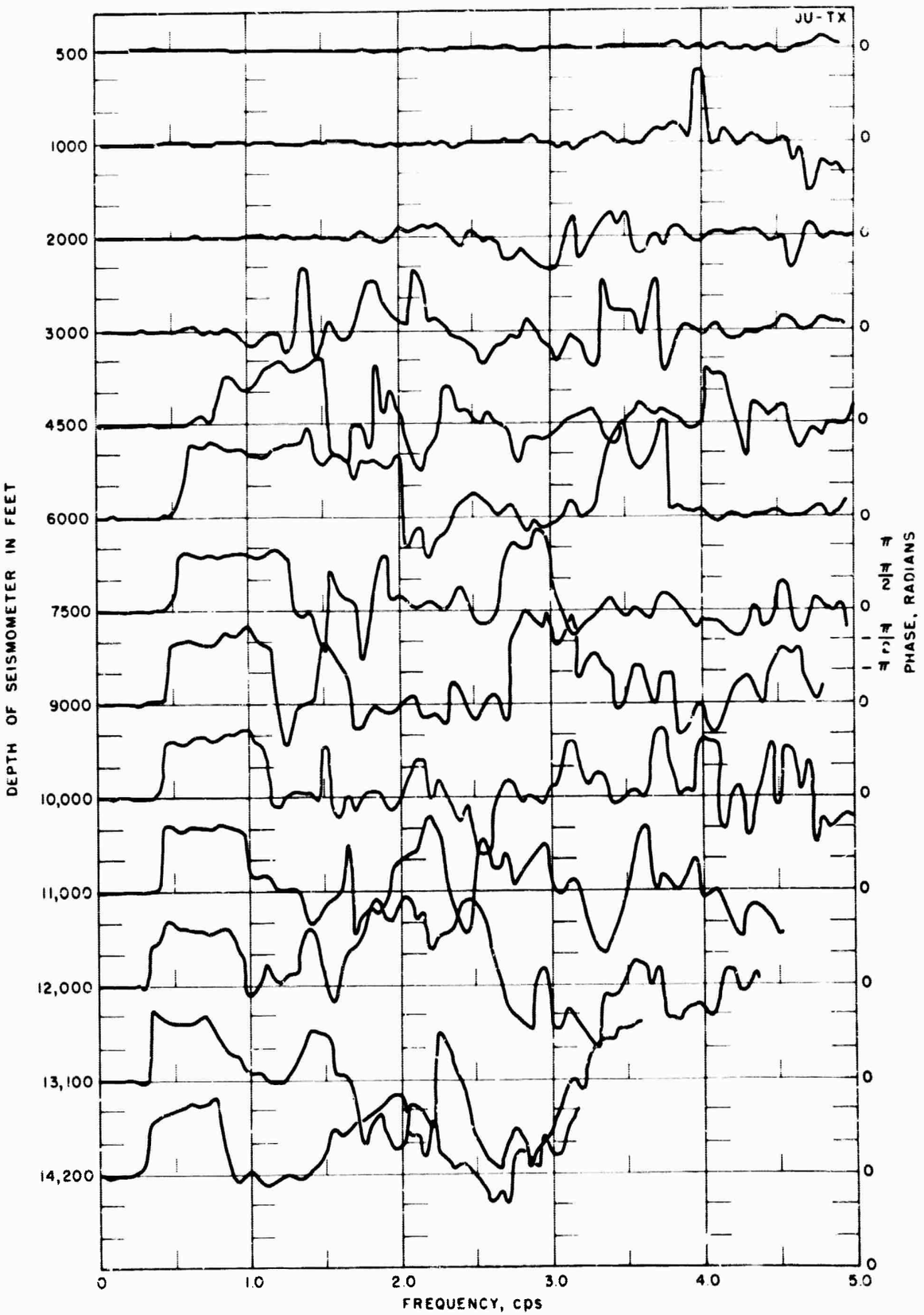

Fig. A3 - Cross-correlation phase of deep well and surface noise at Juno, Texas. Same samples as Figure A1.

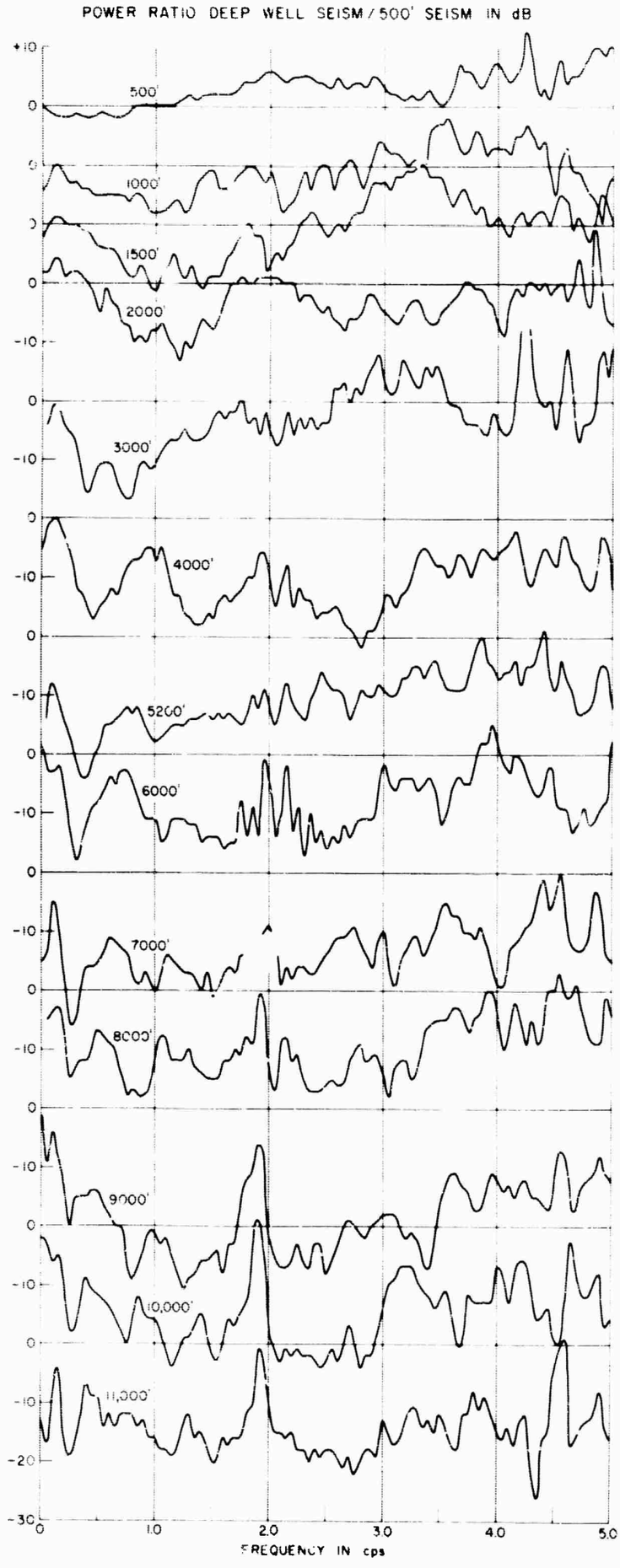

Fig. A4 - Noise power ratio deep well/500-foot as a function of frequency for various depths at Hempstead, Texas. "Typical quiet" night noise samples.

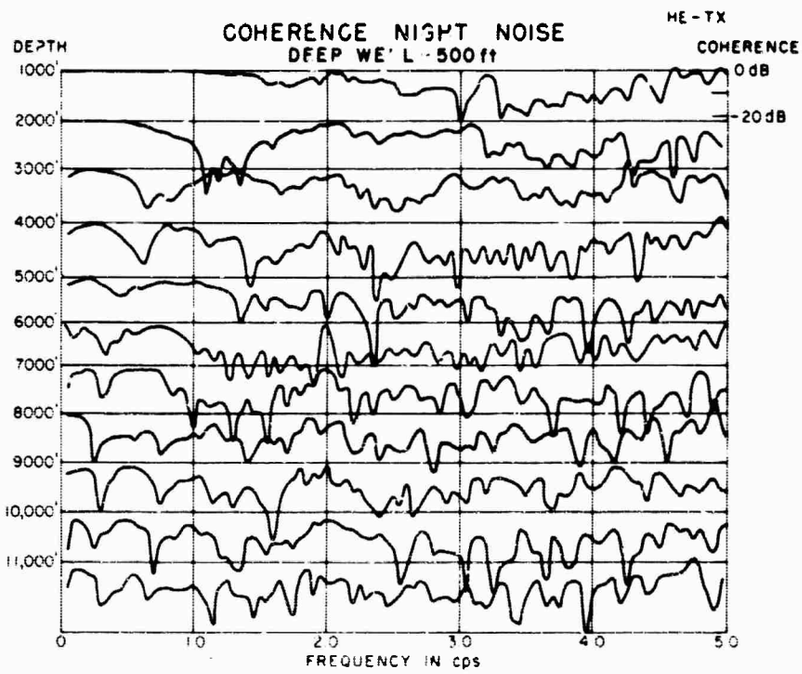

Fig. A5 - Coherence of deep well and 500-foot noise as a function of frequency for various depths at Hempstead, Texas. Same samples as Figure A4.

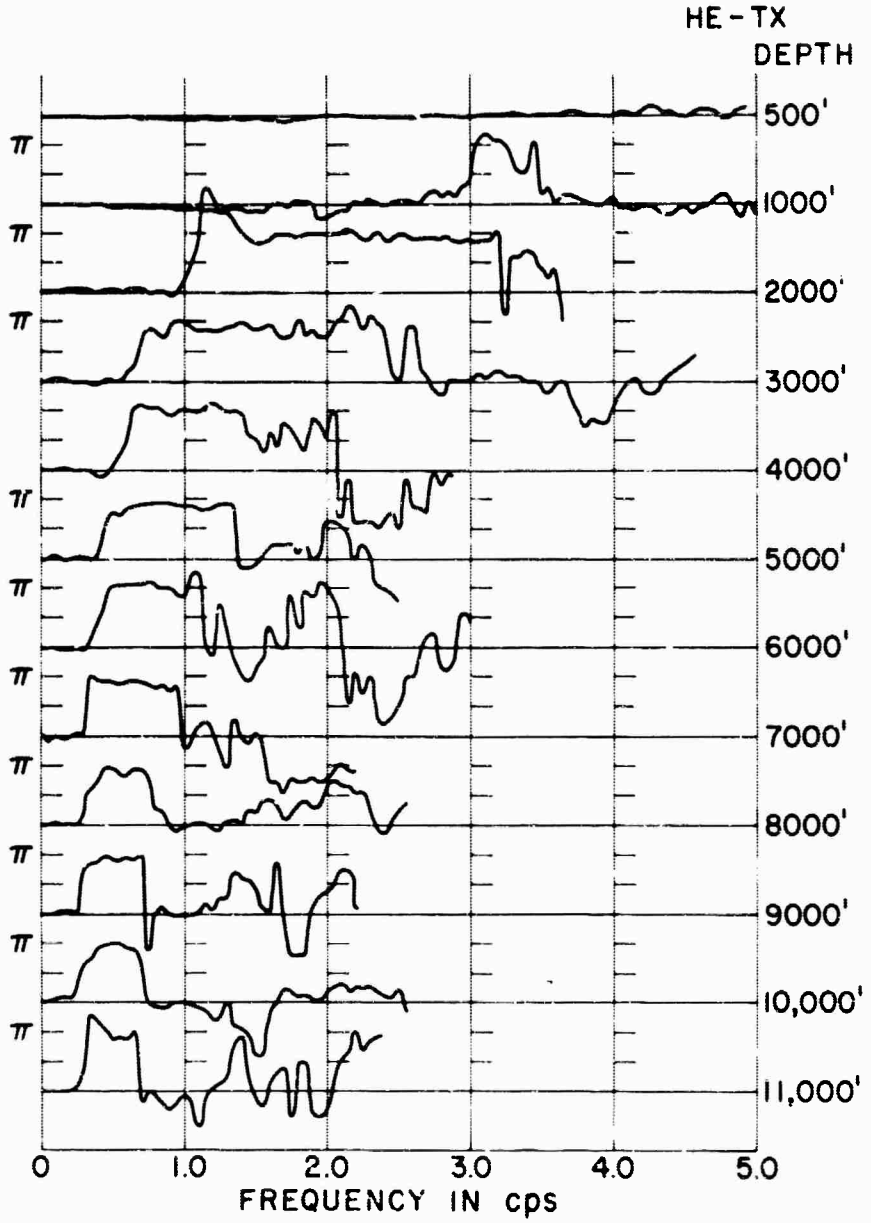

Fig. A6 - Cross-correlation phase of deep well and 500-foot noise as a function of frequency for various depths at Hempstead, Texas. Same samples as Figure A4.